



**HAL**  
open science

# Study and realization of a microwaves system to estimate the moisture content in wood biomass

Maria Merlan

► **To cite this version:**

Maria Merlan. Study and realization of a microwaves system to estimate the moisture content in wood biomass. Physics [physics]. Université Pierre et Marie Curie - Paris VI, 2016. English. NNT : 2016PA066154 . tel-01401304

**HAL Id: tel-01401304**

**<https://theses.hal.science/tel-01401304>**

Submitted on 23 Nov 2016

**HAL** is a multi-disciplinary open access archive for the deposit and dissemination of scientific research documents, whether they are published or not. The documents may come from teaching and research institutions in France or abroad, or from public or private research centers.

L'archive ouverte pluridisciplinaire **HAL**, est destinée au dépôt et à la diffusion de documents scientifiques de niveau recherche, publiés ou non, émanant des établissements d'enseignement et de recherche français ou étrangers, des laboratoires publics ou privés.

**THÈSE DE DOCTORAT DE  
L'UNIVERSITÉ PIERRE ET MARIE CURIE**

École doctorale : Informatique, Télécommunications et Électronique de Paris

réalisée au

**Laboratoire de Physique et d'Étude des Matériaux**

présentée par

**Maria Merlan**

pour obtenir le grade de

**DOCTEUR DE L'UNIVERSITÉ PIERRE ET MARIE CURIE**

ayant pour titre

**Study and realization of a microwaves system to  
estimate the moisture content in wood biomass**

soutenue le 18 février 2016

devant le jury composé de

Catherine Algani	. . . . .	Rapporteur
Frédéric Rouger	. . . . .	Rapporteur
Pierre Ducray	. . . . .	Examineur
Hamid Kokabi	. . . . .	Examineur
Thierry Ditchi	. . . . .	Examineur
Yacine Oussar	. . . . .	Directeur de thèse



# Acknowledgments

First of all, I would like to express my sincere gratitude to the members of the jury Hamid Kokabi, Pierre Ducray, Thierry Ditchi and Yacine Oussar for taking part in the defense of my work, and especially to the thesis reporters, Catherine Algani and Frédéric Rouger who did accept taking the time to read the manuscript of this thesis. I am grateful for the financial investment from the French research agency (ANR) that has supported the MOQAPRO project (2012-2015) concerning the issue "biofuels and energy". The organizations IDSET (*Institut pour le Développement de la Science, l'Éducation et la Technologie*), UCFF (*Union de la Coopération Forestière Française*), ONF (*Office National des Forêts*) and FCBA (*Institut Technologique Forêt Cellulose Bois-construction Ameublement*) were involved in this project to better manage the wood energy sector in France and contribute to fight against climate change. I must say that I have accumulated many debts during this thesis. I would like to thank my main supervisors, Stéphane Holé and Thierry Ditchi for their unflagging assistance in pushing this project along. I am also thankful for not only the time but also moral support that I was given throughout this research. Equally support came from the director of the thesis Yacine Oussar and the academics Emmanuel Géron and Jérôme Lucas. I name Marco Mejia and Tony Hanna who did collaborate during their master's internships in this project, and also Vianney de Courtivron from "*La coopérative forestière Bourgogne Limousin*", who got remarkably involved and provided us facilities throughout the full scale experiment. I am happy to extol the capacity of the LPEM team to manage these three years of my thesis, which have resulted a big step forward concerning this line of research. I reckon that this long experimental research could not be possible without their contribution, which I highly appreciate and particularly enjoyed it quite a lot. I strongly believe that empathy and comprehension in the workplace are key to success.

Finally I would personally like to mention the warmth and kindness received by the whole team LPEM (Julie Iem, Cédric Margo, Nabil Houdali, Basil Salamé, Christine Boué, Céline Corbrion-Fillooy, Charlotte Tripon-Canseliet, Karla Balaa, Manon Pommier, Marie-Christine Leger, Julien Haffner, Ibrahim Mohsen, Binqing Mei, Zied Lassoued, Louiza Hamidouche, Anne Pennillard et Hela Daassi). I remember now with a funny nostalgia Guillaume Trannoy and Nazim Lechea who put up with me the first months when I first arrived and could not say a word in french.

As a personal self reflection, this is my first long professional experience. Intellectual and personal knowledge comes along together with time. Thanks to my friends and family who stay always beside my side.



# Contents

<b>Introduction</b>	<b>1</b>
<b>1 Wood energy sector</b>	<b>7</b>
1.1 Critical condition of current energy consumption . . . . .	8
1.1.1 Ecological footprint and source depletion . . . . .	8
1.1.2 Green tendency . . . . .	9
1.2 Wood biomass energy for heating . . . . .	10
1.2.1 Interest of the industry . . . . .	10
1.2.2 Wood biomass . . . . .	12
1.2.3 Boilers . . . . .	13
1.2.4 Towards a new energy strategy for Europe 2011-2020 . . . . .	14
1.2.5 French energy policy . . . . .	16
1.3 Industrial process . . . . .	17
1.3.1 Production chain . . . . .	17
1.3.2 Importance of standards . . . . .	19
1.3.3 Standards . . . . .	20

<b>2</b>	<b>Background</b>	<b>23</b>
2.1	Thermogravimetric methods . . . . .	25
2.1.1	Freeze drying . . . . .	25
2.1.2	Oven drying . . . . .	26
2.1.3	Infrared drying . . . . .	26
2.1.4	Microwave Drying . . . . .	26
2.2	Analytical methods . . . . .	27
2.3	Rapid or indirect methods . . . . .	28
2.3.1	Radiofrequency methods . . . . .	28
2.3.2	Microwaves methods . . . . .	29
2.3.3	Electrostatic methods . . . . .	30
2.3.4	Optical methods . . . . .	31
2.3.5	Hygrometrical methods . . . . .	33
2.3.6	Radiometric methods . . . . .	34
2.4	Synthesis . . . . .	35
<b>3</b>	<b>Contactless electromagnetic technologies</b>	<b>37</b>
3.1	Preliminary physical background . . . . .	38
3.1.1	Wood chip dielectric properties . . . . .	38
3.1.2	Electromagnetic propagation . . . . .	40
3.2	Transmission-Reflection system . . . . .	41
3.2.1	Experimental prototype . . . . .	42
3.2.2	Optical module . . . . .	43
3.2.2.1	Stereo vision method . . . . .	43

3.2.2.2	Stereo matching process . . . . .	46
3.2.2.3	3D reconstruction . . . . .	47
3.2.2.4	Experimental results and discussion . . . . .	48
3.2.3	Electromagnetic module . . . . .	50
3.2.3.1	Material . . . . .	50
3.2.3.2	Procedure . . . . .	51
3.2.3.3	Direct frequency domain analysis . . . . .	53
3.2.3.4	Direct time domain analysis . . . . .	54
3.2.3.5	Multivariate analysis . . . . .	56
3.3	Conclusions . . . . .	58
<b>4</b>	<b>In contact technologies</b>	<b>61</b>
4.1	Capacitive system . . . . .	62
4.1.1	Principle . . . . .	62
4.1.2	Experimental system and procedure . . . . .	64
4.1.3	Results and discussion . . . . .	66
4.1.4	Summary . . . . .	68
4.2	Resonator technology . . . . .	69
4.2.1	Underlying physics . . . . .	69
4.2.2	Antenna resonators . . . . .	70
4.2.2.1	Half-wave dipole antenna . . . . .	70
4.2.2.2	Quarter-wave monopole antenna . . . . .	71
4.2.2.3	Microstrip rectangular antenna . . . . .	72
4.2.2.4	In-line half-wave dipole antenna . . . . .	73



4.2.3	Simulation analysis . . . . .	74
4.2.4	Experimental analysis . . . . .	75
4.2.5	Study of half-wave dipole antenna performance . . . . .	80
4.2.6	Laboratory-scale system . . . . .	83
4.2.6.1	Equipment . . . . .	84
4.2.6.2	Methodology . . . . .	85
4.2.6.3	Sensor characterization . . . . .	86
4.2.6.4	Multivariate analysis . . . . .	88
4.2.6.5	Summary . . . . .	89
4.3	Full-scale implementation . . . . .	90
4.3.1	Bulk measurements in static piles . . . . .	90
4.3.2	Bulk measurements in a container . . . . .	94
4.3.3	Summary . . . . .	100
4.4	Conclusion . . . . .	101
	<b>Conclusion</b>	<b>103</b>
	<b>Perspectives</b>	<b>107</b>
	<b>Bibliography</b>	<b>109</b>

# Introduction

Global warming is a major problem that is set to increase in the coming years. In the face of this growing concern it is important to focus on reducing emissions of carbon dioxide, which is one of the main causes of global warming. For this, a solution is to use clean energies such as solar or wind energies, or other carbon-neutral energies: lignocellulosic biomass is a source of energy that fits into this second category. 68% of gross inland consumption of renewable energy in Europe was biomass and renewable waste in 2011. Biomass, mainly used for heating, represents 95.5% of the final heat consumption from renewable energies. Wood remains the largest biomass energy source today [1]. Wood chips are an example of secondary residual material produced during forestry processes. Wood that is not directly exploitable for the industry is shredded, and can be burned in boilers in order to produce energy. The levels of carbon dioxide released into the atmosphere during such a process are comparable to the levels released by natural decomposition of the wood chips. It would then be wasteful not to utilize that wood energy [2]. Moreover, since growing plants capture an amount of carbon dioxide equivalent to that released to the atmosphere by burning biomass, the net carbon dioxide footprint is zero over a period of time of around 20 years. Wood chips are then a sustainable energy source [3]. Figure 1 shows this biofuel. Wood chips largest dimension can vary from 3 cm to 12 cm. Their large surface area to volume ratio is ideal for efficient combustion or gasification since fire spread behavior is correlated to the surface area to volume ratio of the fuel. Higher values mean shorter fuel ignition times, and hence faster fire spread rates [4]. Wood chips are more energy efficient than logs because they can form an uniform fuel that can flow or be fed to a boiler. Continuous and uniform fuel feed is indeed key for the performance of the combustion chamber [5].

The calorific value indicates the energy released as heat when a compound undergoes complete combustion with oxygen, usually given in gigajoule per tonne or kilowatt hour per kilogram [6]. The oven-dry calorific value  $NCV_0$  is the calorific value of anhydrous wood and varies slightly between 18.5 to 19 MJ/kg. It is higher in softwood species (evergreen, coniferous) than in hardwoods (deciduous, broadleaved trees) due to the higher content of resin, wax, lignin and oil [7]. Because of the very little variation of  $NCV_0$ , calorific value is directly proportional



Figure 1: Pile of wood chips.

to the mass of fuel and, mostly independent of the kind of wood. However, the main difference between species, if comparing hardwood and softwood species, is the moisture content at the time of felling, and the rate at which this moisture is lost [8]. Indeed hardwoods tend to be denser and softwoods tend to contain more resins. It is not hard to see how moisture content affects the calorific value of a given fuel. When dealing with wet fuel, extra energy is spent on heating and evaporating the water present before combustion can take place. Moreover, more water results in less wood for a given fuel mass, thus still less available energy. It is demonstrated that moisture content of wood has a significant impact on the calorific or energy value of the fuel. The variation of the calorific value between different species when tested at the same moisture content is negligible. Therefore, at the moment of the purchase, the measurement of moisture content determines the calorific value and thus the price in terms of energy content [7, 9]. The Graphic 2 shows the relation between calorific value and moisture content of net wood. The literature gives different definitions of moisture content depending if calculated as the percent of total mass or of wood mass. In this thesis, the moisture content (MC) is calculated on the basis of the total mass of the wet sample as

$$\text{MC}(\%) = 100 \times \frac{m_{\text{wet}} - m_{\text{dry}}}{m_{\text{wet}}}, \quad (1)$$

where  $m_{\text{wet}}$  corresponds to the actual mass (wood and water) and  $m_{\text{dry}}$  corresponds to the mass of the wood as if the fuel were anhydrous. The advantage of this definition is that moisture content gets values between 0 and 100%, 0% indicating anhydrous wood and 100% indicating no wood, only water.

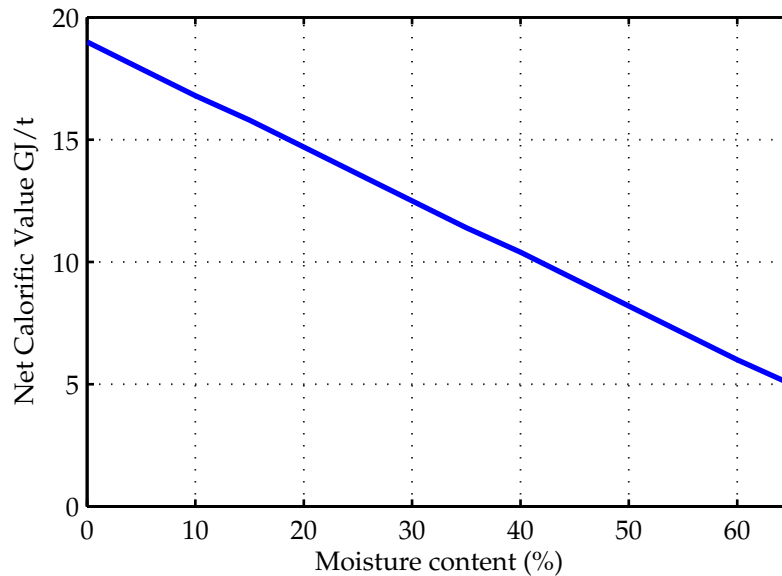


Figure 2: Calorific value of wood versus moisture content [9].

Whole trees, branches or logging residues are mechanically shredded by a shredder machine in order to create wood chips. These wood sources may come from forest thinning, pruning, process fallen or dead trees or even byproducts of sawmills. Due to this variety of sources, the moisture range value can be wide. A pile of dry wood would be around 25% or 30% MC, and a pile of green wood, recently extracted, could reach up to 60% MC. According to the UNECE<sup>1</sup>, which represents 20% of the world population, including some of the world's richest countries like Europe, but also Canada, United States, Central Asia (Kazakhstan, Kyrgyzstan, Tajikistan, Turkmenistan and Uzbekistan) and Western Asia (Israel), wood biomass energy consumption has increased 4% every year between 2007 and 2011 in the UNECE region [10]. This tendency is expected to continue due to many European government strategies promoting this kind of energy in order to get the EU target of 20% of energy consumption from renewable sources by 2020 [11]. These strategies expect to not only reduce climate change, but also increase energy security by encouraging alternatives to imported and increasingly high-priced fossil fuels. Over 40% of the wood raw material in the Nordic forest industries ends up indirectly as fuel. In Finland or Sweden, for example, wood energy consumption is much higher than in other European countries. In France, wood energy consumption is not yet that developed, however, being the second largest of the forest countries in Europe, its wooded territory represents 30% of the metropolitan area. So that, future French wood biomass production is compatible with its stipulated European target, which is to get 23% of energy consumption from renewable energies by 2020 instead of 11% consumed in 2011. To reach this goal it is necessary to improve existing wood chip industries and to optimize quality and price of such energy source. Meth-

<sup>1</sup>United Nations Economic Commission for Europe.

ods and tools for quantitative and qualitative monitoring of the production of wood chips are currently under research.

MOQAPRO project is a scientific project funded by the French National Research Agency whose main target is a large scale integrated approach, from forest land to power plant, of quantity and quality monitoring of the wood chip production chain. Quality monitoring is mainly dependent on moisture content measurement at every step of the production chain. Quantity monitoring is on volume and mass. Monitoring through the production chain implies a constant measurement of wood chip mass and moisture content, which presents complexity due to the large scale circumstances and to the random nature, size and arrangement of wood chips. Although a large amount of moisture sensor technologies exist, the former OMICAGE project showed that none of them can be directly applied to moisture content measurements of wood chips [12]. Therefore, and until now, wood chip moisture content is determined via sampling, each sample being weighted before and after drying. Such a procedure gives only sparse measurements and is very long to implement. Measurements are therefore made by the client who subjectively chooses the samples and indirectly imposes the price of the wood chips. Consequently, bias may be involved and the trade can be unbalanced. The goal of MOQAPRO project is to adapt technologies to complex storage site conditions, as well as to provide automated and economical frequent moisture content measurements for big scale volumes. Give innovative solutions for these monitoring aspects is highly important, especially on moisture content, to promote a high industrial level of woody biomass energy production in profitable situation. Investigations are being led in several European countries to identify production strategies and monitoring tools that could be applied to French industry forest conditions. Results of this project are highly expected by many agents in the wood chip production chain [13].

This thesis is focused on the moisture content measurement in static conditions as one of the most important quality parameters of wood chips. The price of wood chips today depends on the moisture content and both powerplant and supplier are interested in a method for determining payment that is both representative and rapid. As it has been mentioned before, the current reference method called Oven Dry Method (EN 14774-1:2009) is applied [14]. Few small samples are taken from the top of the container and weighed before and after a drying procedure, which it is neither fast nor representative since the moisture can vary greatly in different parts of the container. One way to control the moisture content for payment is measuring it in arriving fuel containers, for which the instrument shall be able to measure an average value within seconds. The objective of this thesis is to estimate the moisture content of large samples of wood chips normally in a truck, as the Figure 3 shows, before delivery to the client.

To accomplish this vision, a technique capable of measuring the moisture content of large quantities of wood chips instantly is necessary. To meet the requirements of a fast measurement



Figure 3: Truck full of wood chips.

method that provides an average value of the moisture content of a larger volume of wood chips, radiofrequency technology (RF) is applied. In the range of the moisture content involved in this system, the effect of temperature or wood fiber direction on the dielectric properties of the wood is rather small when compared to the influence of the water content [15]. According to the literature near infrared radiation is a promising measuring method to be used in a continuous flow, and radiofrequency is today the best-suited method for measuring moisture content in fuel bulks for the ability of measuring large samples [16, 17].

The manuscript consists of 4 chapters and is organized as it follows:

1. *Wood energy sector* (Chapter 1): The first chapter presents the worldwide energy consumption nowadays and the need of a green trend. It follows with a brief description of the production chain of the wood biomass industry market, with general background of operational and quality standards, focused on Europe and France;
2. *Background* (Chapter 2): In the second chapter, a review of several technologies to determine the moisture content in a pile of wood chips are presented, some of which have been already turned into commercialized products;
3. *Contactless electromagnetic technologies* (Chapter 3): The third chapter concentrates on the experimental study of moisture content measurement systems from the outside, that is to say without contact with the fuel, in combination with the theoretical background of far field telecommunication basis;

4. *In contact technologies* (Chapter 4 ): In the fourth chapter, several moisture content measurement technologies from the inside, that is to say in contact with the fuel, are studied, realized and tested, based on different electromagnetic phenomena;

Finally major conclusions and propositions for further experimental investigations are provided.

# Chapter 1

## Wood energy sector

---

<b>1.1</b>	<b>Critical condition of current energy consumption . . . . .</b>	<b>8</b>
1.1.1	Ecological footprint and source depletion . . . . .	8
1.1.2	Green tendency . . . . .	9
<b>1.2</b>	<b>Wood biomass energy for heating . . . . .</b>	<b>10</b>
1.2.1	Interest of the industry . . . . .	10
1.2.2	Wood biomass . . . . .	12
1.2.3	Boilers . . . . .	13
1.2.4	Towards a new energy strategy for Europe 2011-2020 . . . . .	14
1.2.5	French energy policy . . . . .	16
<b>1.3</b>	<b>Industrial process . . . . .</b>	<b>17</b>
1.3.1	Production chain . . . . .	17
1.3.2	Importance of standards . . . . .	19
1.3.3	Standards . . . . .	20

---



This chapter presents the concept of wood energy heating as a possibility to contribute decreasing carbon dioxide CO<sub>2</sub> emissions and therefore global warming. Advantages and disadvantages regarding other renewable energies are presented. A brief description of the steps of the fuel through the production chain in the wood industry is given. Finally, the basis of the necessity of common quality standards are discussed.

## 1.1 Critical condition of current energy consumption

Nowadays the energy consumption has highly increased due to the industrialization of the countries and the increase of population in the world. This trend is expected to continue. There are three kinds of energy production: nuclear sources, fossil fuels and renewable sources. Nuclear energy may cause problems to environment and health in case of nuclear accidents such as Tchernobyl in Ukraine or Fukushima in Japan. However it remains the cleanest high power source with zero CO<sub>2</sub> emission and a real waste control. Fossil fuels are the main world energy resource and are causing global warming by CO<sub>2</sub> emissions, whose levels have increased 31% in the past 200 years. The increase of global temperature means sea level average rate of 1-2 mm every year over the last century. CO<sub>2</sub> emissions caused by the combustion of fossil fuels is the major contribution to the greenhouse effect. On the contrary, renewable energy sources as solar, wind, biomass, geothermal, hydropower and marine can be used to produce energy again and again. They have the capacity of providing energy with zero or almost zero emissions and represent today 14% of total energy consumption. Its use is expected to increase greatly in the coming years from 30% to 80% by 2100. Table 1.1 shows the trend of renewable energy consumption expected until 2040 [18]. Its use is supposed to rise from 16.6% in 2010 to 47.7% in 2040. The main renewable energy nowadays by far is biomass, it represents 75.22% of all the renewable energy consumed in 2010, and it is also expected to follow this trend.

### 1.1.1 Ecological footprint and source depletion

Ecological footprint metric is widely used in ecosystem accounting. It is a measure of mankind demand on the earth's ecosystem. In other words, it measures how fast we consume resources and generate waste compared to how fast nature can absorb our waste and generate new resources. World population has reached 7.2 billion in 2014 and it has doubled in the last 45 years. For several years population has been growing much faster than many vital non renewable sources. Developed countries are consuming water, minerals and forest faster than they

	2001	2010	2020	2030	2040
Total consumption (million tonnes of oil equivalent)	10038	10549	11425	12352	13310
Biomass	1080	1313	1791	2483	3271
Large hydro	22.7	266	309	341	358
Geothermal	43.2	86	186	333	493
Small hydro	9.5	19	49	106	189
Wind	4.7	44	266	542	688
Solar thermal	4.1	15	66	244	480
Photovoltaic	0.1	2	24	221	784
Solar thermal electricity	0.1	0.4	3	16	68
Marine (tidal, wave, ocean)	0.05	0.1	0.4	3	20
Total RES	1365.5	1745.5	2964.4	4289	6351
Renewable energy source contribution (%)	13.6	16.6	23.6	34.7	47.7

Table 1.1: Tendency of renewable sources [18].

can regenerate. Animal and plant species are extincting everyday. Two billion people nowadays live in poverty, more than the world population one hundred years ago. This turns into a scale problem [19]. Not just overpopulation is the only issue but the high levels of energy consumption multiplied by the number of consumers, especially in developed countries. For example, the United States represent 4.5% of the world population and consume 20% of its energy.

Mankind's energy consumption is the main contributor to release greenhouse gases, in particular CO<sub>2</sub> emissions to the atmosphere. Fossil fuels represent 80% of the world energy primary consumption and they are required for global energy needs nowadays [20]. King Hubbert predicted peak oil in the 60s, oil would peak in about 1970 and decline thereafter [21]. The lack of fossil fuels must be replaced to keep current levels of consumption. Depletion of fossil fuels represents a future challenge, World Coal Institute has determined for coal, oil and gas to last 155, 41 and 65 years respectively at 2006 levels of energy consumption. However, different studies of economic models to predict reserves of fossil fuels differ and nobody can predict exactly when supplies will be exhausted. This ambiguity in results show a clear controversial theme. Even so, fossil fuels are limited sources, the time left is imponderable [22].

### 1.1.2 Green tendency

As climate change is one of the major problems of the 21st century, the use of renewable energy sources are being highly promoted. Government policies have been applied in most countries in Europe, Canada and USA to rise the use of renewable energies. These policies involve

funding to develop infrastructure and scientific research, with the aim of optimizing the use of natural resources. Biomass has represented 56% of total research on renewable energies, followed by solar 26% and wind 11% between 1979 and 2009. This is because biomass is a very promising energy. Besides the fact that its price is stable and economical as it comes from waste products, the affordable cost of converting biomass into energy in comparison with other RES<sup>1</sup> makes biomass even more interesting [23]. It also has the advantage of being stored and continuously used regardless of the climate, while other energies as wind and solar are weather dependent, they can only be produced when the natural resource is available [24]. Biomass conversion efficiencies have been continuously improving in the past years. Gasification and direct combustion are the main conversion techniques to generate electricity and heat using biomass. Direct combustion technique is more widely applied, it represents 90% of all biomass plants in the world. This is because it usually requires less cost investments than gasification technologies. Nowadays forestry and agriculture residues are the principal sources of biomass for electricity and heat generation. In 2010 bioenergy has produced 1313 Mtoe<sup>2</sup>, wood biomass represents 87%, 9% comes from agricultural crops and 4% from municipal and industrial residues. The total bioenergy consumption is expected to rise to 3271 Mtoe in 2040. Wood is an abundant source present in almost every country. Among the renewable energy sources, wood biomass is a very convenient alternative for heating and electricity production because of the simple conversion technologies [25].

## 1.2 Wood biomass energy for heating

### 1.2.1 Interest of the industry

At present, within biomass energy based on power and heat CHP<sup>3</sup> generation, wood chips and pellets combustion are the most economically and environmentally convenient options [26]. Biomass co-firing is regarded as one of the most short-term attractive options for power generation. It is based on the combustion of biomass and pulverized coal or gas. Most biomass co-firing systems use existing coal combustion plants so a very low cost investment is required. Replacing old existing coal plants with biomass co-firing has proved to be reducing to almost zero the emissions of CO<sub>2</sub> in North America. But the leading trend is the transition to a complete carbon-free power generation, which is dedicated biomass combustion, based on pellets or wood chip boilers. These firing systems are commercially available to produce hot water or steam. Their main applications are domestic and district heating systems [27].

---

<sup>1</sup>Renewable Energy Sources.

<sup>2</sup>A toe is a tonne of oil equivalent.

<sup>3</sup>Combined heat and power.

The generation of heat by burning wood has important advantages. Since the energy source used is renewable there is no dearth while logging is done in a sustainable manner. The prices are less variable comparing to the fossil fuels. Wood has a neutral balance in terms of CO<sub>2</sub> emissions: that is to say a history of zero carbon footprint. In fact, the amount of CO<sub>2</sub> absorbed during the growth of the tree through the process of 20 years photosynthesis is approximately the same as that released by the combustion of wood [3]. Besides, dead wood that is left in the forest without using for combustion also releases CO<sub>2</sub> by its decomposition [2].

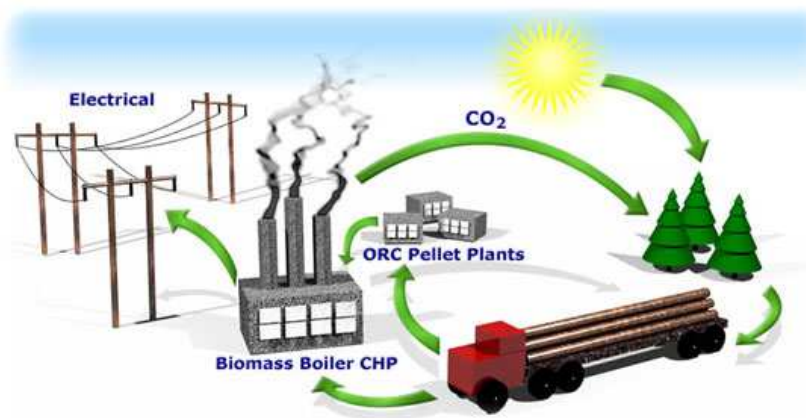


Figure 1.1: Carbon balanced emissions, taken from [28].

It is known that fossil fuels offer higher energy content per mass unit than wood biomass, however they more than double the carbon content, this concludes in higher CO<sub>2</sub> emissions. As a practical example, 20 MWh<sup>4</sup> per year are required to heat a typical domestic house. Using a system based on coal would emit 414 kg/MWh of CO<sub>2</sub>, 314 kg/MWh using oil, 227 kg/MWh with natural gas and only 18 kg/MWh in the case of wood chips at 25% MC [29]. Besides, the price of wood chips is much lower, oil for domestic heating doubles the price of biomass for the same amount of energy. On the other hand, wood biofuel would require a larger stockage space and an initial investment on a wood biomass boiler system.

If the electric power used in thermal energy were replaced by energy from wood biomass, the amount of CO<sub>2</sub> released to the atmosphere would be significantly reduced. The direct consequences on the implementation of timber as a heating source offers positive economic and environmental balance. Wood fuel is much cheaper than fossil fuels and CO<sub>2</sub> emissions would prevent global warming.

Since many years, the use of biomass is basically wood. Its demand is growing fast and this market is expected to reach a value of 70 millions of euros by 2035 in the European Union [30]. The majority of the trade of wood biomass nowadays is between USA, Canada and Europe,

<sup>4</sup>Megawatt-hour represents the product of the power in megawatts and the time in hours.

but Latin America and sub-Saharan African are expected to be large exporters so international trade will be helping the development of biomass sector [27]. It is clear that a sustainable wood to energy industry assisted by a stable source of biofuel, effective fuel transportation and plant performances would bring many advantages, such as the reduction of CO<sub>2</sub> emissions, a proper management of forests reducing the risk of fire, a better environmental preservation, new markets for industries and job opportunities [25, 26].

### 1.2.2 Wood biomass

For many years, wood has been the main source of energy used mostly as heating. Nowadays wood represents an optimistic way to fight the climate change. It can be collected from several sources as timber forests, sawmills or landscaping residues as brush or arboricultural arisings. Wood fuel is presented as logs, sawdust, chips, pellets or briquettes. The efficiency of the fuel depends primarily on the amount of carbon, hydrogen, ash and moisture content. Tables 1.2 and 1.3 show the analysis of several fuels as a percentage of dry fuel weight and their calorific value respectively. We can see the difference between hardwood, softwood, agricultural grain, natural gas and fuel oil to compare [31]. Hardwood species are denser than softwood species because the latter content more resins, but the energy content is considered as equal in both kinds. The only main difference is the time taken during natural drying process of wood. The calorific value of anhydrous wood varies between 18.5 to 19 MJ/kg and it is inversely proportional to the amount of water within the wood, as shown in Figure 1.2.

Logs are not the best option for handling or feeding automatic systems because of their dimension. Moreover, its small surface area to volume ratio is not convenient to combustion efficiency. Sawdust is suitable to be processed into pellets or briquettes. Wood pellets and briquettes are made via drying and compressing sawdust, they are manufactured products, meaning dry and size uniform fuel, so their creation process requires a relatively important amount of energy. Their price is higher making them less interesting for large scale systems. By comparing wood logs to wood chips, it is obvious that chips are advantageous in terms of automation. Chips work as an uniform fuel that flows and can be fed into a boiler as a flow, therefore they could be used in automatic systems. With a higher surface area to volume ratio they can also be burned very efficiently [5]. Wood chips normally come from forest thinning, arboricultural trimming, energy cropping or even residues from activities such as furniture creation, they do not need an extra stage process as pellets or briquettes do, and consequently, their price is considerably lower. They are interesting because of its low price and the fact that they normally can be produced directly in the forest and transported to the client. This process requires little energy. It has been proved that the energy consumption to generate renewable

energy from wood chips combustion represents 2% of the total energy recovered. This means that the contribution of fossil fuels during the chain process of the wood to energy industry could be negligible, resulting in a full renewable carbon neutral source. The powerplants that are dedicated to combustion of biomass mostly use wood chips as biofuel [32].

	Maple	Spruce	Corn	No.2 Oil	Natural Gas
Carbon	48.94	51.97	47.63	86.40	71.60
Hydrogen	5.60	5.59	6.66	12.70	23.20
Nitrogen	0.22	0.43	1.46	0	4.30
Sulfur	0.16	0.10	0.11	0.70	0
Oxygen	43.67	41.24	42.69	0.20	0.90
Ash	1.41	0.67	1.45	trace	0

Table 1.2: Comparison of compounds as a percentage of dry fuel weight [31].

	Maple	Spruce	Corn	Fuel Oil	Natural Gas
Calorific Value (Btu/dry pound)	8.350	8.720	8.120	19.590	22.080

Table 1.3: Comparison of calorific value [31].

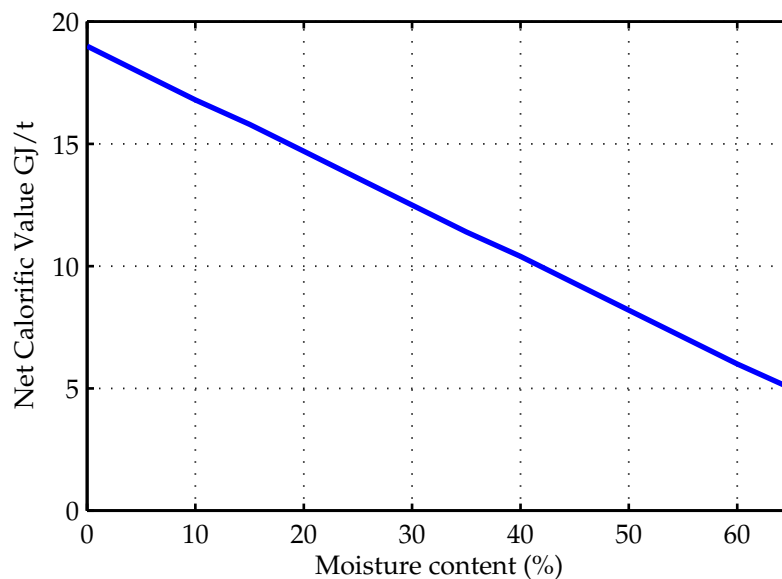


Figure 1.2: Calorific value versus moisture content of the wood [9].

### 1.2.3 Boilers

Nowadays, biomass contribution to primary energy consumption is below to the available possibilities. It mainly consists of burning wood in fireplaces and stoves, often little effective. However, technologies for the use of woody biomass in heating systems have experienced high development in recent years. Modern biomass heating systems basically consist of a biomass

boiler, a space to stock the fuel, a chimney, hydronic systems to distribute the hot water and discharge heating and an outdoor temperature sensor. They have reached levels of efficiency and reliability similar to those of gas or oil boilers, they are fully automatic using low cost fuels that provide ultra low emissions. There are basically three kinds of boilers for wood biomass combustion according to the three main wood fuel categories: wooden blocks, chips and compressed powdered wood (pellets). Combustion of firewood is the most extended way of using biomass in domestic heating. Because of the requirement of a manual feeding, wooden log boilers power is limited to some tens of kilowatt, and they are more suitable for single houses. Pellet and chip boilers are automatic fed systems as fuel behaves as a fluid, their efficiency is comparable to those boilers using gas or petrol. They are normally delivered by large lorries. The fuel stock room must be beside the boiler and preferably underground to ease the loading, it must be protected from water leaks in order not to spoil the biofuel. The fuel is automatically taken from the stock to the boiler where the combustion takes place. Pellets boilers are normally smaller and more simple than chip boilers since the fuel is manufactured, so homogeneous and more expensive. Wood chip boilers use grinded wood of few centimeters size, loaded automatically through feeding systems. These wood chip systems are not limited in size and can reach a heating power of several megawatts. Chipped systems are particularly suitable for heating in buildings of medium or large size, they are normally used in public buildings such as hotels, schools or hospitals. It is very important to ensure that wood chip boilers are supplied with the appropriate type of fuel. This will vary between boiler types and sizes. The two most important variables are the chip size and the average moisture content of the biofuel [33, 34].

#### **1.2.4 Towards a new energy strategy for Europe 2011-2020**

Strong dependence on fossil fuels and inefficient use of raw sources contribute to global warming, turn into high energy prices and threats the economic security. The expansion of the world population and the increase of energy consumption will intensify the damage. Therefore the fight against climate change requires drastic plans. Europe is facing a moment of transformation, the crisis has caused recession and nowadays changes are required. There are very optimistic perspectives for this decade and several goals to achieve. Regarding to energy issues, 2020 promotes more efficient energy resources, more renewable contribution and more economical competitiveness [11]. The "20-20-20" objectives set in the Climate and Energy Package by the European Commission in 2008, represent three key goals that have to be reached by 2020:

- A 20% reduction in emissions of greenhouse gases in the EU, compared to 1990 levels. Trying to reduce them to 30% if conditions are good;

- A 20% increase in participation in the EU energy produced from renewable resources;
- A 20% improvement in energy efficiency in the EU.

Based on these objectives, each country has a national policy to support the energy efficiency and to prevent the climate change. The details for each country are specified in the national action plans for energy efficiency and renewable energy and are defined according to their consumption and resources. Figure 1.3 shows the ratio of renewable energy consumption of each country in 2013, and the ratio that must be reached by 2020. Some of the Northern countries have already developed a competitive structure of renewable sources making easier to reach the goal set by the European Union. Others like France, United Kingdom or Netherlands must double or even triple their renewable consumption in relation to 2011 [35].

Share of energy from renewable sources<sup>6</sup>  
(in % of gross final energy consumption)

	2004	2010	2011	2012	2013	2020 target <sup>5</sup>
EU	8.3	12.5	12.9	14.3	15.0	20
Belgium	1.9	5.7	6.1	7.4	7.9	13
Bulgaria	9.5	14.1	14.3	16.0	19.0	16
Czech Republic	5.9	9.5	9.5	11.4	12.4	13
Denmark	14.5	22.0	23.4	25.6	27.2	30
Germany	5.8	10.4	11.4	12.1	12.4	18
Estonia	18.4	24.6	25.5	25.8	25.6	25
Ireland	2.4	5.6	6.6	7.3	7.8	16
Greece	6.9	9.8	10.9	13.4	15.0	18
Spain	8.3	13.8	13.2	14.3	15.4	20
France	9.4	12.8	11.2	13.6	14.2	23
Croatia	13.2	14.3	15.4	16.8	18.0	20
Italy	5.6	10.5	12.1	15.4	16.7	17
Cyprus	3.1	6.0	6.0	6.8	8.1	13
Latvia	32.8	30.4	33.5	35.8	37.1	40
Lithuania	17.2	19.8	20.2	21.7	23.0	23
Luxembourg	0.9	2.9	2.9	3.1	3.6*	11
Hungary	4.4	8.6	9.1	9.5	9.8	13
Malta	0.1	1.0	1.4	2.7	3.8	10
Netherlands	1.9	3.7	4.3	4.5	4.5	14
Austria	22.7	30.8	30.9	32.1	32.6	34
Poland	6.9	9.2	10.3	10.9	11.3	15
Portugal	19.2	24.2	24.7	25.0	25.7	31
Romania	17.0	23.4	21.4	22.8	23.9	24
Slovenia	16.1	19.3	19.4	20.2	21.5	25
Slovakia	5.7	9.0	10.3	10.4	9.8	14
Finland	29.2	32.5	32.9	34.5	36.8	38
Sweden	38.7	47.2	48.9	51.1	52.1	49
United Kingdom	1.2	3.3	3.8	4.2	5.1	15
Norway	58.1	61.2	64.7	65.9	65.5	67.5

\* Eurostat estimates based on the national data transmission under Regulation (EC) No 1099/2008 on energy statistics.



Figure 1.3: Renewable energy consumption goals by 2020, taken from [35].

The strategy "20-20-20" represents helping the environment, contributing to fight the climate change and create new business and employment opportunities. If EU leads the market of



green technologies, the industrial competitiveness and economical security would be greatly reinforced. Meeting these energy goals could result in creating over 1 million of new jobs and €60 billion investment less in oil and gas imports by 2020, which is key for energy security [36]. They are the first step to a long term goals leading to an environmentally-friendly energy consumption. The European energy security strategy presents long term measures to ensure Europe's security of supply. Reports for EU energy trends to 2030 and 2050 are planned. Higher investment in renewable energies, low carbon technologies and energy efficient are expected. These trends lead to reduce greenhouse gas emissions by 80% to 95% compared to 1990 levels by 2050, as well as to reach 75% consumption from renewable energies. A situation based on sustainable energy consumption is pursued [37].

The forests in Europe represents around 40% of the territory, and continues to grow by 0.4% annually in last decades. Currently, it is used only 60-70% of the annual increment of European forests, so stocks are enlarging. Today, 58% of all wood harvested in Europe is used in carpentry, furniture, paper and pulp. The remaining 42% is used for energy. Currently forest biomass is the most important renewable energy source, representing 50% of total consumption of renewable energy in the EU. So it has an important role to achieve the target of 20% increase in the consumption of renewable energy in the EU. Wood is a natural material and if it comes from sustainable forests it will minimize the effects on the climate. Therefore, Europe needs a well managed and balanced way to run forest industry, covering the demand for wood while protecting biodiversity. There is no common EU forest policy and that is why a new EU strategy for the forestry sector is proposed. This proposal leads to set the forest sector as the main path towards a green economy. So to make the most of sustainable forest ensures a balanced production and consumption of wood, and thus minimizes the impact on the environment [38].

### 1.2.5 French energy policy

France is in the top ten list of countries with higher energy consumption in the world with 253 Mtoe in 2013, 18.4 Mtoe of which are coming from renewable energy sources. The French target is to reach 23% of renewable energy consumption by 2020. Therefore, the annual renewable energy production rate should double from 18.4 Mtoe to 37 Mtoe. Wood for renewable energy and forest policies were not a priority until 2007 when Grenelle environmental forum changed the forest policy, it was turned into a harvesting policy, and higher priority was given to the collection and the use of wood as biomass. There is no target for the production of energy from wood biomass but its demand is expected to highly increase by 2020, therefore most European policies encourage the use of forest biomass for electricity. The last French annual finance law project (2013) has set as main goal the increase of the wood market. Reducing the climate change is the central interest of this forest policy [39].

## 1.3 Industrial process

Wood chips are the most inexpensive form of woody biomass nowadays, and they are used for heating in chip boilers with precise fuel specifications of size and moisture content (MC). They are normally purchased in sawmills using the MAP<sup>5</sup> unity. One net cubic meter of solid wood represents 2.5 MAP, in other words 2.5 m<sup>3</sup> of chipped wood and air. MAP is the french volume terminology and it is translated in english as bulk cubic meter. The large volume of this fuel is a parameter to take into account because it requires a large enough storage site and a monitoring technology suitable for rough conditions.

### 1.3.1 Production chain

Figure 1.4 briefly explains the industrial process, from collection, manufacture and maintenance of wood chips until delivery to the customer.



Figure 1.4: Production chain of wood chips, taken from [40].

After the felling process, the logs recollected can be directly chipped in the forest or transported to a warehouse. Generally in warehouses, logs are left to dry naturally, either inside or outside, sometimes covered by a special tarpaulin. The drying natural process of logs takes in between 4 and 12 months before the chipping, depending on the nature of wood, hardwood is denser so it implies a slower drying. It must be settled in a good open air space location during dry weather season. It must be properly protected during the rainy season. Stacking wood chips in large piles can cause mold, overall in the case of wet chips. This makes the temperature in the middle of the pile to rise, the pile could get on fire when is is very big, that is why piles of

<sup>5</sup>MAP unity means *un metre cube apparent de plaquettes* in french which represents 1 m<sup>3</sup> of wood chips and air.

chips in warehouses are normally limited to 8-10 meters high [41]. The drying natural process can reduce the MC to 25%-30%. In the case of chipping green wood chips directly in the forest, they would have a moisture content of 50%-60%, so that they must be used earlier because they take the risk of being decomposed. However, nowadays some techniques of artificial or forced drying are being considered. Unheated drying air as fans or heated drying air based on solar energy can be used to reduce MC of the fuel, when heat cheap energy is available. The idea is to reduce MC using low energy investment. A lower MC allows a long term storage of chips with little microbial activity, resulting in less losses and more fuel available. It also increases the efficiency of the fuel and reduces its emissions [42, 43]. This technique is not standardized and it is hardly applied.

To produce wood chips, green parts must be left over in the forest. The Figure 1.5 shows a chipping unit, some of them have crane-tip mounted scales that check the quantity of wood that is being harvested. Once the wood is chipped and specified by size and MC, it is kept in warehouses until the moment of the purchase. Then they are priced according to the calorific value offered, and delivered to the client typically in trucks. The particle size distribution of wood chips depends on the type of the chipper. The CEN<sup>6</sup> standard classifies chips in classes: particle classes P16, P45, P63 and P100 have a minimum size of 3.15 mm, and a maximum size respectively of 16 mm, 45 mm, 63 mm and 100 mm. In terms of quality, the commercial classes P16, P45 and P63 describe high grade chips, suitable for the feeding of small domestic boilers. The CEN standard classifies chip moisture content in classes: M20, M30, M40, M55 and M65, indicating the maximum value of moisture content that the fuel has. A fuel delivered under the label M40 means that it represents a moisture content between 30% and 40%. Storage of wood chips is not advisable over M40 due to risk of decomposition. When produced from freshly felled trees, MC can be very high, up to 70%. Larger boilers can burn wet wood chips. Smaller boilers need chips of a moisture content of 30% or less. The CEN standard also classifies wood chips ash content in classes: A0.7, A1.5, A3.0, A6.0 and A10 that indicates the maximum percent of ash content per weight [44].

Forests, handling and storage techniques (see Figure 1.6) through the full industrial chain must meet some minimum quality requirements in order to obtain a final high quality fuel. Different stages as the method to harvest and care of handling the fuel determine the presence of impurities in wood fuel like stones, soil or other materials left over in the forest that can damage a boiler system. A clean fuel and storage room ensures the efficient performance of the system. A well managed industrial process makes easier to get good quality final product, so the process of harvesting must be a controlled standardized process to avoid impurities at all handling stages, from the felling stage until the delivery to the client.

---

<sup>6</sup>European Committee for Standardization.



Figure 1.5: Chipping unit machine taken from [45].

### 1.3.2 Importance of standards

In the late nineties the European Commission gave CEN the mandate to develop standards for solid biofuels to support the energy policy of Europe. With this policy the European Commission set targets to be reached by 2020 to reduce greenhouse gas emission and to become less dependent on oil and gas. The mandate of the European Commission to CEN was to develop quality standards for solid biofuels. The import of biomass in Europe was increasing so the development not only of European standards but also global standards became more and more important. The development of standards for sampling and testing solid biofuels as well as fuel quality assurance is a key element to unblock fuel markets and trans European fuel trade. This contributes to reach the environmental, social and economic goals of the European Commission. The standards are made in response to private or public institutions needs. In this particular case of biofuels, the standards provide an accurate description of the product for both sellers and buyers. Thus, the functioning of the biomass industry gets harmonized and promotes transparency in the market and in the price of biofuel. This provides a better customer-seller relationship. There is a broad spectrum of biomass that can be used for heat energy. The differences are mainly due to different parameters such as moisture content, ash content or kind of chipper size [49]. As a rule, biomass equipment as boilers and fuel chip conveyed systems are designed to operate effectively with a specific fuel [50]. Low quality fuel means inhomogeneous particle size, ash content and MC. A boiler using wood chips with different specifications than those that are required, will reduce efficiency, increase emissions and even get ruined. Some boilers can use a range of fuels, but they may need to be manually re-calibrated to inform the control system about the changes in the fuel properties. Fuel Standards provide then an accurate description of the wood chip fuel physical parameters and performance characteristics. The physical description covers the maximum size and maximum moisture content, origin or ash content, ensuring that the correct wood fuel can be matched to



Figure 1.6: Handling wood chips in the warehouse taken from [46, 47, 48].

the biomass boiler. For example a tonne of chips would be characterized by a label P40-M30-A1.5. These fuel standards describe accurately the product and they are key to give reliability in the purchase. This reassures the user that the biomass fuel is efficient, and that their equipment will operate correctly. Clear biomass standards avoid possible buyer-client misunderstandings, protects both sides and give mutual confidence, making life easier for everyone involved. A large scale standardized approach of quantity and quality monitoring of the wood chip production chain aims to ensure cost-efficient production of wood, high-value fuel and satisfied costumers [51]. In the following paragraphs a more detailed explanation of European standards for biofuel is presented.

### 1.3.3 Standards

The European Committee for Standardization CEN is an association that gathers the National Standardization Bodies of 33 European countries. CEN contributes to the development of European Standards regarding different materials, services and processes [52]. The technical committee CEN/TC 335 Solid biofuels was founded in 2000 within the scope of solid biofuels,

including wood chips. Table 1.4 shows its equivalent nomenclatures corresponding to worldwide, european and national level (France). Regarding to biofuel standards, there were several national standards such as the Austrian ÖNORM M7 133 and the German DIN 66 165 in 2004, but there was no common standard in Europe yet. CEN/TC 335 was then established by the European Commission to develop the relevant European Standards for the market of solid biofuels. Its objectives were: facilitate international trade, supply boiler heating systems and improve the development of agricultural and forest biomass [53]. These specifications have been translated into French experimental standards by *l'Association Française de Normalisation* (AFNOR). CEN/TS for solid biofuels have been upgraded to Euro-Norms as ÖNORM or DIN, and also used as the basis for new ISO standards (ISO/TC 238). Many standards for solid biomass were published or are under construction with the goal of reaching a Standardized fuel quality certificate in Europe. The standards that belong to the committee CEN/TC 335 are mainly focused on three major groups:

- The group of descriptions and definitions where fuel specifications and classes are described;
- The group that determines the different parameters that characterizes the fuel, such as MC, chip size, calorific value or ash content;
- The third group is mostly focused on monitoring through the supply chain [54].



Figure 1.7: Samples of wood chips drying in an oven.

There is no requirement to give a more detailed description of existing standards. However, a brief explanation about the specifications of the standard method to determine the MC in wood chips is presented, giving a general idea of the advantages and disadvantages of it. The standard total moisture reference method belonging to the committee CEN/TC 335 Solid biofuels was last published in 2010 and is implemented since 2004 [14]. This standard method is divided

in three rapports (see Table 1.5) and is applicable to all solid biofuels. The way of determining the MC is taking samples of 300 g of biofuel and drying them in an oven at a temperature of 105° in air atmosphere until the mass remains constant. This process is shown in Figure 1.7. Then the MC is calculated by

$$\text{MC}(\%) = \frac{m_{wet} - m_{dry}}{m_{wet}} \times 100, \quad (1.1)$$

where  $m_{wet}$  corresponds to the actual mass (wood and water) and  $m_{dry}$  corresponds to the mass of the wood as if the fuel were anhydrous. This method does not demand a complex laboratory equipment, it is considered precise and independent from parameters like fuel density or ambient temperature. However, it is neither fast nor representative as it usually takes 24 hours and the MC of the taken sample can vary largely depending on the part of the fuel bulk. The term MC when drying biomass materials can be not entirely truthful because untreated biomass contains amounts of volatile compounds that can be evaporated during the drying process [55].

On worldwide level: International Standardization Organization (ISO)	ISO/TC 238 'Solid Biofuels' Developing International standards
On european level: European Committee for Standardization (CEN)	CEN/TC 335 'Solid Biofuels' Developing European standards
On national level: <i>L'Association française de normalisation</i> (AFNOR)	<i>La Commission de normalisation X34B est le miroir du CEN/TC 335 'Solid Biofuels'</i>

Table 1.4: Standards for solid biofuels.

European standards (EN)		International standards (ISO)	
Physical and mechanical properties		Physical and mechanical properties	
EN 14774-1:2009	Part 1: Total moisture, Reference method	ISO 18134-1	Part 1: Total moisture, Reference method
EN 14774-2:2009	Part 2: Total moisture, Simplified method	ISO 18134-2	Part 2: Total moisture, Simplified method
EN 14774-3:2009	Part 3: Moisture in general analysis sample	ISO 18134-3	Part 3: Moisture in general analysis sample

Table 1.5: Standard correspondence for solid biofuels, determination of moisture content, oven dry method.

# Chapter 2

## Background

---

<b>2.1</b>	<b>Thermogravimetric methods</b>	<b>25</b>
2.1.1	Freeze drying	25
2.1.2	Oven drying	26
2.1.3	Infrared drying	26
2.1.4	Microwave Drying	26
<b>2.2</b>	<b>Analytical methods</b>	<b>27</b>
<b>2.3</b>	<b>Rapid or indirect methods</b>	<b>28</b>
2.3.1	Radiofrequency methods	28
2.3.2	Microwaves methods	29
2.3.3	Electrostatic methods	30
2.3.4	Optical methods	31
2.3.5	Hygrometrical methods	33
2.3.6	Radiometric methods	34
<b>2.4</b>	<b>Synthesis</b>	<b>35</b>

---



Combustion of biomass for heat and energy production is expanding due to the trend of renewable alternatives to fossil fuels. The wood chips, shredded wood of some centimeters, have many advantages for the production of thermal energy. They come from wood that would not be valued otherwise, their production represents 2% of the energy recovered and it is a natural abundant source available that can provide a significant amount of energy supplies of many countries like France. It has been justified that the main goal of European Standards is to harmonize the trade market, improve the quality of the final product as well as the producer-client relationship. Solid biofuels are by nature heterogeneous, they are composed by a mix of different moisture contents (MC), densities and sizes of chips. Since wood chips come mainly from forest thinning and residues from logging operations, their MC varies largely, from around 10% to 60%. Today the commercial value of wood chips depends on the MC. Since it is the most important parameter to determine for optimizing the performance of a power plant. Variation in MC of the fuel affects the combustion process since the water does not take part in the reaction, it just absorbs heat energy as it evaporates. This represents a problem specially for smaller plants whose technical or economical resources are more limited than large ones [56, 57].

The current method, called Oven Dry Method (EN 14774-1:2009) is nowadays the official method to determine MC in wood chips. Some differences in the results of this method have been noticed (<1%), when using several temperatures in the drying process. This happens because of the possible presence of volatile compounds in the fuel, that evaporate when determining the MC in the oven [58]. This method is viable since it does not require complex equipment, and it is accurate and independent of parameters such as room temperature or fuel density. The fact remains that it is not rapid and does not offer a representative value of MC of a large amount of heterogeneous fuel, since just several small samples are taken to be dried [59, 55]. Owing to these issues, a continual research on new technologies more suitable to the industrial requirements is carried out.

In this chapter several technologies to determine the MC of wood chips are presented, some of which have been already turned into commercialized products, and others have not been tested owing to complex performance requirements or no reasonable cost limits. Technologies for fuel characterization reported in the literature can basically be separated in two major groups: Direct measurement methods that refer to measuring exactly the fuel itself and indirect measurement methods that are based on determining MC from other parameters. Thermogravimetric and analytical methods are direct methods while electrical, optical, radiometric, hygrometric and acoustical are indirect methods [56].

## 2.1 Thermogravimetric methods

The thermogravimetric methods are based on the weight loss determination after a drying process. The sample must be weighed before and after the drying process finishes. The quantity of water is established between the initial weight of the material and its weight after it has been dried. The end of the drying process is achieved when weight losses do no longer vary. These methods are based on oven drying, freeze drying, infrared drying and microwaves drying. They are reliable but relatively slow, from 10 minutes (microwaves drying) to several days (freeze drying). The lower the temperature the longer the time required, however the evaporation of volatile compounds is reduced. All thermogravimetric methods operate destructively.

### 2.1.1 Freeze drying

This technique is mostly used in alimentary industry, the absence of liquid water and the low temperatures required results in less deterioration of the product so it gives a final product of better quality when compare with oven drying method. Despite of these advantages, freeze-drying is seen as the most expensive process of drying [60]. It consists on freezing the sample at  $-20\text{ }^{\circ}\text{C}$  which then is dried into a vacuum chamber at ambient air temperature during several days. When applying freeze and oven drying on wood chips, the resulting MC is slightly lower if using freeze drying due to the absence of volatile non-water compounds [58]. Figure 2.1 presents a commercialized model of freeze dryer (Christ ALpha 1-2 LD Freeze dryer) whose ice condenser capacity is 2.5 kg and operating temperature down to  $-55^{\circ}\text{C}$ . This process lasts 24 hours for drying a 2-kg sample. There is a wide range of size capacity available [61].



Figure 2.1: Christ ALpha 1-2 LD Freeze dryer, taken from [61].

### 2.1.2 Oven drying

This standard method, EN 14774-1:2009 or ISO/CD 18134-1, is applicable to all solid biofuels. The way of determining the MC is taking a sample of biofuel of about 300 g and drying it in an oven at a temperature of 105°C in air atmosphere until the mass remains constant. This process usually takes 24 hours. Figure 2.2 shows a typical oven applied to the standard method EN 14774-1:2009 or ISO/CD 18134-1. Its use is common in industry and science since provides a precise drying performance. This specific model (Universal Oven UN55plus) works for a temperature range from 5°C above ambient up to 300°C, it holds a 53-L volume and 80-kg maximum loading. Temperature, air flap position and time can be programmed [62].



Figure 2.2: Universal Oven UN55plus, taken from [62].

### 2.1.3 Infrared drying

Infrared driers are designed for industrial and professional sectors. They are scale driers that determine the weight while drying. Humidity can be quickly and accurately detected in many different materials such as: powder materials, food, pallets or wood chips. The samples are small, less than 60 g and the time required for wood chips drying is between 7 to 48 minutes [56]. Figure 2.3 presents a moisture analyzer balance based on infrared drying, this model (Infrared Moisture Analyzer MA35M-000115V1) is a simple model that measures samples up to 35 g with 1 mg resolution [63].

### 2.1.4 Microwave Drying

They are scale driers, like the infrared driers. Unlike conventional oven drying, microwave drying yields accurate results in less than 20 minutes, making it ideal for process control [56]. Figure 2.4 gives a moisture content measurement device based on microwave radiation. Its range of moisture is from 0% to 100% with a 0.2 % bias [64].



Figure 2.3: Infrared Moisture Analyzer MA35M-000115V1 taken from [63].



Figure 2.4: Moisture Analyser PCE-MWM 300 taken from [64].

## 2.2 Analytical methods

Contrary to thermogravimetric methods, analytical methods take the possible volatile compounds lost into account. Avoiding the combustion of treated or impregnated material, analytical methods are chemical methods based on the mixture of the fuel with a chemical element. Azeotropic distillation with water immiscible solvents like toluene or xylene are used to determine MC in lignocellulosic biomass. Water distills with the solvent and after condensation, these get separated so the quantity of water can be determined [65]. Xylene distillation experiments were performed in reference [58] and compared to results obtained by the standard oven method. The deviation in the results are explained by the amounts of volatile compounds released in the drying method. Karl Fisher method is also used in the determination of MC in wood, dry methanol displaces the water in the sample. Afterward, the water is titrated via the Karl Fisher method. This method is neither affected by possible volatile compounds. Automated Karl fisher titrators are commercially available and they offer excellent measuring accuracy. Figure 2.5 introduces this technology. It can either be used as stand-alone titrator or integrated into an overarching network. The Karl Fisher Titrand family of titrators includes

a variety of coulometric, volumetric, and combined titrators, enabling to analyze any water content from 0.001 to 100% [66].



Figure 2.5: KF Titrator: Metrohm's instrument, taken from [66].

## 2.3 Rapid or indirect methods

The increasing use of wood chips as fuel implies more bulk MC measurements, which are nowadays based on the time-consuming standard methods. Deliveries and contractor numbers are growing rapidly, expecting accurate delivery control for the bulk fuel. In order to be able to apply feed forward control, moisture content for chips bulk or flow should be measured automatically and online. The importance of saving time and obtaining information on the MC prior to incineration is the main motivation for using rapid test methods for moisture determination. Rapid measurements of the MC are based on using electrical, optical, radiometric or hygrometric methods.

### 2.3.1 Radiofrequency methods

The dielectric properties of the material depend on its physical properties, especially MC. This fact is utilized in microwave and RF measurements [67]. The term radiofrequency RF theoretically represents electromagnetic waves of frequencies between 3 Hz and 300 GHz. However the term microwaves is commonly used for frequencies between 1 GHz and 300 GHz. So radiofrequency refers here to frequencies lower than around 1 GHz.

RF and microwave methods can use the attenuation, phase shift, or resonance sensors for moisture metering. The most common way is to use absorption, that is, energy attenuation. Measurement results depend on the sample temperature, which can be easily compensated for. It is also necessary to know the sample density or to measure a certain fixed dimensions of a sample. If the material changes, a new calibration will be applied respectively. An electrical system for MC determination is basically a personal computer, a network analyzer and two antennas. An electromagnetic field is transmitted and its phase shift and attenuation are calculated. Calibrations are needed because density, temperature and mass affect the signals.

A RF method based on reflection technology to determine MC in large samples of biofuels is based on the attenuation shift in frequency and time domain. This technique is studied in reference [68]. The proposed method is a small scale version of an application for large volumes of biofuel in a container. The idea is to measure the reflection energy from the material under test with a RF antenna placed above the container that holds the sample. Two 57-cm diameter and 85-cm height barrels made of steel were joint, simulating a waveguide with a short circuit at the end. The upper barrel holds the RF antenna and absorbent material, and the bottom barrel contents the sample, sawdust in this case. Results show that attenuation is higher for higher MC in the frequency domain until 800 MHz. The time delay of the pulse between 310 MHz and 1300 MHz does not change with MC but the amplitude does, the reflection from the surface of the material and from the bottom of the barrel are clearly differentiated. In fact, it is demonstrated that the higher the MC, the stronger the reflection from the surface and the weaker the reflection from the bottom. Calibration is necessary in this method to avoid interferences. The adaptation of this technology to a real application would turn into a giant waveguide, that might be not quite practical for the wood industry requirements.

### 2.3.2 Microwaves methods

The basis for microwave measurements is similar to RF. But microwaves are more suited for flow measurements due to their lower penetration depth. Methods based on microwaves transmission technology are reported in literature [69, 70]. The attenuation and shift phase of an electromagnetic signal are studied to determine the moisture content of a solid sample of timber. A transmitter and receiver placed at each side of the sample, are used to study the transmitted signal. The density of the material under test is a very important parameter when using microwaves techniques because it influences the measurement of the MC. It has been demonstrated that a moisture measurement of timber independent of the density can be achieved by measuring two microwave parameters. Methods based on this idea are reported in literature [71]. They are based on measuring attenuation and phase shifts of a transmitted signal at a

single frequency, on measuring changes of attenuation and phase shifts versus frequency or on measuring two phase shifts at two different frequencies. The latter method is reported as the more accurate because attenuation can be a complex parameter to study due to the multiple reflection, however this phenomena influence less the phase measurement.

In reference [72] a method for MC determination of bulk wheat grain is based on a rectangular waveguide at 1.5 GHz. Firstly, a sample of 40 g of the material is compressed into a semi solid block. The scattering parameters are measured in the waveguide and the complex permittivity is determined. Results show that real and imaginary part of the permittivity are strongly dependent on MC and independent on the compression forced applied. MC between 5% and 18% were tested. This method can be a basis for a robust MC technique of larger samples for granular materials. Reference [73] proposes a method for simultaneous measurements of density and MC by measuring dielectric properties in static samples of wheat. The method assures to be also valid for other particular materials and the possibility to be applied in real time on-line measurements applications.

It is also possible to perform measurements in time domain. Electrical time domain is a technique based on dielectric property behavior in time-varying electric field. These variations are used to determine permittivity or electrical conductivity. The main application is the determination of MC in porous materials. This technique was first applied in wood in 1996. It measures the MC of a sample via measuring the time needed for an electromagnetic pulse to travel forth and back through the sample [74].

The basis of MC determination using microwave technology is the relaxation of the molecules of water present at high frequency. The higher the frequency, more changes in the investigated parameters. The properties of dielectric materials are determined by its permittivity. Transmission or reflection sensors investigate these parameters. However the highest sensitivity is achieved by resonator sensors. Using this technique, the sensor is in contact with the material under test, therefore the field penetrates the material up to certain depth. Since the global permittivity is a function of water content, dry matter and air, the resonance frequency and quality factor of the sensor change according to the dielectric constant and the loss factor, respectively. Coaxial and planar resonators at microwave frequencies are used to study MC in soil or granular materials such sand in [75, 76, 77].

### 2.3.3 Electrostatic methods

One of the earliest applications was to correlate electrical resistance or conductance of the material under test and its MC. For dielectric devices it has been seen that the density of the fuel

affects the measurement so, calibrations for several types of fuel should be considered [59]. A capacitive sensing method is studied in [78]. A robust vessel made of printed circuit board (PCB) material and open at the top is filled by wood pellets. There are several electrodes in a vessel (20 cm × 15 cm); either three pairs of electrodes located on one wall of the vessel, or one pair of electrodes located in both parallel walls of the vessel. A temperature calibration is needed. Results show that larger gap between receiver and transmitter (parallel electrodes) is better than small gaps for heterogeneous material such as pellets. Measurements are less sensitive to grain direction and bulk density in this case, therefore capacitive measurements show higher reproducibility for the parallel geometry. Methods based on studying conductance or capacitance are very extended in lumber industry but they often require a superficial measurement. FMG 3000 is a commercial device based on capacitive technology, it is presented in Figure 2.6, its weight is 12 kg, it measures a range between 0% and 55% MC samples of 60-L volume [79].



Figure 2.6: FMG 3000 - Moisture meter taken from [79].

There are many probes based on static measurements [80]. Wood moisture meter PCE-HMM is a device to determine moisture and temperature of chips. It is presented in Figure 2.7 (left) and it is available in four different lengths of measuring probe: 25 cm, 50 cm, 100 cm or 270 cm. The measuring range of the moisture meter covers from 9% to 50% and a temperature range of  $-10^{\circ}\text{C}$  to  $+100^{\circ}\text{C}$ . Another device called Meter GMH 3830 and based on resistive technology is shown in Figure 2.7 (right). There is always few centimeters penetration in these devices.

### 2.3.4 Optical methods

Infrared-reflectometric method is based on electromagnetic energy being absorbed by the sample when this one is reached by light. This light consists of two kinds of waves that are applied through the fuel. One of them at a frequency able to get the maximum absorption by free water, and a second one at a frequency hardly absorbed by water or by any other component of the





Figure 2.7: Moisture meter PCE-HMM (left) and moisture meter GMH 3830 (right), both taken from [80].

sample. The relation between the intensity of both kind of reflected waves determine the MC of the fuel. The Near-infrared radiation (NIR) method (Mesa MM710) was tested and it is advisable to apply individual calibration function for different bulk densities [59]. NIR, penetrates further into the sample than IR (a few millimeters) and is therefore more suitable for biofuel. Both IR and NIR are surface measurement methods and can only be used on biofuel conveyed on a belt in a full scale application. These methods only study the surface, so the density of the sample is therefore not relevant. NIR is seen as the most promising method to be used in a continuous flow of wood chips. Compensation for frozen water and surrounding light can be applied using multivariate calibration and especially Partial Least Squares (PLS) [57]. Products based on Infrared-reflectometric method are commercially available [81, 82]. NIR spectrometer (Series KJT70) for moisture determination in process applications and the humidity analyzer (GRECON IR 5000) are both devices designed for belt applications based on infrared radiation, see Figure 2.8 and 2.9.



Figure 2.8: Optical Spectrometer Series KJT70, taken from [81].



Figure 2.9: Grecon IR 5000, taken from [82].

### 2.3.5 Hygrometrical methods

In the field of moisture measuring, there are two kinds of moisture. The absolute moisture of the material, in this case wood, that indicates the percentage of water content referred to the dry mass. And the relative equilibrium moisture content that indicates the relative moisture of the ambient air counterbalancing the material, in this latter case, the material does not absorb or release any moisture. Air humidity balance method is based on the property of wood of absorbing or releasing water from or to the atmosphere (hygroscopic properties) [83]. When the atmosphere and the material present the same water vapor pressure inside a container, this means that the sample is under constant conditions. As the equilibrium air humidity is a function of the MC of the sample and the temperature, MC can be determined via studying these two parameters. In spite of the accuracy of the humidity balance method, it is not applicable for wood chips because it reaches precision up to 14% MC (wet base) [56]. Sven Hermansson presents the option of determining the MC of wood chips via measuring the oxygen and moisture content of the flue gases inside a furnace. The furnace must be equipped with flue-gas condenser. Relative humidity sensors can be used in gases up to 200°C, qualifying the method for this application. Results indicate that the method can predict changes in MC. By knowing the fluctuations in fuel on-line, parameters of the furnace can be regulated to ensure good performance, but it has been found that the accuracy of the sensor deteriorates with the presence of water. Condensation phenomena influences the relative humidity measurement so that this method just allows measurements of wood chips with very low MC [84].

Measurements of wood chips based on flue-gas in Sweden consist of determining efficiency via several measurements (inlet air, water steam to the air and combustion, flue-gas) after the combustion chamber and outdoors [57]. Commercialized products based on this technology are available [85]. Figure 2.10 presents an example of humimeter for 12-L sample volume. It covers a range from 5% to 70% water content and its resolution is up to 0.1% water content.



Figure 2.10: Humimeter BMA, taken from [85].

### 2.3.6 Radiometric methods

A technique that uses dual X-ray radiation on wood chips was performed in Sweden, using frozen and non frozen spruce and pine that are the main species in the region. The method consists on X-raying a sample inside a 3-L vessel at two different photon energies. Both energies are attenuated through the sample. A detector registers this attenuation at two frequencies that are correlated with the effective atomic number of the material under test, the latter is dependent on the quantity of water within the sample. Results show that there is no difference between frozen or unfrozen water, and that better results are obtained when using calibration models developed for a single specie rather than for both [86].

Nuclear magnetic resonant method senses the quantity of hydrogen in the material under test. Hydrogen atoms align themselves in a magnetic field and can be excited with the application of a certain electromagnetic wave. This excitation is registered with NMR spectroscopy. Lawrence Berkeley National Laboratory developed a MC measurement that consists of a permanent magnet, this include an enclosure where the material under test is measured. A solenoidal coil was wrapped around the sample tube, neither the sample tube nor the RF coil influence the NMR signal. Temperature changes affect the field, so this studies are performed into a temperature-controlled box. The magnet dimensions are 32 cm×28 cm×19 cm, its mass is about 68 kg and the magnetic field applied is 0.47 T. Tests performed in several samples of wood chips show that this method is as accurate as the standard method. It takes just a few seconds and it differentiates between liquid water and frozen water, which can be very exploitable for the forestry industry. The questionable issue is if this technology is cost effective [87].

Neutron activation analysis (NAA) is a nuclear process, the sample is radiated with a source of neutrons, resulting in gamma-ray emissions from the material under test. This chemical separation of elements allows the determination of the composition of the material. This technique is normally used to analyze elements in small concentrations. Neutron moisture measures are

also used to determine moisture dependent factors in several industrial processes [88]. The basis is that the neutron parameters vary according to the quantity of hydrogen concentration in the material under test, that is to say, the water content volume. The probe presented is assumed to be located in an homogeneous and constant density material and is formed by an internal neutron source and a line detector for thermal neutrons. Calibration for bulk density is applied. Results show that the probe is sensitive to the water, overall when the source is closer to the detector.

## 2.4 Synthesis

It is obvious why time-consuming thermogravimetric methods are not suitable for the wood-to-energy industry requirements. They are very slow when an automatic measure is essential. Moreover they take small samples to give a MC value. The analytical methods are less time-consuming but also suffer from the same limitation. Unlike these direct methods, the indirect or rapid determination methods operate non-destructively, and the results are available within seconds or minutes. Several of the methods presented are not technically or economically suitable, or they are simply not commercially available for rapid testing.

The infrared-reflectometric can be independent of the density of the material since it is basically affected by the surface. However, the capacitive, microwave and time-domain reflectometry (TDR) sensors are influenced by this parameter up to 5% to the total variation [56]. Both infrared (IR) and near infrared (NIR) are surface measurement methods and can only be used on biofuel conveyed on a belt in a full scale application. Microwaves have a penetration depth of approximately 15 cm and are more suitable also for small samples or a conveyor belt application. Radiofrequency (RF) has a larger penetration depth than microwaves and is suitable for measurements of large sample volumes. More research in this area is expected in the future [57]. Multicalibration is required because the density, mass and temperature of the material affect the signals. Hygrometric method is rather slow for the expectations of real applications, it takes more than 15 minutes. There is no evidence about nuclear magnetic resonance (NMR) being good as a research field for MC determination [57]. Although NMR can measure MC and locates where the water is in the sample, it is a high cost technology. It is not a suitable method, either because the measurement time is too long for use in on line applications or because the dimensions of the device would be extremely big for the sample size under test [87]. Neutron activation analysis (NAA) could be adapted to a real applications but it presents disadvantages regarding security of users.

A lot of research in this field has been going on in recent years because of the importance of the biomass in the production of heating. Many patents have been filled in to protect convenient

technological instruments for this industry in the last decades. Instruments to determine humidity on a stream of wood chips based on RF and NIR have been patented [89, 90], as well as devices for humidity determination in bulk small samples, based on waveguides [91, 92], transmission technologies [93], dual X-ray and gamma radiation [94, 95] or freezing drying [96].

According to the literature NIR is a promising measuring method to be used in a continuous flow, and RF is the most promising method for the measurement of the MC of bulks of biofuel, due to its ability to measure large samples [59, 57].

Now that moisture is known as the first parameter of the quality of wood chips, its determination currently becomes difficult for the wood energy industry because the technologies available on the market are not accurate or too restrictive. A rapid and accurate evaluation of the MC is required by a cost effective technology. None of the methods applied nowadays is convenient for the requirements of the wood-to-energy industry. The project MOQAPRO presents as a goal to track the quality and quantity of wood chips during the production chain. This tracking involves measurements of the mass, volume and MC of the fuel at every stage of the production chain, which implies adapting technology to rough site conditions. This thesis is specifically focused on providing automatic and economical frequent MC bulk measurements, for big volumes. In view of this literature, the most promising technologies involve capacitive, resistive, and radiofrequency methods. All are tough technologies and penetrate in the material, being less dependable on the changeable conditions that affect the surface, such as climate, natural evaporation or condensation. They must be applied on line and provide a good sensitivity on site. They do not require either too large or too expensive devices. Therefore, an electromagnetic technology is supposed to be studied to determine the moisture content of big volumes of wood chips (several cubic meter). On the basis of the above, this thesis is focused on RF measurements.

# Chapter 3

## Contactless electromagnetic technologies

---

<b>3.1</b>	<b>Preliminary physical background</b>	<b>38</b>
3.1.1	Wood chip dielectric properties	38
3.1.2	Electromagnetic propagation	40
<b>3.2</b>	<b>Transmission-Reflection system</b>	<b>41</b>
3.2.1	Experimental prototype	42
3.2.2	Optical module	43
3.2.3	Electromagnetic module	50
<b>3.3</b>	<b>Conclusions</b>	<b>58</b>

---

In this chapter a remote technique to determine the moisture content (MC) of large samples of wood chips is presented. The electromagnetic theoretical basis are explained. The description, design and experimental setup of a laboratory-scale prototype are exposed as well as its possible application to the industry.

## 3.1 Preliminary physical background

### 3.1.1 Wood chip dielectric properties

Wood is a polar dielectric. Its relative permittivity strongly changes in the presence of water. Molecules of water generally present a random orientation. However, when an electric field is applied, the molecules orient themselves according to the direction of the field [97]. The dielectric properties of a material result from its response under the influence of an electric field and can be expressed by its permittivity  $\epsilon = \epsilon_0 \times \epsilon_r$ , where the permittivity of the vacuum  $\epsilon_0$ , is a constant and only depends on the units used. In the general case  $\epsilon_r$  is a complex number which depends on the angular frequency  $\omega$  as it follows

$$\epsilon_r(\omega) = \epsilon_r'(\omega) - i\epsilon_r''(\omega), \quad (3.1)$$

where the real part  $\epsilon_r'$ , known as the dielectric constant, expresses the ability of the material to store energy and the imaginary part  $\epsilon_r''$ , known as the dielectric loss factor, is a measure of the energy absorbed from the applied field. The symbol  $i$  referred to as the square root of  $-1$ . Similar expressions exist for the magnetic properties of the material. However, the relative magnetic permeability  $\mu_r$  is usually equal to 1 for most materials except for ferromagnetic materials such as iron, cobalt and nickel. The relative permeability  $\mu_r$  is therefore equal to 1 in the context of MC estimation. The dielectric properties of a media are dependent on its density, temperature and the frequency of the electric field.

Wood chips are a material formed by wood, air and water, the wood relative permittivity  $\epsilon_{wood}$  varies between 1.6 and 2.6 and the one of air is approximately 1. This dielectric constant changes hardly with frequency or temperature as seen in Figure 3.1a. Water has a high dielectric constant compared to other materials and the MC of a material therefore influences its dielectric properties to an appreciable degree. Water dielectric constant  $\epsilon_r'$  is around 80 at frequencies between 500 MHz and 2 GHz, for temperatures ranging from 1.5°C to 45°C, as illustrated in Figure 3.1b. Therefore, the global permittivity of a material composed by air, wood and water strongly varies with the presence of water. Whole trees, branch wood or logging residues are mechanically grinded by a grinder machine in order to create wood chips. Due to this variety

of sources, the MC range value can be wide. A pile of dry wood would be around 25%, and a pile of wood recently extracted could reach up to 60% MC. In the range of MC involved in this system, the effect of temperature or grain direction on the dielectric properties of the wood is rather small when compared to the influence of the water content [98].

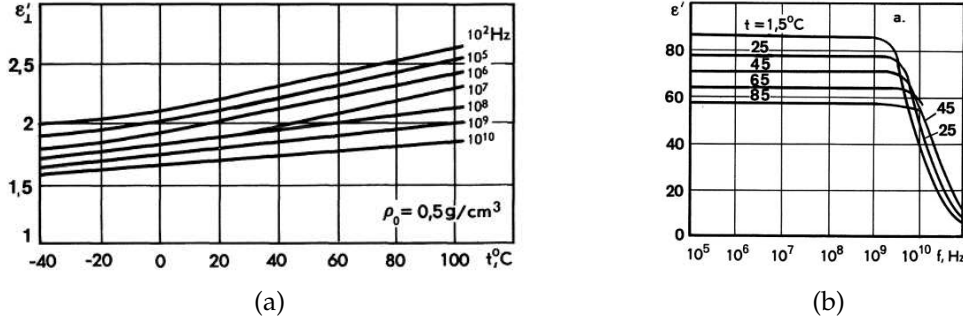


Figure 3.1: (a) Dependence of the dielectric constant of oven-dry wood on the temperature. (b) Dependence of the dielectric properties of free water on frequency, both taken from [98].

The MC of wood chips is defined in this thesis by

$$\text{MC}(\%) = \frac{m_{\text{water}}}{m_{\text{wet}}} \times 100 = \frac{m_{\text{water}}}{m_{\text{water}} + m_{\text{dry}}} \times 100 = \frac{m_{\text{wet}} - m_{\text{dry}}}{m_{\text{wet}}} \times 100. \quad (3.2)$$

It varies largely from around 20% to 50%, where  $m_{\text{wet}}$  represents the mass of the wet sample,  $m_{\text{dry}}$  the mass of dry wood and  $m_{\text{water}}$  the mass of water within the sample. The electric properties of wood can be defined by polarization process. Polarization is caused by the change in the arrangement of electrically charged particles of wood in space, under the influence of an electromagnetic field. The influence of the magnetic field is negligible but the electric field strongly affects the material. The polarization  $\vec{P}$  effect is characterized by

$$\vec{P} = \chi \epsilon_0 \vec{E} = (\epsilon'_r - 1) \epsilon_0 \vec{E}, \quad (3.3)$$

where  $\chi$  is the susceptibility of the material, in other words, the ability of a material to polarize in an electric field. The polarization effect is composed by the contribution of several polarization phenomena: electronic polarization, ionic (atomic) polarization, dipole (orientation) polarization, interfacial (structural) polarization and electrolytic polarization. Depending on the electric field frequency, dipole (orientation) polarization and interfacial (structural) polarization are the most noticeable for frequencies between  $10^5$  Hz and  $10^{10}$  Hz.



### 3.1.2 Electromagnetic propagation

Microwaves correspond in the electromagnetic spectrum, illustrated in Figure 3.2, to frequencies between 1 GHz to 300 GHz. Microwave radiation itself is non-ionizing radiation, distinctly different from ionizing radiation such as X rays and gamma rays. Some similarities with visible light are that they may be reflected or absorbed by a material, they may be transmitted through materials, and they experience a direction change when traveling from one material to another. The penetration depth can be small, so the refraction of the wave at the interfaces and the heat dissipation in the vicinity are phenomena to take into account. Although plane wave is an abstract concept, it is very useful because any radiated electric field can be considered as a superposition of plane waves [99]. In a loss media the propagation constant  $\gamma$  is

$$\gamma = i\omega\sqrt{\epsilon\mu} \text{ with } \epsilon = \epsilon' + i\epsilon'' \text{ thus } \gamma = \pm i\omega\sqrt{(\epsilon' + i\epsilon'')\mu} = \alpha + i\beta, \quad (3.4)$$

where  $\alpha$  is its real part and is called the attenuation constant,  $\beta$  is its imaginary part and is called the phase constant. The propagation of an electromagnetic wave results in a field which amplitude is

$$E = E_0e^{i\omega t - \gamma x} = E_0e^{-\alpha x}e^{i(\omega t - \beta x)}. \quad (3.5)$$

It represents an exponentially attenuated pseudo-periodic wave. The factor  $e^{-\alpha x}$  represents a damping in the direction of the propagation of the wave, this results in a damped plane wave which velocity is  $v = dx/dt = \omega/\beta = 1/\sqrt{\epsilon\mu}$  [100].

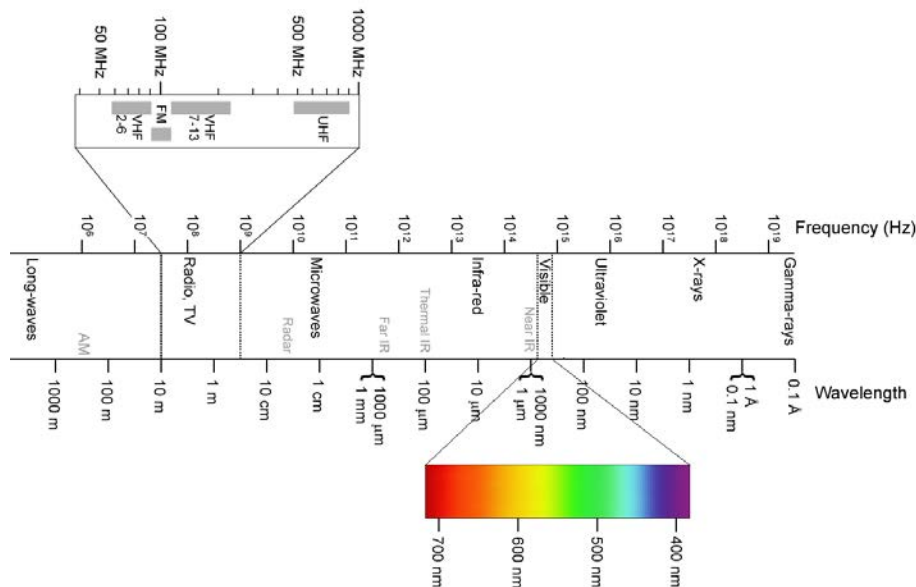


Figure 3.2: Electromagnetic spectrum, taken from [101].

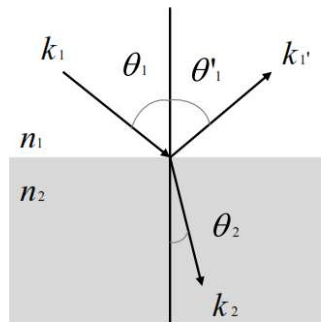


Figure 3.3: Snell-Descartes Principle.

When an electromagnetic wave is incident on the surface of a medium with dielectric properties different from those of the medium in which the wave originates, part of the incident energy is reflected and part is transmitted with an attenuation and phase shift. Figure 3.3 presents the Snell-Descartes principle. In the case of wood chips, the material under test is heterogeneous formed by wood, water and air. Electromagnetic propagation through wood chips involves therefore many complicated physical phenomena. The process includes multiple reflections and refractions, absorption of the electromagnetic energy, transport of the generated heat, dimension changes of the wood, phase changes in the water or transport of the water through the wood material. In order to control this process one needs to understand the various phenomena involved. This understanding is achieved by experimental measurements.

## 3.2 Transmission-Reflection system

The experimental part consists of a system with two modules, a transmitter (TX) and a receiver (RX), both above the sample, as sketched in Figure 3.4. A combination of different measurement techniques is applied in order to determine several parameters: the relief of the chips and content of water. An optical imaging module is used to determine the relief of the surface of chips, which is very relevant because this can play an important role in the waves reflections. An electromagnetic module is used to determine the content of water in the wood that is considered as an homogeneous material, the power reflected by the wood is analyzed in order to get the attenuation and phase, which are strongly related with the relative permittivity of the dielectric. This system should work at microwaves frequencies and must be independent of the thickness of the sample. In this research, the study of the reflected power by the material under test is analyzed on frequency and time domains.

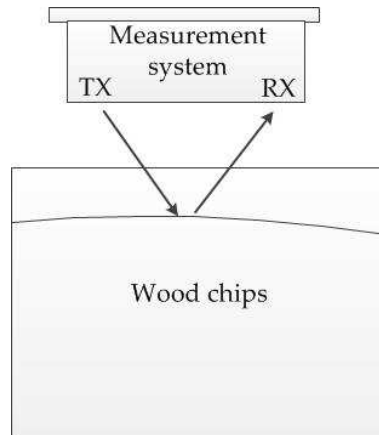


Figure 3.4: Principle of the transmission-reflection system.

### 3.2.1 Experimental prototype

The idea is to simulate a real scale gantry that holds a measurement system composed by an optical module and an electromagnetic module. It would be located over the weighbridge of a powerplant. In general, when a truck arrives to the powerplant, it is weighted in a weighbridge to check the coming stock, as shown in Figure 3.5. A mobile gantry holding the measurement system can probe and record all along the surface of the container. This allows the study of the relief of surface and the study of the reflected electromagnetic energy by the material. This information can therefore provide a MC value of a large volume of biofuel. This method is fast and easily conceivable for real application.



Figure 3.5: Weighbridge in a powerplant.

The experimental part is based on a small-scale system for bulk measurements of wood chips, presented in Figure 3.6. The contribution of the thesis is a small scale version of what could

be applied in arriving fuel containers to powerplants, to optimize the industrial process. The structure is composed of two different parts, a fixed inferior section and the crossbar that holds the measurement system. The inferior part is a fixed shell with an electronic weighbridge that supports the container and calculates its weight. Its two superior transversal bars hold the crossbar that supports the measurement system. The crossbar can be moved horizontally and vertically if necessary. The woods chips are stored in the container that simulates the truck. This laboratory-scale system is used for instrumentation purpose, keeping in mind the restrictions of the industrial application.

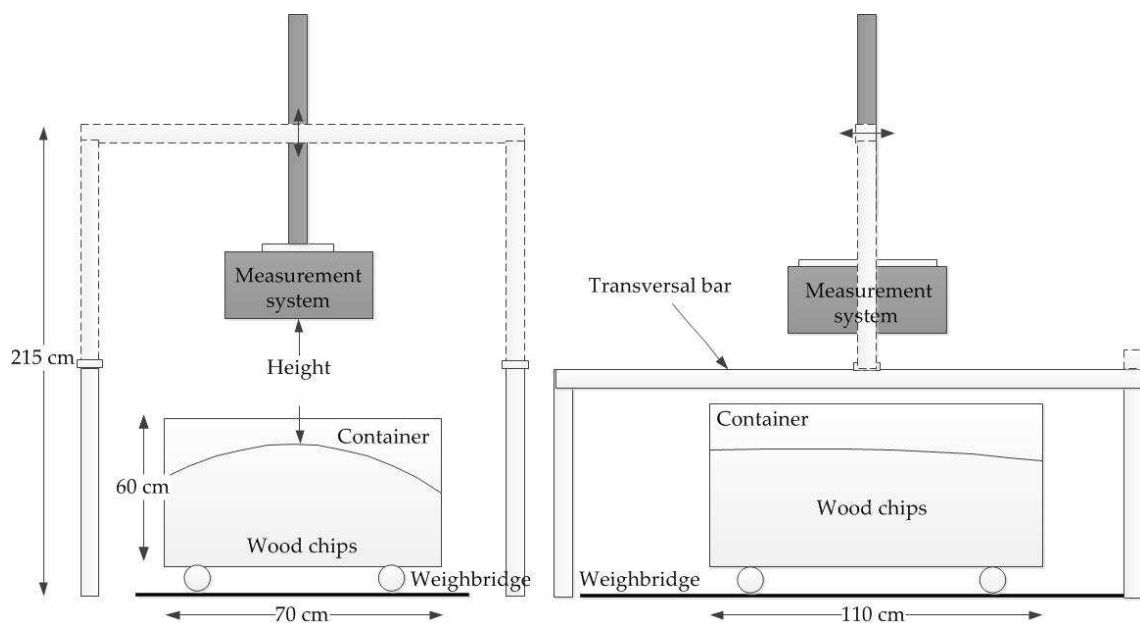


Figure 3.6: Laboratory-scale system.

### 3.2.2 Optical module

There are several ways for measuring the shape of a surface [102, 103]. Since wood chips can be considered as a textured material that is to say a non-uniform material, stereo matching is a good and economical compromise.

#### 3.2.2.1 Stereo vision method

Computer stereo vision is the creation of a 3D image from at least two digital 2D images, such as obtained by a CCD<sup>1</sup> camera. By comparing images of an object from two vantage points, a 3D

<sup>1</sup>Charge-Coupled Device.

rendering can be formulated by determining the relative positions of the object from two angles. By comparing these two images, the relative depth information can be obtained [104, 105]. A stereo vision system is used in order to analyze the shape of the pile of chips. Figure 3.7a details a stereo vision system in which the stereo cameras have left and right image planes, they have the same focal length  $f$  and their optical axes are parallel and perpendicular to the image planes. The distance between the cameras  $\Delta x$ . An object in a 3D space is projected onto the image planes. The object is located at the distance  $D$  from the image planes and is projected at the position  $x_L$  on the left image and at  $x_R$  on the right. The difference between  $x_L$  and  $x_R$  refers to an offset between the two images, this offset referred to as disparity is measured in pixels. The relative depth information can be obtained by

$$\frac{D+f}{a} = \frac{f}{x_R} \quad \text{and} \quad \frac{D+f}{b} = \frac{f}{x_L} \quad \text{thus} \quad a = \frac{D+f}{f}x_R \quad \text{and} \quad b = \frac{D+f}{f}x_L,$$

$$\text{and since } \Delta x = a + b = \frac{D+f}{f}(x_R + x_L) \quad \text{one has } D+f = \frac{\Delta x \times f}{x_R + x_L},$$

$$\text{therefore } D = \left( \frac{\Delta x}{x_R + x_L} - 1 \right) \times f. \quad (3.6)$$

Figure 3.7 shows the CAMHED3DCAM stereo webcam (Heden brand) that has been used for testing the measurement concept. The distance between the lenses is 3.948 cm. The images taken by this stereo camera are gif animated image format, so Matlab<sup>®</sup> Image Acquisition Toolbox was installed in order to extract a single image of  $480 \times 640$  pixels from a prerecorded video stream.

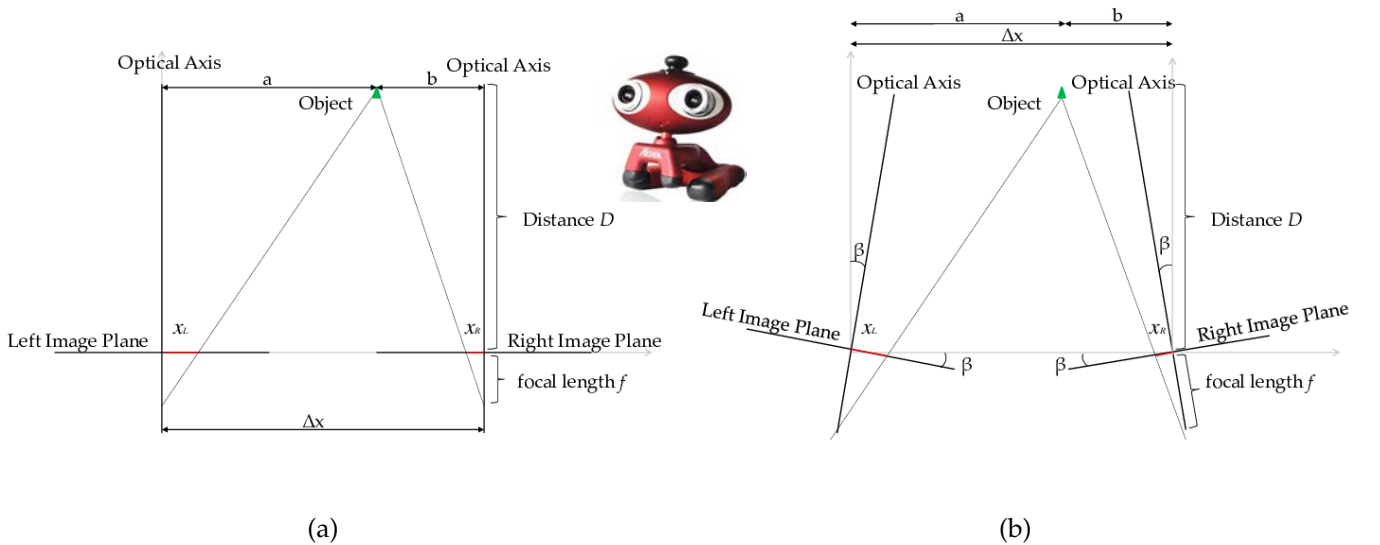


Figure 3.7: (a) Stereo vision system with parallel axes. (b) Stereo vision system with no-parallel axes. The photography shows the stereo vision camera used (taken from [106]).

As a proof of concept, a small quantity of chips are taken in order to perform the first measurements and results. Both cameras, parallel and placed horizontally to one another are used to obtain two different views of the sample, in a similar manner to human binocular vision, as illustrated in Figures 3.8 and 3.9. A disparity is observed between the two images. The relation between the disparity of two images is reported as a function of the distance between the object and the camera. This is the stereo vision principle.



Figure 3.8: Photography of the experiment.

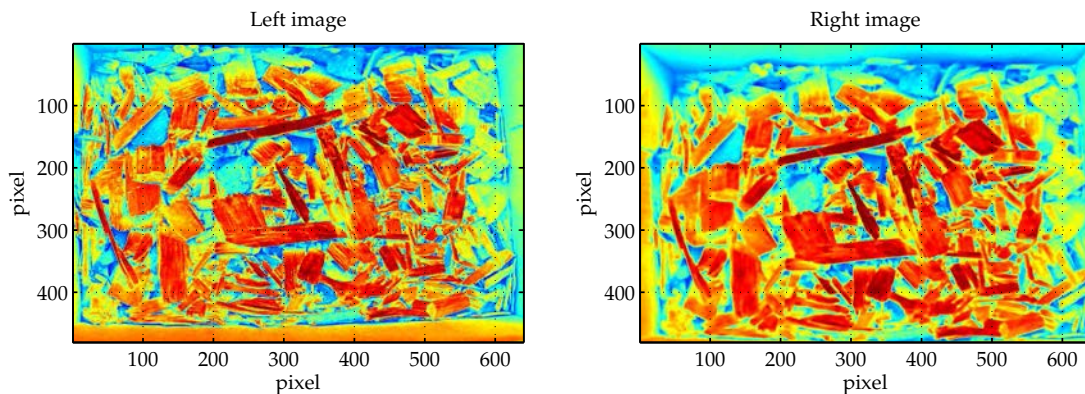


Figure 3.9: Left and right image taken by the camera.

Theoretically both cameras should present the same image when the distance between camera and object tends to infinite. Experimentally however, the cameras used are not perfectly lined up, that is to say that they are not parallel. The offset of the two images therefore is not zero at the infinite but at a certain distance from the camera. The distance at which camera axes intersect is obtained as 286 mm, which means there is a  $7.9^\circ$  deviation between the axes. Therefore, it is necessary to modify the stereo vision distance estimation presented in (Equation 3.6) and to correct the parameters of the camera in order to simulate the ideal situation. In other words, in order to simulate the cameras parallel and therefore to achieve the correct height at every

target point. For that purpose (Equation 3.6) becomes:

$$D = \frac{\Delta x(\cos 2\beta(x_L x_R - f^2) + f(x_R + x_L)\sin 2\beta - x_L x_R - f^2)}{2\sin(2\beta)(x_L x_R - f^2) - 2f\cos(2\beta)(x_R + x_L)} + \frac{2f^2\cos(\beta)(x_R + x_L) - 4f\sin(\beta)x_L x_R}{2\sin(2\beta)(x_L x_R - f^2) - 2f\cos(2\beta)(x_R + x_L)}, \quad (3.7)$$

where the deviation of each axis is an angle  $\beta$ , as illustrated in Figure 3.7b.

### 3.2.2.2 Stereo matching process

The Stereo matching process consists of identifying specified target points of an object on a pair of left and right images. Their disparity value between each image is used to obtain a 3D coordinate calculation. The correlation of digital images is a method for measuring the disparity between the two images. The correlation (also referred to as matching) between two images  $im_L$  and  $im_R$  is called cross-correlation and is defined as

$$im_L(x, y) * im_R(x, y) = \iint im_L(x', y') im_R(x' + x, y' + y) dx' dy'. \quad (3.8)$$

It is a standard approach to feature detection and it is used as a measure for the degree of similarity calculation between two images. In the case of discrete function one has

$$im_L(m, n) * im_R(m, n) = \sum_p \sum_q im_L(p, q) im_R(p + m, q + n). \quad (3.9)$$

The correlation algorithms use images as gray-scale matrices as input. Since the disparity depends on the position of the image, one of the images is decomposed in a series of small images. Having the small images in the reference image a correlation is made with the other image in order to find the best correspondence. The peak of the cross-correlation occurs where the right and left images are best correlated and it is called the match, or target point. Because all the correlations would take a long time and since disparity does not change a lot between images, a rough correlation is made first with an area corresponding to half the image in order to find a rough disparity  $(\Delta x, \Delta y)$ . Then the correlation is made between the reference image at position  $(x, y)$  and a few shifts  $(S_x, S_y)$  in the other image at the position  $(x + \Delta x + S_x, y + \Delta y + S_y)$ . This speeds up the calculation. The size of the chips is also considered in this program to optimize the size of the small reference images. Figure 3.10 presents the left and right images that take part in the cross-correlation.

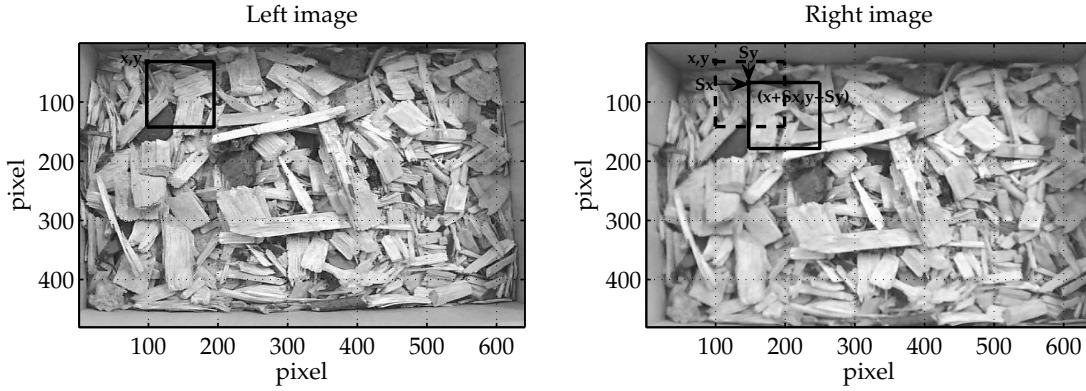


Figure 3.10: Correlation between the two images.

### 3.2.2.3 3D reconstruction

Once the object is targeted and the stereo matching operation is completed, the object depth can be estimated for 3D coordinate calculation by the (Equation 3.7). Figure 3.11 shows the trigonometric explanation for 3D reconstruction using an tilted Stereo Vision cameras, each with an angle  $\beta$ , and having a half field of view (FOV)  $\theta$ . The distance between the cameras  $\Delta x$ , distances  $x_R$  and  $x_L$  have however to be estimated from the disparity expressed in pixel. Only the disparity in the  $x$ -axis is taken into account. The actual axis of the cameras seems to be relatively well aligned compared to the angle. The object is seen by the left camera at the angle  $\varphi_L$  from the camera axis and it is seen by the right camera at an angle  $\varphi_R$  from the camera axis. If  $2Pix$  represent the width of the image and  $n_L$  and  $n_R$  the position of the object in the left and right images respectively, the

$$\frac{n_L}{Pix} = \frac{\tan \varphi_L}{\tan \theta} \quad \text{and} \quad \frac{n_R}{Pix} = \frac{\tan \varphi_R}{\tan \theta} \quad (3.10)$$

In addition, it can be seen from Figure 3.11 that

$$D \tan(\varphi_L + \beta) + D \tan(\varphi_R + \beta) = \Delta x, \quad (3.11)$$

thus

$$D = \frac{\Delta x}{\tan(\varphi_L + \beta) + \tan(\varphi_R + \beta)}. \quad (3.12)$$

Both tangents can be estimated with the (Equation 3.7)

$$\tan(\varphi_L + \beta) = \frac{n_L \tan \theta + Pix \tan \beta}{Pix - n_L \tan \beta \tan \theta} \quad \text{and} \quad \tan(\varphi_R + \beta) = \frac{n_R \tan \theta + Pix \tan \beta}{Pix - n_R \tan \beta \tan \theta}. \quad (3.13)$$



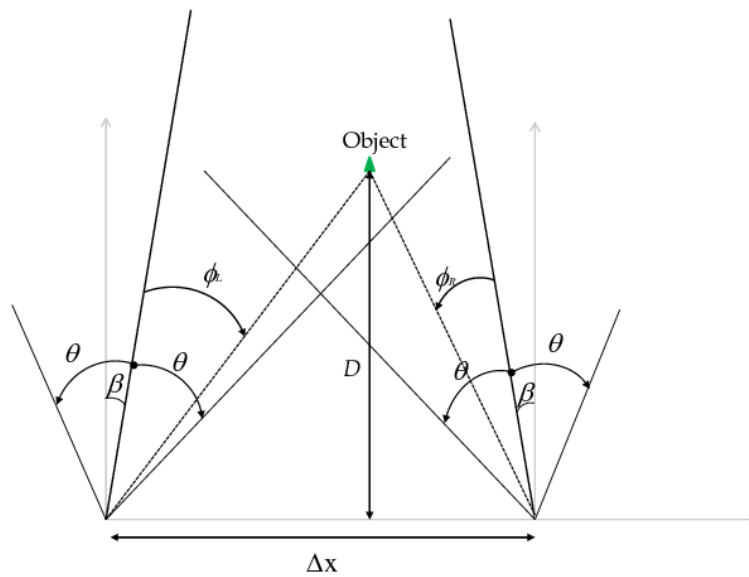


Figure 3.11: Theoretical 3D reconstruction.

#### 3.2.2.4 Experimental results and discussion

Figure 3.12 shows the experimental setup. The distance between the camera plane and the base of the box containing the wood chips is 22 cm. The pile of chips is around 7 cm high at the peak. The images are acquired via a Heden Stereo Vision camera. The images have been taken as to include both detailed and non-detailed regions, as illustrated in Figure 3.13.



Figure 3.12: Experiment.

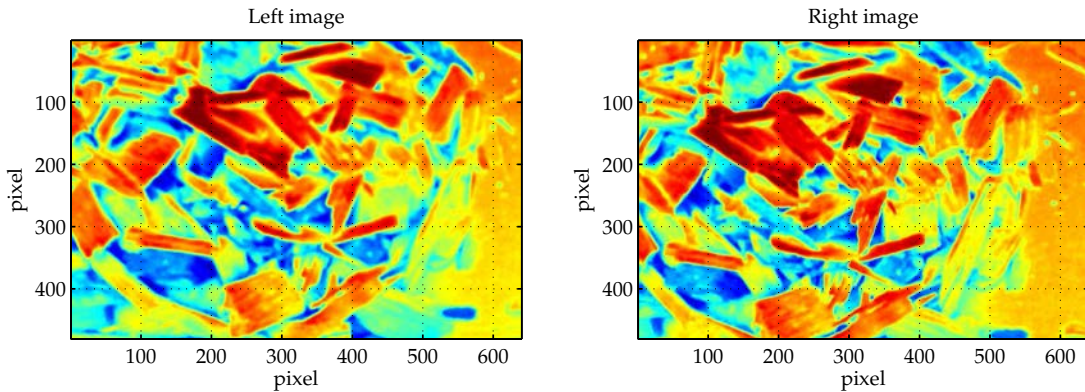


Figure 3.13: Images taken by the stereo vision camera in this experiment.

Figure 3.14a shows the matrix that contains the calculated distance between every target points of the object and the camera plane. The lowest distance between the camera and wood chips in this experiment is to around 15 cm. It can be noticed that this distance is well estimated. Figure 3.14b is analogous to Figure 3.14a but it shows the distance from the bottom of the pile of chips. Most of the chips are located in the left part of the image. In the part of the image that shows a lack of chips the calculated distance has not been taken into account because there is no sufficient correlation to estimate a disparity. In order to detect such situation automatically, the curvature of the correlation peak have been taken into account. The higher the peak, the higher the curvature and thus the better the matching confidence.

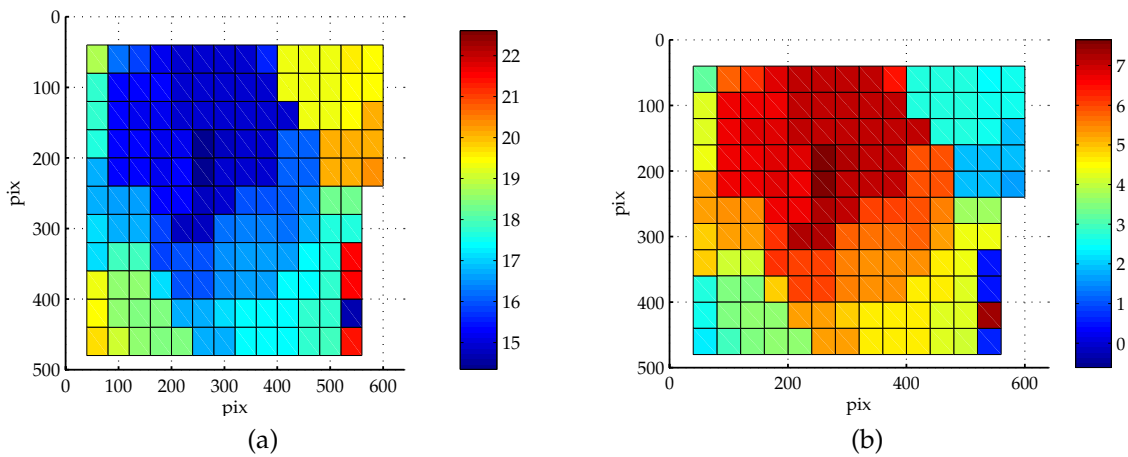


Figure 3.14: (a) Distance  $D$  from the pile to the camera. (b) Height of the pile of chips.

The values of the peak of the correlation functions differ a lot depending which target areas are being correlated. The right parts of the images show a lack of chips, so the curvature value is very low, an average value around 1. This means that the correlation function is basically flat because there are several target areas that share the same similarity. This implies a high probability of error when time comes to choose the peak of the correlation function. The average value of the peaks in the regions full of wood chips is in the order of  $10^2$ . Depending

on the values of the curvature, a minimum curvature value must be determined from which the system can be considered as reliable. Below that value the data would be omitted. That is why no correlation is presented in Figures 3.14a and 3.14b in that region. Also, an error of the algorithm in the right part of the region is observed caused by a flat correlation function. Notice that either the error or the absence of correlation is equivalent to no wood chips since the particularity of wood chips is that it gives high contrast image, and thus good correlation peaks.

### 3.2.3 Electromagnetic module

#### 3.2.3.1 Material

To determine the water content, an electromagnetic module is applied. The power reflected by the wood is analyzed in order to get the attenuation and phase, which are strongly related with the relative permittivity of the wood chips. The antenna chosen as the transmitter is a Double Ridged Waveguide MODEL 3115 operating from 1 GHz to 16 GHz. The antenna chosen for the reception is a Log periodic antenna EM-6952, operating in the frequency range from 1 GHz to 18 GHz. Figure 3.15 shows both antennas respectively.



Figure 3.15: Transmission and reflection antennas.

The reflection coefficient  $\Gamma$  between the antennas after the reflection on the wood chips is measured using a 8722ES Vector Network Analyzer (VNA) calibrated with the 85033E Mechanical Calibration Kit, 3.5 mm, from Agilent Technologies. The frequency range of the VNA is from 500 MHz to 40 GHz, and the kit is specified from DC to 9 GHz. The VNA is used via a GPIB<sup>2</sup> port in order to control the experiment and data acquisition from a Matlab<sup>®</sup> program. For that

---

<sup>2</sup>General Purpose Interface Bus.

purpose , the compact National Instruments GPIB-USB-B able to control up to 14 programmable GPIB instruments has been used.

Plastic containers with dimensions 120 cm×80 cm×70 cm are used to hold the samples. Oak chips whose size is P100 are humidified manually to reach different moisture content values. The weights of the dry samples are approximately 60 kg. Different quantities of water are added to each container, the samples are stirred regularly in order to absorb the water and get an homogeneous wet material. Table 3.1 shows the resulting samples, referring just to the weight of chips. Using the electronic weight T3200P model from PMC-MILLIOT the weight of an empty container and wheels is 67.5 kg.

	Container 1	Container 2	Container 3
Wet sample (kg)	81.5	99.5	108.5
Dry sample (kg)	59.5	66.5	64
MC (%)	27	33	41

Table 3.1: Information of the samples.

### 3.2.3.2 Procedure

A bistatic configuration using two antennas is preferred than a monostatic configuration to get rid of the non perfect matching of the antenna in the measuring range. The reflection from the wood chips is indeed small and could be not visible in the reflection from the antenna. It has also been verified that measurements at frequencies above 2 GHz are strongly influenced by the position of the wood chips, giving no reproducible results. In order to avoid interferences, the frequency must be chosen according to farfield or footprint limitations, as well as wood chips and structure scale dimensions. Therefore, two antennas, a transmitter and a receiver have been used to emit a sweep of frequencies below 2 GHz. An absorbent material is located between both antennas in order to avoid the direct cross talk. In order to estimate the penetration of electromagnetic waves in wood chips, a metallic plate has been buried at different depths in the container, from 0 cm to 51 cm. Wood chips are 21% MC and the reflection coefficient signal  $\Gamma$  corresponding to the reflection on the wood chips has been measured from 500 MHz to 2 GHz. This is illustrated in Figure 3.16. It can be noticed from the Graph 3.17 that the metallic plate can be detected when the thickness of the sample is smaller than 35 cm . The curve that represents the sample of thickness 25 cm of wood chips clearly behaves differently at frequencies under 1.3 GHz, however a similar response is obtained when the depth of the material under test is up to 35 cm.

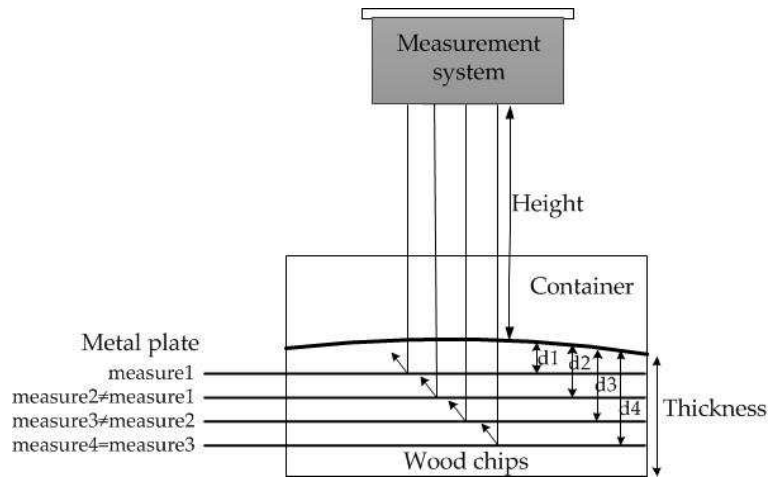


Figure 3.16: Determination of the penetration depth.

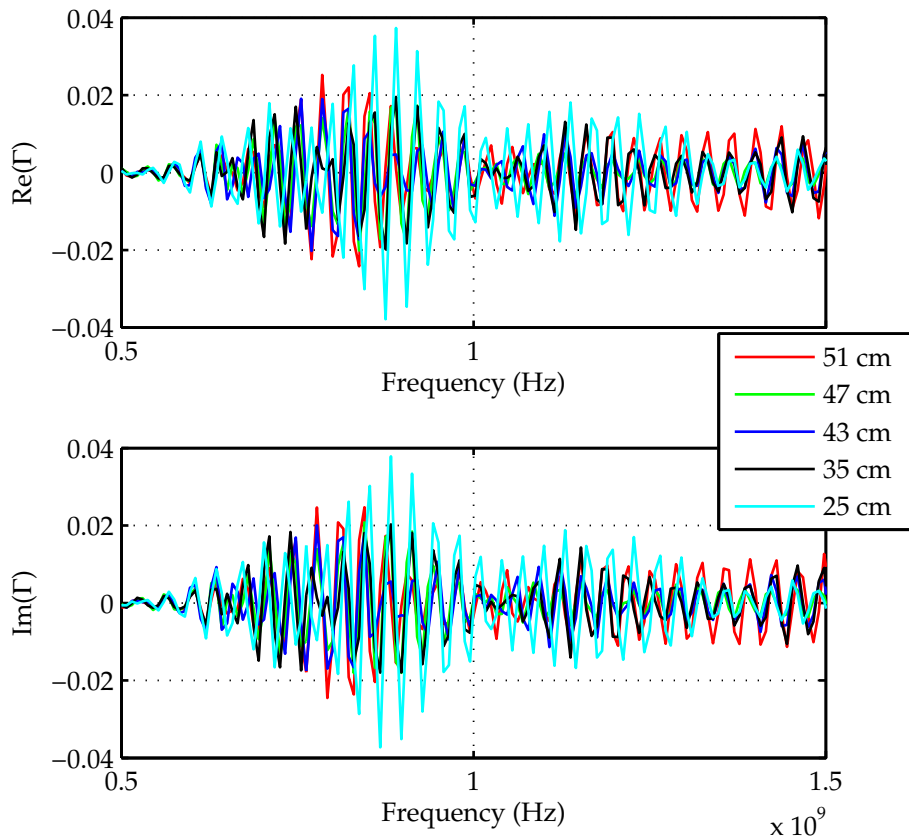


Figure 3.17: Real and imaginary part of the reflection coefficient  $\Gamma$ .

The influence of the MC has been tested with 3 containers filled with wood chips at different MC values, this makes it possible to test the samples exactly in the same environment and conditions. In addition, 6 different heights of the antennas in order to evaluate the influence of that parameter have been tested. The measurement system is shown in Figure 3.18.



Figure 3.18: Antennas at several heights.

The reflection coefficient  $\Gamma$  is measured for three samples of oak at different MC values, 27%, 33% and 41%. The thickness of the samples are 36 cm to make sure the signal is not affected by other material than wood chips. Every MC measurement has been performed four times, modifying the arrangement of the wood chips between measurements.

### 3.2.3.3 Direct frequency domain analysis

Figure 3.19 shows the module of the reflection coefficient  $\Gamma$  at three different MC values when the antennas and the surface are separated by two distances, 41 cm and 56 cm. The chosen range frequency is from 500 MHz to 2 GHz but reproducible measurements are not observed above 1 GHz. No common patterns have been found for the different heights. It is clear that the contribution of MC to  $\Gamma$  is not obvious. Although the pattern are totally different for each distance from wood chips to the antennas, each MC gives very close values of  $\Gamma$  whatever the wood chips arrangement. Reflection phenomena yields a very complex signal since it depends not only on MC but also slightly on the relief of the surface and on the entire environment through the room. Moreover, wood chips is a granular material which implies the diffusion phenomenon. Therefore, the reflection phenomenon can be observed as a superposition of many reflected waves on the surface and many retrodiffused waves. The reflection on the surface increases with MC while the retrodiffused waves from the inner of the wood chip pile decreases. This combination leads to a very complex reflection phenomenon.

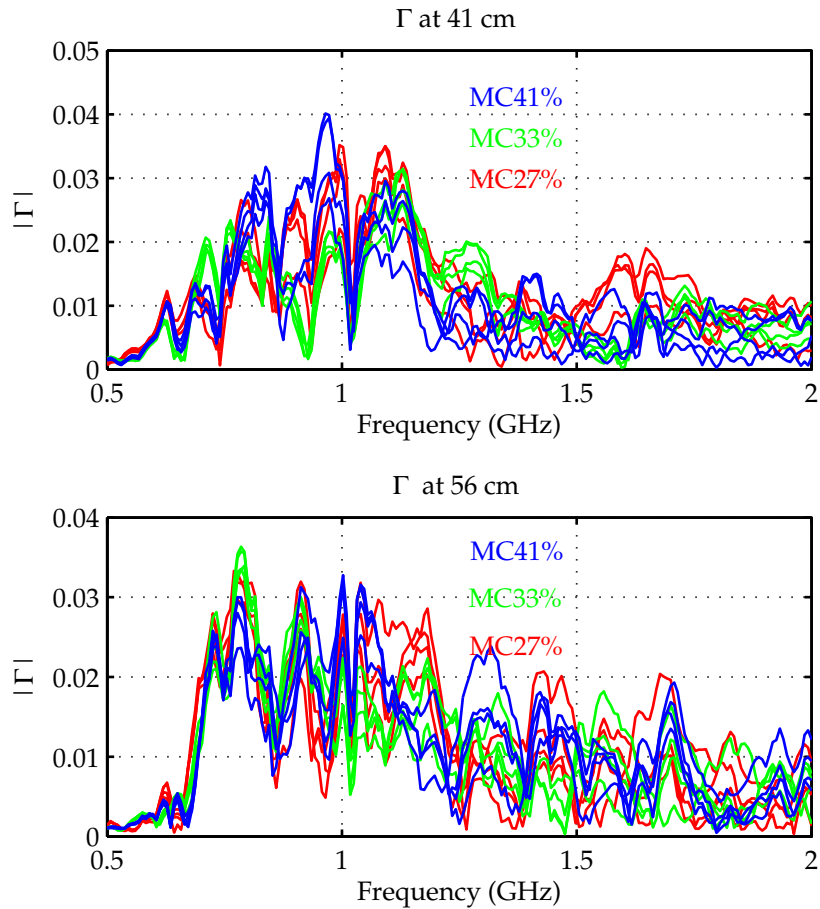


Figure 3.19:  $\Gamma$  for three different MC at two different heights: 41 cm (top) and 56 cm (bottom).

The current identified phenomena do not allow to draw more conclusions on this analysis approach.

### 3.2.3.4 Direct time domain analysis

In order to separate the different contribution in the signal a time domain analysis is carried out instead of a frequency domain analysis. Before presenting measurements in time domain using 8722ES Vector Network Analyzer, a brief explanation of this mode is necessary. To study the transmission and reflection phenomena in time domain,  $50 \Omega$  loads and coaxial cables as transmission lines are used. Propagation velocity in these lines is  $2 \times 10^8$  m/s. If the line is 2 meters long the time required by the wave generated by the source to travel in the line is 10 ns. As a simple representation, two coaxial cables are used, one of 1-m long (5 ns) representing the reflection by the surface of the material, and another of 2-m long corresponding to the reflection after penetration inside the sample. Figure 3.20 shows an illustration of the experiment and

results. The Graph shows the coefficient  $S_{21}$  measured by the VNA. The two contributions are clearly visible in the signal, one at 5 ns and another at 10 ns.

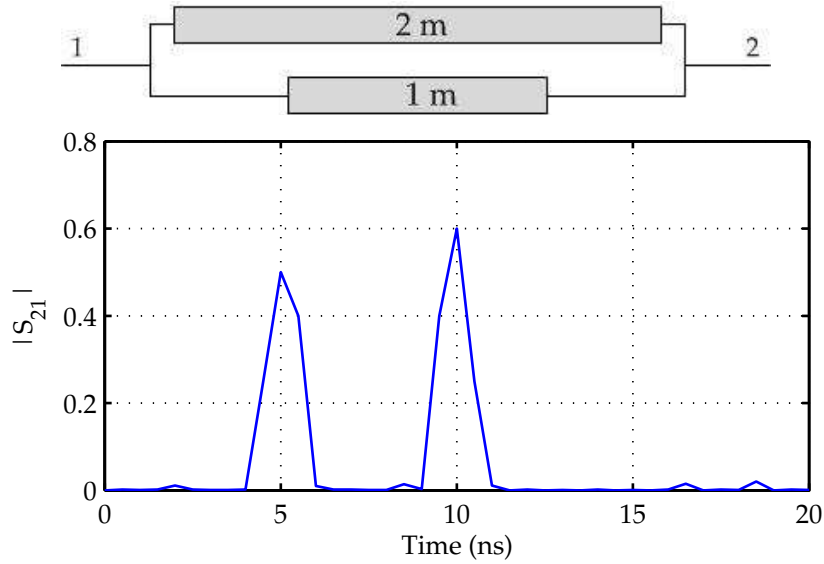


Figure 3.20: Schema-principle time domain analysis

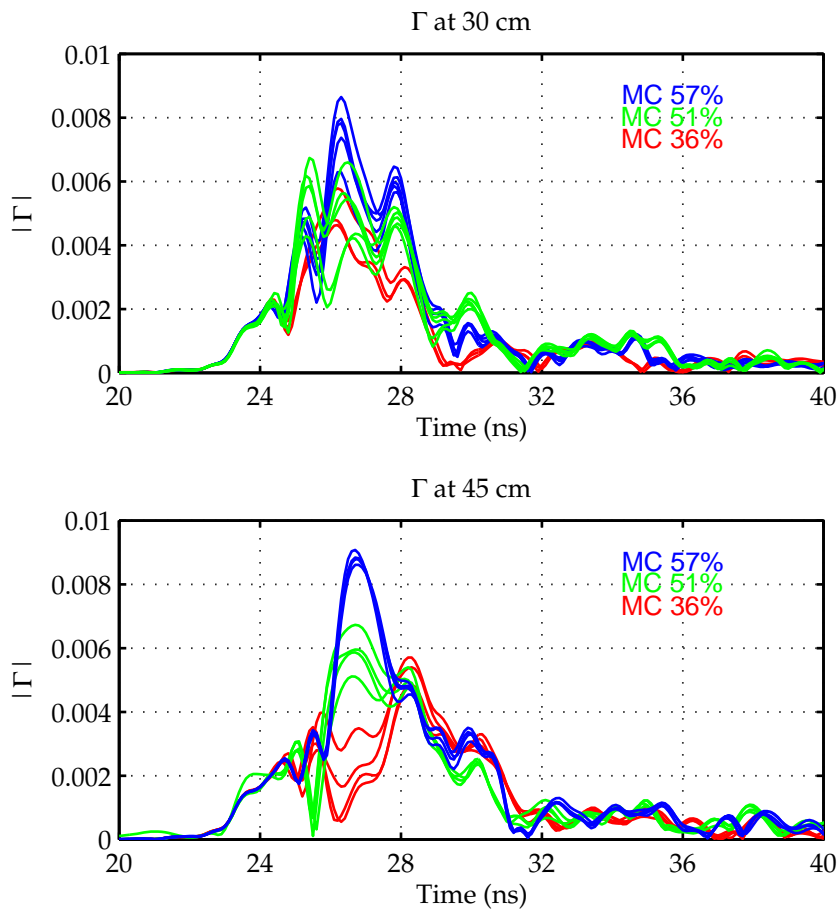


Figure 3.21: Comparison of MC time domain at different heights. (a) 30 cm. (b) 40cm.



The time domain analysis can thus separate the time at which the reflection is generated. In the case of wood chips, it is interesting to separate the signal of the retrodiffusion from the signal of the surface. Several samples of different MC are evaluated at different heights of the antennas, analogous to the frequency domain experiment. Three samples of oak P100 chips at 36%, 51% and 57% MC have been analyzed four times each, changing the arrangement of the chips between measurements. Preliminary results are encouraging since the amplitude of the reflection coefficient  $\Gamma$  seems to change according to the MC of the sample. Figure 3.21 shows the reflection coefficient  $\Gamma$  when the antennas are separated from the sample by 30 cm and 45 cm, this implies a time shift of 1 ns. Therefore both images must be compared taking this time shift into account. No correlated results can be found. It is clear that the reflection coefficient  $\Gamma$  behaves differently depending on the distance between the sample and the antennas.

It can be noticed that the same order can be found around 28 ns in Figure 3.21(a) and 26.5 ns in Figure 3.21(b) respectively, in these regions the reflection coefficient seems to be proportional to the value of MC. This is however by chance since (a) correspond to antennas closer to the wood chips than (b). As a consequence the same location would have been earlier instead. The fact that the response of the system changes in relation to the distance of the antennas presents several disadvantages. Even if the optical module estimates the relief of the pile and the distance from it to the antennas, the accuracy may not be enough for assuring a reliable measurement of MC.

### 3.2.3.5 Multivariate analysis

There is much mixed information in the measured signals. Multivariate analysis allows to find relationships in this information. Learning machine methods are promising techniques for the design of box models. These methods are significantly helpful if measurements are available and the variable to predict is not supported by a clear physical principle or a knowledge based model, which is clearly the case. Therefore it is interesting to process the measurements performed in the frequency domain with, for instance, the Support Vector Machine (SVM) technique [107]. In this particular case the 3 piles of chips at different MC presented in subsection 3.2.3.3 are used. As a reminder, the following paragraph summarizes the experimental setup.

For each of these piles, see Table 3.2, 4 measurements of the reflection coefficient  $\Gamma$  with different arrangements of chips are available for 201 different frequencies between 500 MHz and 2 GHz. These experiments are repeated six times at different distances  $d$  from the antennas to the surface of the pile of chips, 31 cm, 36 cm, 41 cm, 46 cm, 51 cm and 56 cm. Therefore there are 24 measurements of the reflection coefficient  $\Gamma$  for each container, that is to say, for each MC.

	Container 1	Container 2	Container 3
Wet sample (kg)	81.5	99.5	108.5
Dry sample (kg)	59.5	66.5	64
MC (%)	27	33	41

Table 3.2: Information of the samples.

There are not enough containers with different values of MC to create a MC prediction model. Therefore, regression can not be implemented. However, data separation can be implemented as a 3-class problem using Support Vector Machines. Thus, linear classifiers have been designed in the laboratory by a postdoc researcher<sup>3</sup> with machine learning skills [108]. Input variables are ranked and selected using the Recursive Feature Elimination (SVM-RFE) technique [109, 107]. Since 3 different values of MC are available, 3 classes are considered. The one-vs-one classification approach is preferred. Thus, for a  $n$ -class problem,  $n(n-1)/2$  linear SVM classifiers are implemented. Each implementation designs a 2-class classifier which compares 2 classes at the time. In our study three different implementations are made to compare the three MC under test. The problem takes into account 202 available features, 201 frequencies and the distance  $d$ . The process of 2-class separation by linear SVM tries to find an optimal separation between the two classes in the input variables space (202 dimensions in this case because it is the number of available features). The SVM-RFE method proceeds iteratively to rank these features according to their relevance. A validation procedure is commonly implemented to select the classifier that achieves the best generalization capabilities [110]. In our study a 2-fold cross validation method has been implemented. The achieved classifiers require limited computational power therefore they can be involved in real-time industrial applications.

Table 3.3 shows the recognition rates for the three pairwise comparisons. The results are promising since for a given sample (container 1, 2 or 3, see Table 3.2), the method predicts the container which it belongs with 95.83% probability. The global recognition rate is calculated using a decision rule based on the most attributed class by the three classifiers. It is observed that the relevant features selected by the SVM-RFE method are 12, 6 and 12 for the three implementations respectively. It is also important to notice that the distance from the antennas to the surface of the pile  $d$  has never been selected as a relevant feature by the SVM-RFE method. This means that  $d$  is redundant in this analysis.

---

<sup>3</sup>Hela Daassi-Gnaba.

Classes (containers)	Linear SVM	
	Recognition rate	Number of relevant features
MC1 versus MC2	91.7%	12/202
MC1 versus MC3	100%	6/202
MC2 versus MC3	100%	12/202
Global recognition rate: 95.83%		

Table 3.3: Recognition rates.

### 3.3 Conclusions

In this chapter a contactless measurement system to determine the moisture content (MC) of wood chips has been proposed. This method can be automatic and therefore easily applicable to the industry. It consists of a crossbar holding the measurement equipment that probes all the upper part of an industrial container. The measurement equipment is based on two modules, an optical module to study the shape of the pile and an electromagnetic system at microwave frequencies that study the reflected energy by the material, the latter being related to the permittivity of the material and therefore to its MC. An optical module based on a stereo vision system has been presented. This module provides the relief of the surface of a pile of wood chips. This parameter is very significant in order to be able to study more accurately the reflected energy by the material. Thus, this system proposes a MC prediction based on the knowledge of this two parameters, relief of the pile and reflected energy by this one. Various analysis have been studied. Either time domain and frequency domain analysis give not satisfactory results due to many uncontrolled parameters taken into account in the signal.

A statistical analysis has also been applied reaching a degree of recognition of 95.8% between three different MC values, 27%, 33% and 41%. Though these results are obtained regardless the distance from the antennas to the chips, this is far from the expected target, which is to predict any MC value within a range of 20% and 50% with 1% accuracy. However, our results have been achieved with a small amount of data. Investigations can be carried out further if more data is available. In particular, the implementation of regression methods can be also considered if many different MC values are measured.

The complexity of the reflection phenomena swings the efficiency of the MC prediction mainly due to the contribution of the reflected signal by the surface which is mixed with the reflected power that crosses through the material. This drawback has many implications since the surface of the pile may be at random conditions in the real situation. Indeed, the surface of a big pile of chips in the forestry industry is very changeable. A MC measurement based on it is not reliable, rough conditions in the forest and warehouse, weather changes and type of delivery truck can very easily affect the state of the surface. Sometimes delivery trucks are not covered,

and if they are, a plastic canvas covering the chips contributes to the evaporation phenomena, which results in extra water content just over the surface of the material. This could give a false value of the MC. Moreover the penetration depth of the microwave radiation is about 35 cm at most, when the MC is minimum. This does not provide a representative value of MC of a large bulk fuel.

In conclusion, results are not promising enough to carry out this line of research towards a real size experiment and real application.



# Chapter 4

## In contact technologies

---

<b>4.1</b>	<b>Capacitive system</b>	<b>62</b>
4.1.1	Principle	62
4.1.2	Experimental system and procedure	64
4.1.3	Results and discussion	66
4.1.4	Summary	68
<b>4.2</b>	<b>Resonator technology</b>	<b>69</b>
4.2.1	Underlying physics	69
4.2.2	Antenna resonators	70
4.2.3	Simulation analysis	74
4.2.4	Experimental analysis	75
4.2.5	Study of half-wave dipole antenna performance	80
4.2.6	Laboratory-scale system	83
<b>4.3</b>	<b>Full-scale implementation</b>	<b>90</b>
4.3.1	Bulk measurements in static piles	90
4.3.2	Bulk measurements in a container	94
4.3.3	Summary	100
<b>4.4</b>	<b>Conclusion</b>	<b>101</b>

---

Chapter 3 has shown some disadvantages of contactless technologies owing to the surface of the material under test. In view of these issues, this chapter is focuses on in-contact technologies. The presented technologies in the following sections aim to avoid the influence of the surface, to be independent of external parameters such as the weather and truck geometry. For instance, sensors directly installed in the container could provide a first value of moisture content (MC) while chipping in the forest or in the warehouse, and also a value at the moment of the delivery to any client to determine the price of the fuel.

Capacitive system and resonator system are first tested in laboratory experiments, then a full scale experimentation is presented before conclusion.

## 4.1 Capacitive system

A MC measurement system based on capacitive technology is presented and analyzed in the following subsections. The principle is to scale up a commercialized device based on a capacitive bucket to the container of a truck [79]. After a brief description of capacitive sensors, a laboratory scale experiment is presented and results are discussed.

### 4.1.1 Principle

A capacitor is formed by two parallel conductors separated by a dielectric material see Figure 4.1. Under voltage, the capacitor carries equal and opposite charges. The capacitance  $C$  of the capacitor is defined as the ratio of the accumulated charge  $Q$  on the positive electrode by the voltage  $V$  applied to the electrodes. The capacitance is related to the dielectric constant of the material between the conductors. Due to the strong difference between the value of the permittivity of dry wood and water, capacitive techniques are well suited for MC measurements in bulks. The relation of capacitance  $C$  of a parallel-plate condenser when neglecting boundary effects is defined by:

$$C = \epsilon_0 \epsilon_r \frac{A}{d}, \quad (4.1)$$

where  $\epsilon_r$  is the relative dielectric constant of the material between conductors,  $A$  is the area of the electrodes and  $d$  is the distance between the electrodes. The electric field is normal to the surfaces [100]. This relation is acceptable if  $d$  is much smaller than the size of the conducting surfaces. Otherwise, if the conducting plate size is larger or comparable to the distance between them, the capacitance is influenced by the boundary effects. In that case the capacitance  $C$

between two conductors can be calculated from:

$$C = \int \epsilon_0 \epsilon_r \zeta^2 \partial v, \quad (4.2)$$

where  $\zeta$  is the electric field when one electrode is held to 1 V while the other is grounded. As charge  $Q$  and voltage  $V$  are connected by  $Q = C \times V$ , the current  $i$  flowing in the circuit due to a voltage variation is directly proportional to the capacitance of the system by:

$$i = \frac{\partial(CV)}{\partial t}. \quad (4.3)$$

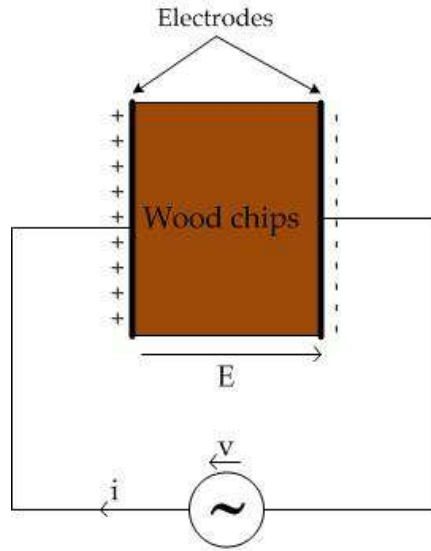


Figure 4.1: Capacitive sensing.

The currently applied commercialized capacitive device consists of a metallic bucket filled with wood chips, see Figure 2.6 in Chapter 2. An electrode immersed in the middle of the sample forms a capacitor with the metallic bucket with a dimension of  $64 \text{ cm} \times 50 \text{ cm} \times 50 \text{ cm}$  (*height*  $\times$  *depth*  $\times$  *width*), the device provides capacitance in the range of 1 to 50 pF. The dimensions of the system can be extended while keeping the same capacitance if the electrodes area and distance between electrodes increase with the same factor. In our case, the dimensions of the container of the delivery truck are  $2 \text{ m} \times 4 \text{ m} \times 2 \text{ m}$  (*h*  $\times$  *d*  $\times$  *w*) so the ratio between the surface of both sides of the container divided by the container width is the same order of magnitude than the ratio of the capacitive bucket. This implies the modification of an industrial container by installing a couple or more metal plates in the internal walls. A huge amount of fuel could then be probed. This system could provide measurements of MC in the woods while chipping, during transportation between warehouses and before final delivery to the client.



### 4.1.2 Experimental system and procedure

As it is not possible to use a truck during months to make the study, instead a plastic container  $120 \times 80 \times 70 \text{ cm}^3$  is equipped with two aluminum plates of  $100 \times 50 \text{ cm}^2$  and 1-mm thickness. The aluminum plates are attached to two parallel surfaces of the container, separated by 70 cm. Figure 4.2 presents the equipped container mounted on wheels so it can be easily weighted. The electrodes of each plate are connected to a capacitive sensor board with coaxial cables to avoid signal bias as much as possible. The container is filled with a 72 kg sample of P45 dry wood chips from oak. The capacitive sensor board presented in Figure 4.3 provides the value of the capacitance between both electrodes, one being held to the voltage  $V_p$  and the other being grounded. The sensor board output is given by

$$\Delta Q = C_0 \times V_0 + C \times V_p, \quad (4.4)$$

where  $V_0$  is a reference voltage,  $\Delta Q$  is the variation of the accumulated charge on the electrodes,  $C$  is the value of the capacitance depending on wood chips and  $C_0$  is a reference capacitance. The flow of charges accumulated on the electrode is easy to determine by a simple charge-transfer circuit. This consists of charging and discharging iteratively during  $n$  cycles the capacitor with the voltage  $V_p$ . The value obtained by the sensor board is the variation of charges  $\Delta Q$ .



Figure 4.2: Capacitor implemented in a plastic container.



Figure 4.3: Capacitive sensor board.

In order to measure the capacitance between terminals, the reference capacitance  $C_0$ , the reference voltage  $V_0$  and polarization voltage  $V_p$  must be calibrated. The sensor board provides values within a specific range. The smaller the range, the better the accuracy but some measurements may be missed by saturating the system. More variation of capacitance can be obtained with a bigger range but if it is too big the accuracy is degraded. A calibration that allows measuring the whole range of capacitance under test accurately is required. Therefore, the maximal and minimal values obtained by the sensor board must be adjusted. These values correspond to the capacitance of wood chips at 20% and 50% MC, which are the minimal and maximal MC under test. This range is defined by:

$$\Delta Q_{min} = C_0 \times V_0 + C_{min} \times V_p = 0 \quad \text{then} \quad C_0 \times V_0 = -C_{min} \times V_p$$

and

$$\Delta Q_{max} = C_0 \times V_0 + C_{max} \times V_p \quad \text{then} \quad \frac{\Delta Q_{max} - \Delta Q_{min}}{C_{max} - C_{min}} = V_p.$$

This way, saturation is avoided during all the experimental measurements. Once the working range is adjusted, the calibration process of the sensor board can be performed. The reference point must not change when adjusting  $C_0$ ,  $V_0$  and  $V_p$  so a value within the range is used. Several measurements with different values of capacitance are performed. The reference capacitance is  $C_0 = 150$  pF. According to the reference value, the sensor card measures  $C_{12}$ , the capacitance between the electrodes 1 and 2. The bulk of wood chips under test is homogeneously humidified up to almost 50% MC. The capacitance between the two metal plates has been measured continuously during 5 weeks while decreasing the weight of the sample, that is to say while

decreasing the MC. P45 size wood chips are homogeneously dried and stirred using fans. 16 capacitance values corresponding to 16 different MC values are evaluated. Every measurement day, the calibration process and measurements are performed in the same place under equal environmental conditions all along the experiment, otherwise measurements obtained by the sensor card would have not been really comparable. Capacitive measurements are indeed very sensitive to the environment, since electrodes are not shielded, they are influenced by every thing in the room. Figure 4.4 illustrates the experimental setup of this experiment.



Figure 4.4: Capacitive sensing performance.

### 4.1.3 Results and discussion

The results show that the system is sensitive to the MC of the material under test. Table 4.1 shows the pair of values obtained (MC, Capacitance) during the 5 weeks of the experiment. It is clear that the capacitance decreases with the MC since less water implies a lower permittivity and therefore a lower capacitance. Figure 4.5 presents the evolution of the capacitance related to the MC. The behavior of the system is not linear during the whole range of MC under test. The variation of the capacitance is stronger for values of MC between 20% and 30%. For values of moisture higher than 30%, the variation of the capacitance becomes smaller comparing to the variation of moisture. This phenomena is well known [98]. It is caused by the way the water is

trapped in the wood. Above 30% MC the water accumulates freely whereas below 30% MC the water is bounded to wall cells (hygroscopic water). The saturation point of wood, which is 30% MC, is considered as the state in which the cavity of the fiber is free from moisture and its wall is completely saturated. Below the fiber saturation point of wood many important physical properties of wood are tremendously affected by the variation of moisture. Over this point the relation tends to be less dramatic [111].

Capacitance measurements			
MC (%)	Capacitance (pF)	MC (%)	Capacitance (pF)
48	192	38.46	161.5
47.44	182	35.71	158
47.05	180.6	31.75	153.5
46.6	181.5	29.41	152
45.6	175.6	27.27	149.2
44.61	174.8	23.4	117
43.3	172.6	22.16	87
41.2	165.4	20.4	65.41

Table 4.1: Obtained values (MC, Capacitance).

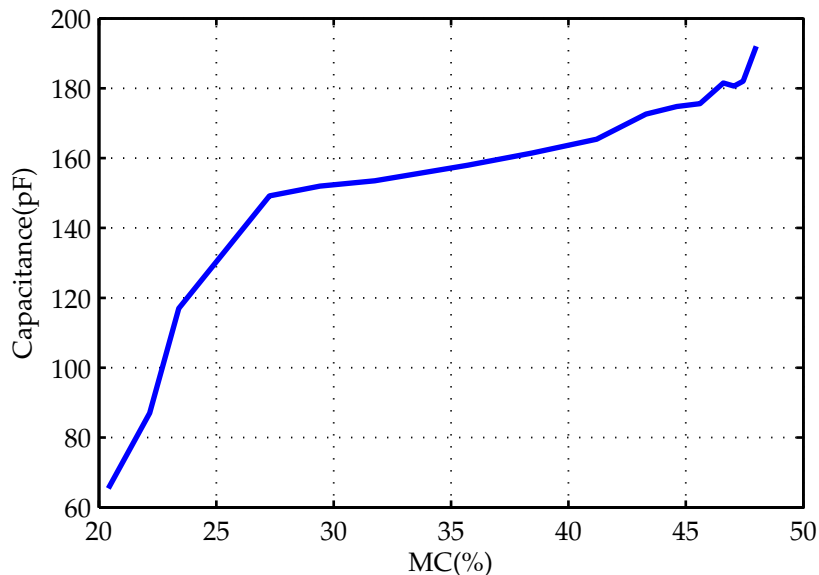


Figure 4.5: Capacitance versus MC.

The system is very sensitive to the variation of the MC, overall below the fiber saturation point. However, special conditions are necessary for its performance. The measurements must be always performed at the same position because the system is too sensitive to the environment. The repeatability is poor since the presence of something or someone around the container or over the plates modifies the result. This is due to the fact that lines of the electric field are not

fined inside the container. Therefore the lines of the electric field that get out the container are sensitive to the environment.

#### 4.1.4 Summary

A system to measure the MC of wood chips in bulk based on capacitive technology is presented. It is based on the installation of two metal parallel plates in two faced walls of a container. It is clear that the MC of the dielectric material between two electrodes and its permittivity are proportional. This allows an estimation of the MC by measuring the capacitance. A small-scale system has been designed, implemented and tested. This technology presents several advantages, it provides an average measurement of the MC of a large quantity of fuel and it is a robust technology able to resist to the rough expected conditions of the forest industry. However, the installation of a huge capacitor in the container of a truck may not be economical neither practical in regards to an industrial application. The electrode must indeed be sufficiently far from the boundary of the truck to still be sensitive to the wood chips. A capacitor based on another geometry could be considered. For instance with the electrode held to  $V_p$  in the middle of the container while the boundary of the container becomes the second electrode. Results in the laboratory have shown that the system is sensitive to the MC under test but also to possible changes in the environment surrounding. In addition, the metal plates must not be wet before the measurement otherwise the result would be unreliable. This is almost impossible to happen in real conditions since rain, temperature or water left over at the bottom of the container can easily interfere in the reliability of this system.

## 4.2 Resonator technology

At higher frequency, resonators are very interesting for characterizing dielectric material and thus it is a promising technique for MC measurement.

### 4.2.1 Underlying physics

Power transfer between a source and a device through a transmission line is maximized when all parts are matched. This means that the impedance of all parts, if real, are equals. Otherwise a fraction of the energy is reflected back to the source. Usually sources and transmission lines are matched to  $50 \Omega$ , therefore maximum energy is transferred when the impedance of the device is  $50 \Omega$ . The reflection coefficient  $\Gamma$  is defined as

$$\Gamma = \frac{Z - Z_0}{Z + Z_0} \quad (4.5)$$

where  $Z_0$  is generally  $50 \Omega$  and  $Z$  the impedance of the device, reaches a minimum at a frequency where  $Z$  is the closest to  $Z_0$ .

In the case of an antenna or resonator as the device, the maximum power transferred to the material is thus at the minimum of  $\Gamma$ . As the impedance of an antenna or a resonator depends on the electrical characteristics of surrounding material, the frequency at which the maximum power is transmitted to the material depends on its electrical characteristic and obviously on its permittivity. The frequency of the minimum of  $\Gamma$  is therefore a good indicator of permittivity, thus of MC.

If resonators generally require to introduce the material in a small chamber, an antenna can be used to directly probe surrounding material when introduced inside this material. Therefore a resonant antenna buried inside the material under test can provide information about the moisture content of the material.

The antenna radiation field is divided into three different regions, which are illustrated in Figure 4.6 for a certain antenna [112]. In these different regions the characteristics of the electromagnetic waves are different. They are not firm boundaries but provide information about the radiated field as a function of the distance from the antenna. The far-field (Fraunhofer) region is defined for distances  $d \geq 2D^2/\lambda$ , where  $D$  is the largest linear dimension of the antenna, and  $\lambda$  is the wavelength. This region is used for communication. The electric and magnetic field vectors are orthogonal to each other and the radiation pattern is formed and constant. As a consequence the gain does not change according to the distance, it depends only on the angle.

The reactive near-field region is usually defined for distances  $d \leq \lambda/2\pi$ . This region is very close to the surface of the antenna and  $E$  and  $H$  are very complex to predict. The gain of the antenna varies drastically with the distance even at a fixed angle. Between far-field and reactive near-field regions, there is the radiating near-field region, also called the transition region. In this region, the antenna pattern is taking shape but is not yet fully formed.

In the case of MC measurement purpose, one is interested in the properties of a material and not in the transmission of information. The monitoring of the working frequency is thus a good indicator. Therefore the proposed technology is focused on the study of the reflection coefficient  $\Gamma$  in the near field radiation region of a resonator antenna.

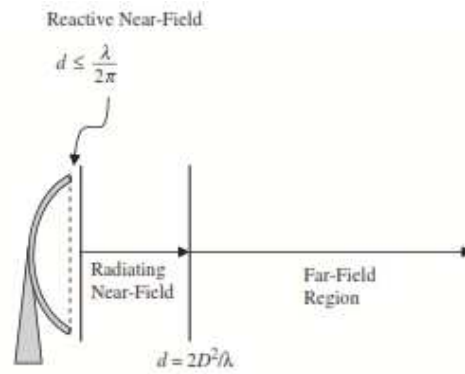


Figure 4.6: Boundaries for antenna radiation regions, taken from [112].

## 4.2.2 Antenna resonators

As it has been mentioned above, the idea is to determine the moisture content of wood chips through measuring the reflection coefficient  $\Gamma$  of a resonant antenna in contact with the material under test. As the antenna impedance depends on the material under test the maximum power is transferred to the antenna at a specific frequency. This frequency is directly connected with the permittivity of the material under test and thus to the MC.

### 4.2.2.1 Half-wave dipole antenna

The half-wave dipole antenna is a special form of the dipole antenna. Half-wave means that the length of the dipole is equal to a half-wavelength in vacuum at the frequency of operation. The directivity of a half-wave dipole antenna is 2.15 dB and the half-power beam width (HPBW) is  $78^\circ$ . When the antenna is at resonance, its input impedance is  $73 \Omega$ , with no reactive component. This maximal power transfer occurs because the wavelength complies with the limit conditions

of a null current at both ends of the antenna. Notice that a null current limit conditions implies that the antenna is fed at its center. Such antenna resonates in vacuum at the frequency  $f_0$  given by

$$f_0 = \frac{0.47c}{\text{length}}, \quad (4.6)$$

where  $c$  is the speed of light. At this frequency the power transferred to the surrounding media is maximal resulting in a minimum of the reflection coefficient [113]. The resonance occurs as well for frequencies multiple of  $f_0$  which is referred to as harmonics in what follows.

Finally, a half-wave antenna inside a specific dielectric provides a resonant frequency related to the speed of light in that media, which is directly connected to its relative dielectric constant  $\epsilon'_r$  by

$$f_{\text{resonance}} = \frac{f_0}{\sqrt{\epsilon'_r}}. \quad (4.7)$$

In the far-field region, the radiation pattern, see Figure 4.7, of the antenna emits electromagnetic waves perpendicularly to the antenna axis.

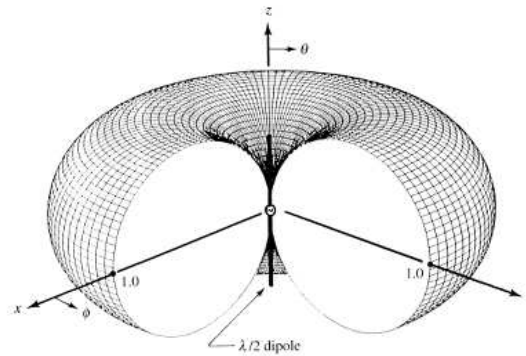


Figure 4.7: Three dimensional radiation pattern of a  $\lambda/2$  dipole, taken from [113].

#### 4.2.2.2 Quarter-wave monopole antenna

A monopole antenna is one half of a dipole antenna mounted above a ground plane. It is normally one quarter wavelength long. The vertical monopole antenna is highly used for land mobile communications, with the vehicle itself being the required ground plane. An ideal quarter-wave antenna has a radiation resistance of  $36 \Omega$ . Quarter-wave antennas mounted on the earth result in high power loss due to the poor ground conductivity, therefore a ground screen must be installed to improve the efficiency. This ground screen generally consists of radial wires extending from the base of the antenna as shown in Figure 4.8. The screen is normally slightly buried and improves the efficiency of around 95%. The performance is similar to the half-wave



dipole however just half of the surrounding material is probed [114]. Its radiation pattern is shown in Figure 4.9.

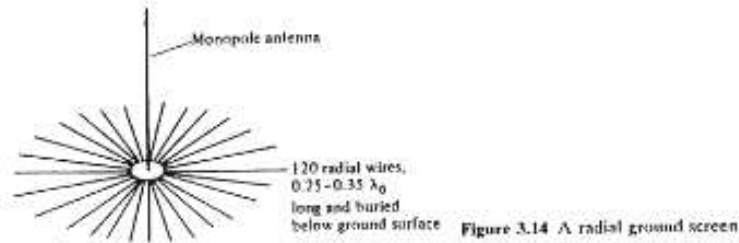


Figure 4.8: A radial ground screen buried below ground surface, taken from [114].

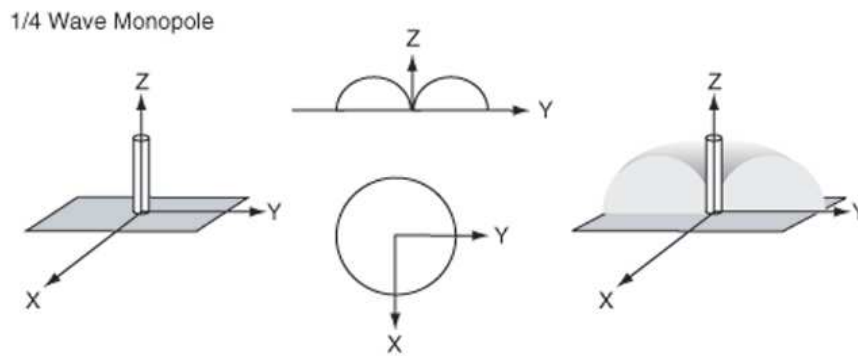


Figure 4.9: Radiation pattern of a quarter-wave monopole, taken from [114].

#### 4.2.2.3 Microstrip rectangular antenna

The microstrip rectangular antenna is another simple and inexpensive antenna, mechanically robust and very versatile in terms of resonant frequency. The patch is of length  $L$ , width  $W$ , and sitting on top of a circuit board of thickness  $h$  with permittivity  $\epsilon_r$ . All of the parameters in a rectangular patch antenna design ( $L, W, h, \epsilon_r$ ) control the properties of the antenna. The frequency of operation of the patch antenna is determined by the length  $L$ . The relationship between the resonant frequency and the patch length is approximately

$$f_{resonance} = \frac{c}{2L\sqrt{\epsilon_{eff}}} = \frac{1}{2L\sqrt{\epsilon\epsilon_0\mu_0}}, \quad (4.8)$$

As for other kinds of antennas the resonant frequency depends on the relative permittivity, referred to as  $\epsilon_{eff}$ . Here, however  $\epsilon_{eff}$  refers to a mixture between the permittivity of the substrate and the permittivity around the antenna. Therefore the sensibility of the patch antenna should be lower than that of the half or quarter-wave antenna. The gain of patch antennas is approximately 5 to 7 dB. The width  $W$  controls the input impedance and the radiation pattern.

The wider the patch, the lower is the input impedance [113]. Figure 4.10 shows a microstrip line, its electric field lines and effective dielectric constant geometry.

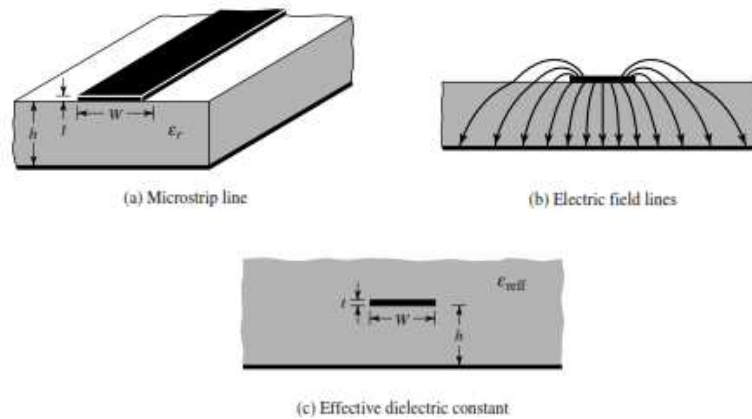


Figure 4.10: Electric field lines of a rectangular patch antenna, taken from [113].

#### 4.2.2.4 In-line half-wave dipole antenna

Considering the density of the material under test and its tendency to act as a solid block, the fact of plunging an antenna inside a pile of chips is significantly rough. An antenna fed in-line is obviously less likely to be damaged when plunged in a pile of chips than an antenna fed perpendicularly. The performance is similar to the half-wave dipole. It is presented in Figure 4.11 and the radiation pattern of this antenna is simulated using HFSS (Figure 4.12) and is illustrated in Figure 4.13.



Figure 4.11: Antenna half-wave dipole antenna fed in-line.

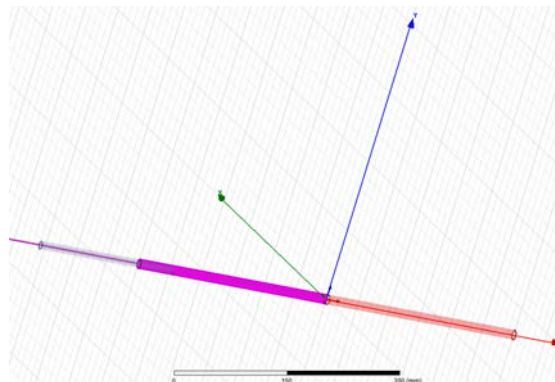


Figure 4.12: Antenna half-wave dipole fed in-line.

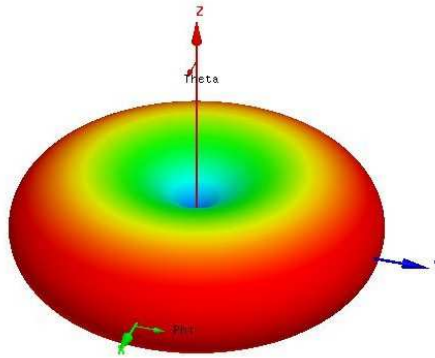


Figure 4.13: Dipole fed in-line radiation pattern simulated using HFSS.

### 4.2.3 Simulation analysis

HFSS<sup>1</sup> and ADS<sup>2</sup> softwares are used to study the behavior of the reflection coefficient  $\Gamma$  when the antenna is surrounded by wood homogeneously wet. The permittivity of dry and wet wooden logs are known [98]. Simulations have been performed according to different moisture contents of wooden logs.

Several microstrip antennas printed in an epoxy substrate and fed from underneath via a probe have been simulated, using (ADS) to obtain the optimal source position at frequencies 300 MHz, 500 MHz, 800 MHz and 1 GHz. The reflection coefficient  $\Gamma$  hardly presents differences when changing the permittivity of the material surrounding as expected. This is due to the electric field distribution in the antenna, which is mostly concentrated in the epoxy and hardly penetrates in the material under test.

A  $\lambda/2$  dipole at 250 MHz fed in-line is simulated using HFSS, see Figure 4.12. , as well as several  $\lambda/4$  monopoles and  $\lambda/2$  dipoles at frequencies between 250 MHz and 1 GHz, see Figure 4.14. The reflection coefficient  $\Gamma$  is very sensitive to the variation of the permittivity of the surrounding media. Different values of permittivity provide different resonant frequencies.

Contrarily to microstrip resonators,  $\lambda/4$  monopoles and  $\lambda/2$  dipoles have a more convenient electric field distribution which penetrates deeper in the material under test and therefore are much more sensitive to the variation of the permittivity of the surrounding media. The fact that the  $\lambda/4$  monopoles require a ground plane can be a problem in terms of a real application since it implies a transformation of the container of the truck. Therefore  $\lambda/2$  dipole seems the best option for this research, it does not need a ground plane and also probes at least twice as much volume as the monopole.

<sup>1</sup>High Frequency Structural Simulator.

<sup>2</sup>Advanced Design System.

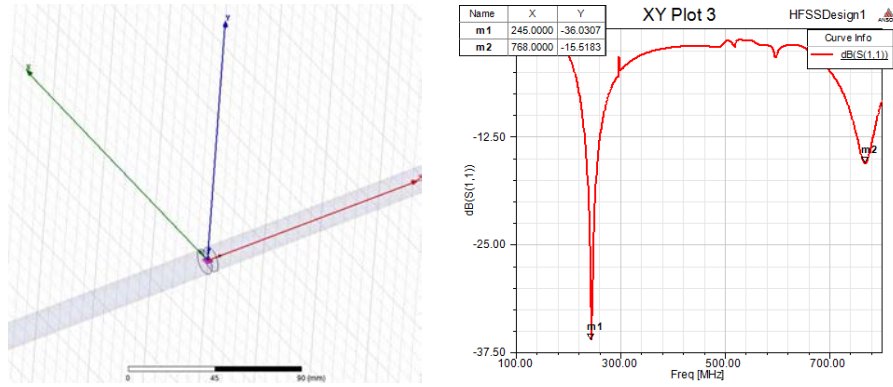


Figure 4.14: 56-cm long half-wave dipole antenna in the vacuum simulated using HFSS.

### 4.2.4 Experimental analysis

Simulations have been performed in wet wood, which permittivity is fully known. However wood chips are a highly inhomogeneous material and thus may differ from dense material. Experimental analysis have been carried out in order to better understand the performance of these sensors in presence of this material and especially the influence of wood chip size on the antenna size. All printed sensors have been built using a contact printer Hellas 38 from Bernier Electronik and an etching machine from Socem-Elec to create circuit boards. SMA connectors are welded on the board to supply the antennas,  $\Gamma$  is measured using a 8722ES Vector Network Analyzer calibrated with the 85033E Mechanical Calibration Kit, 3.5 mm, from Agilent Technologies.

P100 Oak	Container 1	Container 2	Container 3
Wet sample (kg)	81.5	99.5	101.5
Dry sample (kg)	59.5	66.5	64
MC (%)	27	33	36

Table 4.2: Samples under test.

Given the optimal dimensions by previous simulations, several rectangular microstrip antennas have been realized in order to study its behavior in the wood chips at different frequencies, corresponding to 300 MHz, 500 MHz, 800 MHz and 1 GHz. They are fed from underneath that is to say from the ground surface in order to reduce the influence of the cable. The outer conductor of the coaxial cable is connected to the ground plane, and the center conductor is extended up and welded to the patch antenna as shown in Figure 4.15. The glass epoxy dielectric is of 1.6-mm thick with permittivity  $\epsilon_r=4.3$ . The reflection coefficient  $\Gamma$  is measured in the three containers of  $120 \times 80 \times 70 \text{ cm}^3$  at the 3 different MC described in Table 4.2. At high frequencies,  $\Gamma$  hardly presents differences in between the 3 samples, see Figure 4.16. The reproducibility of the measurements is influenced by the arrangement of the chips and also by the

possible gaps of air in between the chips. At lower frequencies the reproducibility is improved but the amount of field lines that cross the material are not sufficient to make any significant difference between the 3 permittivities as observed from the simulations.



Figure 4.15: Microstrip patch antenna operating at 1 GHz,  $W = 91.3$  mm,  $L = 71.3$  mm.

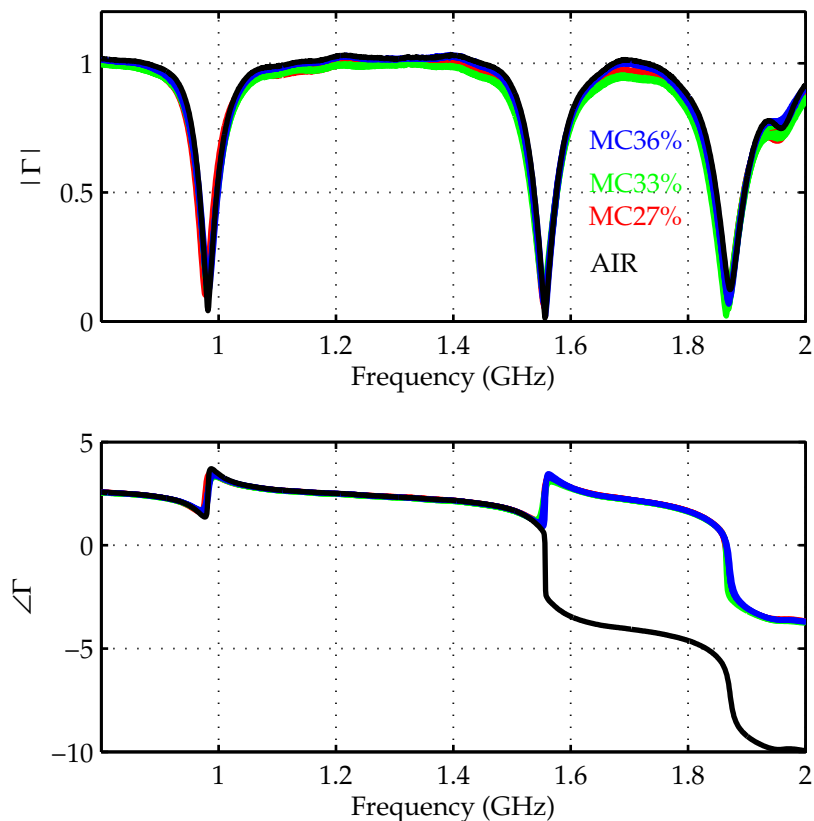


Figure 4.16: Reflection coefficient  $\Gamma$  of a 1 GHz microstrip antenna.

Concerning the wire antennas, half-wave dipoles present advantages compared to monopoles since the mechanisms are simpler and the volume probed is double, therefore several half-wave

dipoles have been built. Dipoles fed perpendicularly are fed at their center and built using double sided PCB<sup>3</sup> Epoxy Fiber FR4 with a relative permittivity of  $\epsilon'_r = 4.3$  and 1.6 mm thickness. One branch is one side and the other branch is the ground side of the PCB, so no connection between the sides is necessary. Experiments have been carried out using the containers described in Table 4.2, with antennas whose length is either 15 cm, 23 cm, 32 cm, 36 cm, 45 cm, 54 cm and 60 cm. Figure 4.17 shows three of these antennas. Figures 4.18 and 4.19 show the amplitude of the reflection coefficient of two half-wave antennas, 27 cm and 54 cm long, in the same range of frequency. The reflection coefficient  $\Gamma$  at the antenna input is measured repeatedly changing the chip arrangement. For small sized antennas, the size of chips and the gaps of air in between the wood chips affect more the effective dielectric constant of the sample to a larger extent and therefore the reproducibility of the results. Higher reproducibility has been achieved by the 54 cm half-wave dipole, see Figure 4.19.



Figure 4.17: Half-wave dipoles.

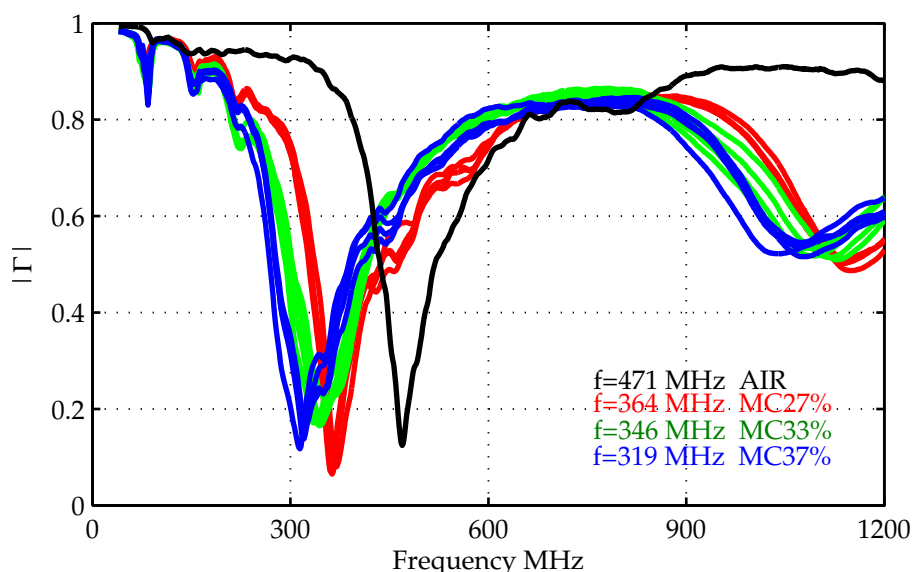


Figure 4.18: Reflection coefficient  $\Gamma$  of a 27-cm long half-wave dipole immersed in samples at different MC.

<sup>3</sup>Printed circuit board.

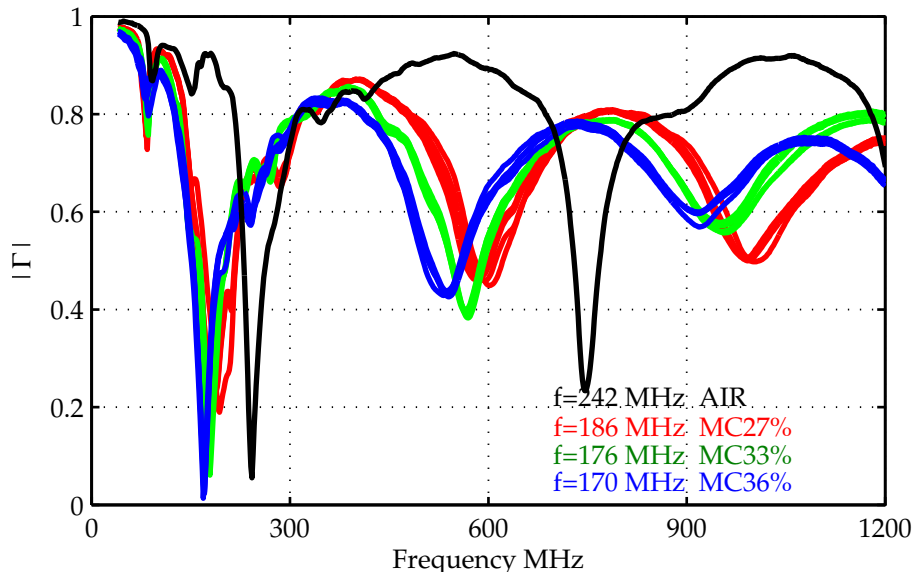


Figure 4.19: Reflection coefficient  $\Gamma$  of a 54-cm long half-wave dipole immersed in samples at different MC.

A half-wave dipole fed in-line has been built and tested to study its performance. It is formed with two copper cylinders of 1-cm diameter and 28-cm long. The coaxial cable goes through inside the cylinder until the middle where it is welded to the two branches, see Figure 4.20. The reflection coefficient  $\Gamma$  of the dipole fed in-line has been tested inside a pile of chips of oak (P45) to study the behavior of its resonant frequency according to the MC. Experimental results show that this antenna is not as sensitive as the antenna that is fed perpendicularly. The presence of the coaxial cable beside one branch of the dipole influences the current distribution and therefore their usual behavior. This results in electromagnetic perturbations that reduce the reliability of the measurement. A non-metallic power supply different to a coaxial cable such as optical fiber would be more convenient in order to avoid perturbations while keeping the in-line geometry. Figure 4.21 shows the average value of the  $\Gamma$  of the 56-cm long dipole fed in-line and perpendicularly for several values of MC within a sample of oak. If one compares both performances, the difference between the quality of the signal is clearly observed.



Figure 4.20: Photography of half-wave dipole fed in-line.

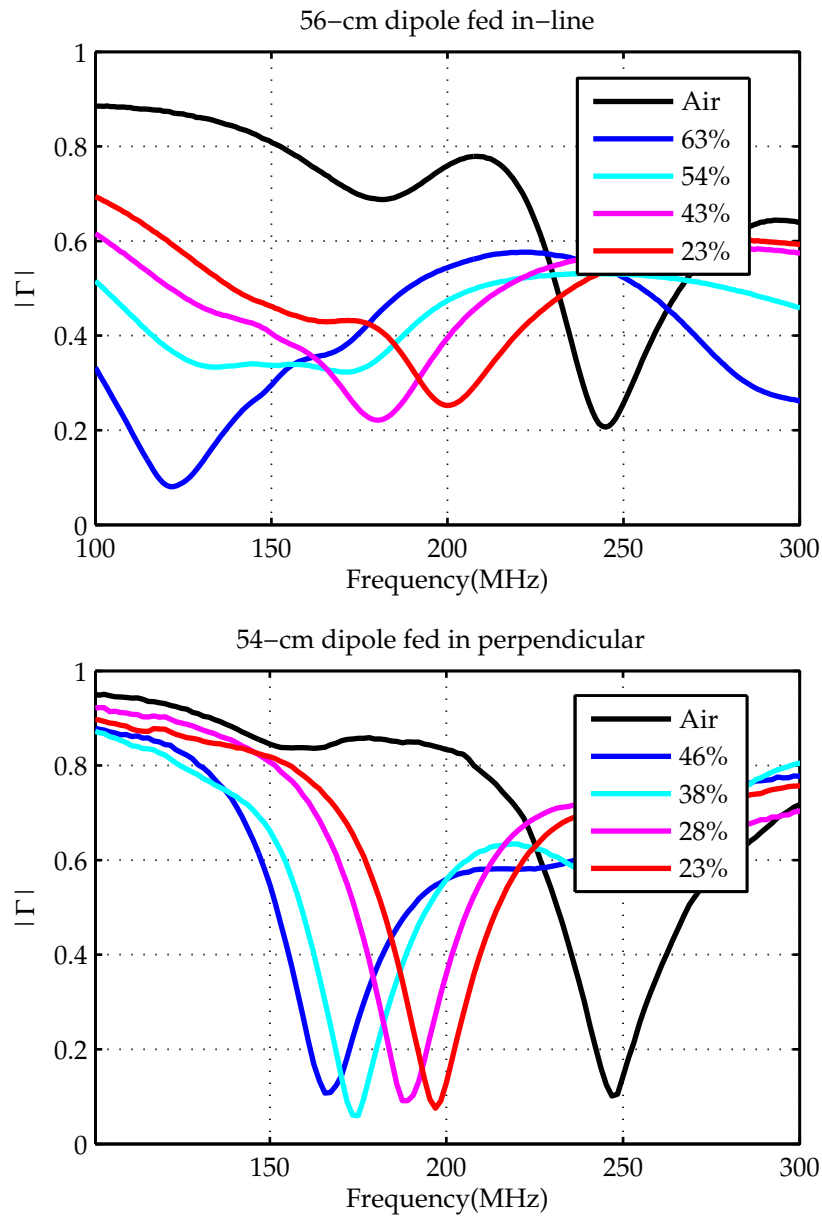


Figure 4.21: Comparison of  $\Gamma$  given by a half-wave dipole fed in-line and perpendicularly.

All experiments presented in this subsection allow to study the behavior of the antennas in real samples of wood chips and validate the performance obtained by the simulations. The patch antennas are not sufficiently sensitive to the material around. Half-wave dipole is a good compromise, it is very sensitive to the moisture of the surrounding media and probes an appreciable volume of material. In order to have good reproducibility the working frequency is limited by the size of the chips. Notice that half-wave antennas have also been successfully used with other material such as concrete [115].



### 4.2.5 Study of half-wave dipole antenna performance

It has been demonstrated that the reflection coefficient  $\Gamma$  of a half-wave dipole antenna changes according to the permittivity of the surrounding material. In order to go further and determine which volume does really affect the antenna, an experiment using a known material has been performed. Sunflower oil is an insulating material which permittivity is well known, 2.4 at the operating frequency [116]. Sunflower oil has been chosen because it is an insulating liquid and simplifies the complexities of the experiment. A 15-cm long wire dipole antenna of 1.7-mm diameter wire has been placed in the middle of a plastic bucket of 25.6-cm diameter and 35-cm height. The bucket of 16.7 L capacity is surrounded by electromagnetic absorbents. The dipole is perfectly placed parallel to the surface of the oil. This way the proximity to the sunflower oil is equal all along the wire. The reflection coefficient  $\Gamma$  of this antenna placed at the height of 16.25 cm within the bucket is measured while slowly filling the bucket with sunflower oil with 400 mL added between each measurement. In the middle of the experience 100 mL is added instead between measurements to increase accuracy. A volume of 400 mL represents a level increase of 0.778 cm and 100 mL represents 0.1945 cm level increase. Figure 4.22 sketches this experience. The antenna is very sensitive to the material in a nearby region as shown in Figure 4.23. Indeed the transition from 90% to 10% of the resonant frequency from about 900 MHz to 550 MHz occurs  $\pm 0.95$  cm above and below the sunflower level. The change is clearly visible around  $\pm 3$  cm around the sunflower level. It is interesting to see if the wire diameter has an influence on the results. The experiment is repeated using a 16.4-cm long dipole made of 3-mm diameter wire. No significant difference is found between both values of diameter as shown in Figure 4.24.

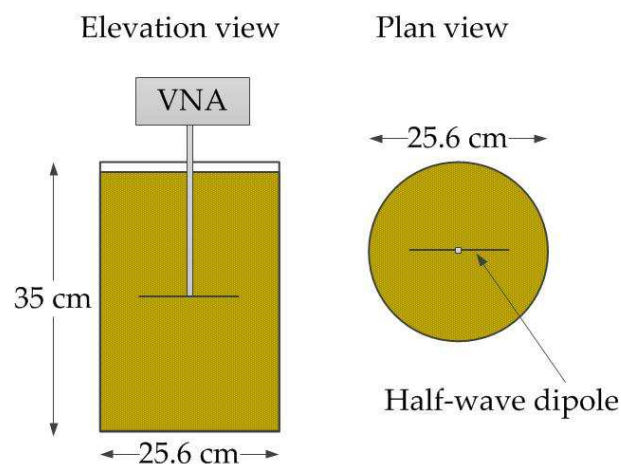


Figure 4.22: Schema of the sunflower bucket.

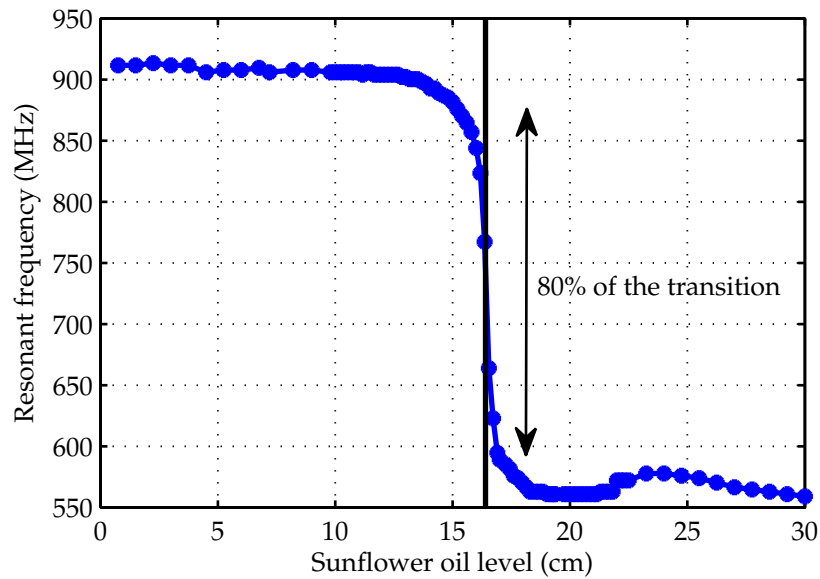


Figure 4.23: Evolution of the resonant frequency of a 15-cm long dipole, made with 1.7-mm diameter wire.

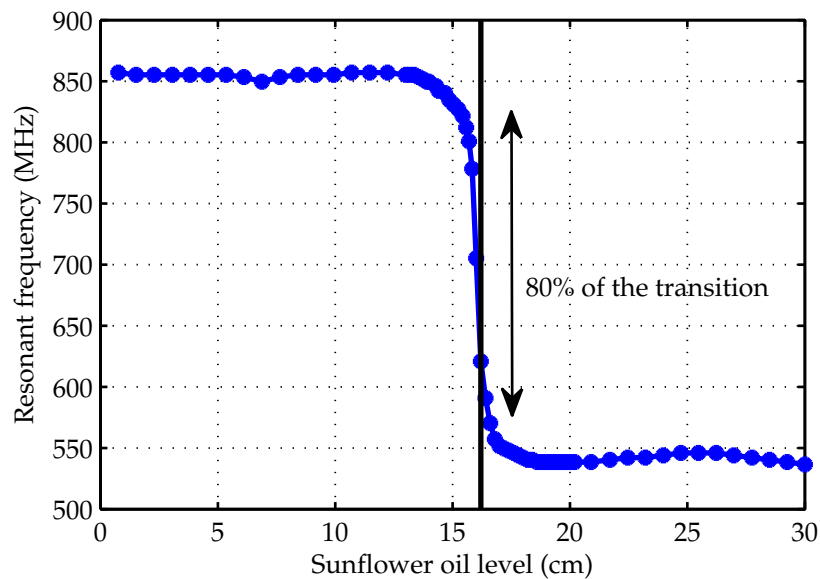


Figure 4.24: Evolution of the resonant frequency of a 16.4-cm long dipole, made with 3 mm diameter wire.

This experiment is also simulated using HFSS in order to estimate the accuracy of the model, specially the boundary conditions. A 15-cm long wire dipole antenna has been placed in the middle of a plastic bucket. Dimensions of the bucket and dielectric properties of the sunflower oil are equal to the experimental setup performed. Figure 4.25 shows the evolution of the resonant frequency of this antenna in presence of sunflower oil. It is clear that the strong change

of the resonant frequency occurs in the closest region to the antenna, this simulation gives a nearby region of 1.2 cm at each side of the antenna and a 90% to 10% transition of  $\pm 0.76$  cm around the sunflower level. This simulation agreed with the experimental results.

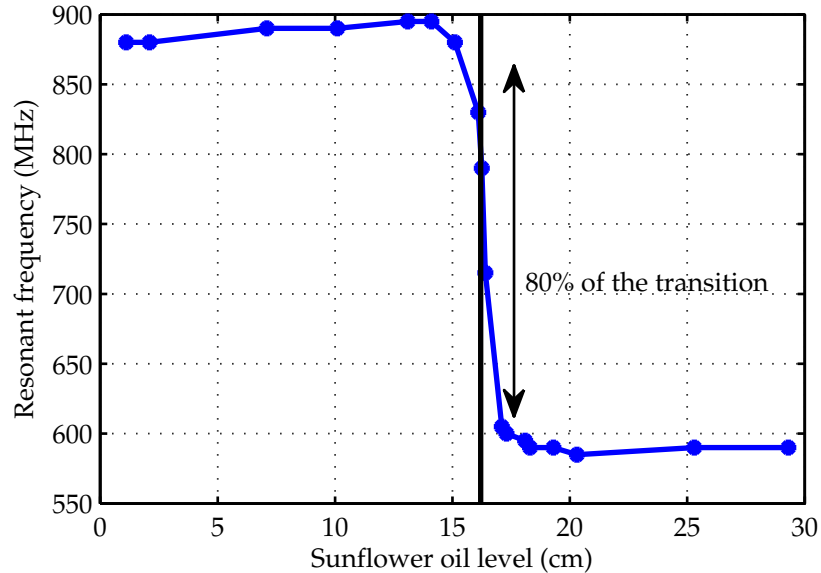


Figure 4.25: Evolution of the  $\Gamma$  of a 15-cm long dipole simulated by HFSS.

Wood chips is however a heterogeneous material composed by wet wood and gaps of air in between, therefore the limited nearby region is likely to be bigger under these circumstances. It would be interesting to see how a bubble of air located in different positions within the sunflower oil could affect the reflection coefficient  $\Gamma$ . This would allow a closer point of view to our particular case. But it is almost impossible to control it experimentally. As simulation is very close to the experiment, simulations have been performed using HFSS to evaluate the behavior of a half-wave dipole under these circumstances. Seven bubbles of air of 15-mm diameter are placed in the bucket full of sunflower oil, this is presented in Figure 4.26. The diameter of these bubbles is  $\lambda/20$ , where  $\lambda$  is the wavelength of the antenna in the air. 7 bubbles are located in a line facing the dipole. Their location is changed in order to study the region nearby the antenna that really affects the value of the resonant frequency. Figure 4.27 shows the evolution of the resonant frequency of the antenna as a function of the position of the bubbles within the bucket. The bubbles are filled either with air or with water in order to present an increase or a decrease of permittivity according to that of the sunflower oil. The resonant frequency of the antenna seems to be sensitive to the presence of air when the surface of the air bubbles is at 2.5 cm from the wire. However the frequency shift is significant only if the gap is around the wire. The same yields with water bubbles though the frequency shift is higher due to its larger permittivity. 10% of the frequency shift is obtained when the bubble center is at 1 cm from the wire. All these results are consistent with the fact that the sensor is sensitive to the

mean permittivity value of  $\pm 1$  cm around the wire. The presence of heterogeneity modifies the resonance frequency according to the average value of the permittivity around the wire in its sensitive region.

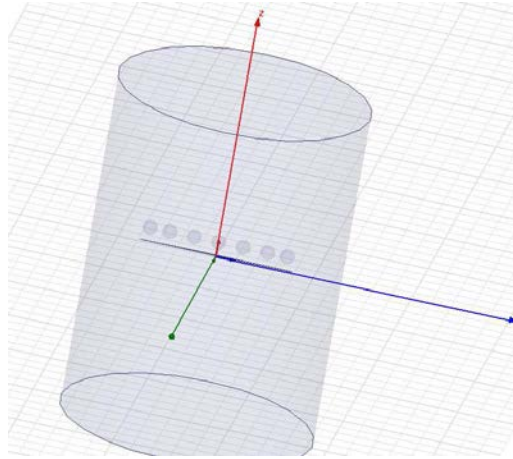


Figure 4.26: HFSS simulation with bubbles of air or water in the sunflower oil.

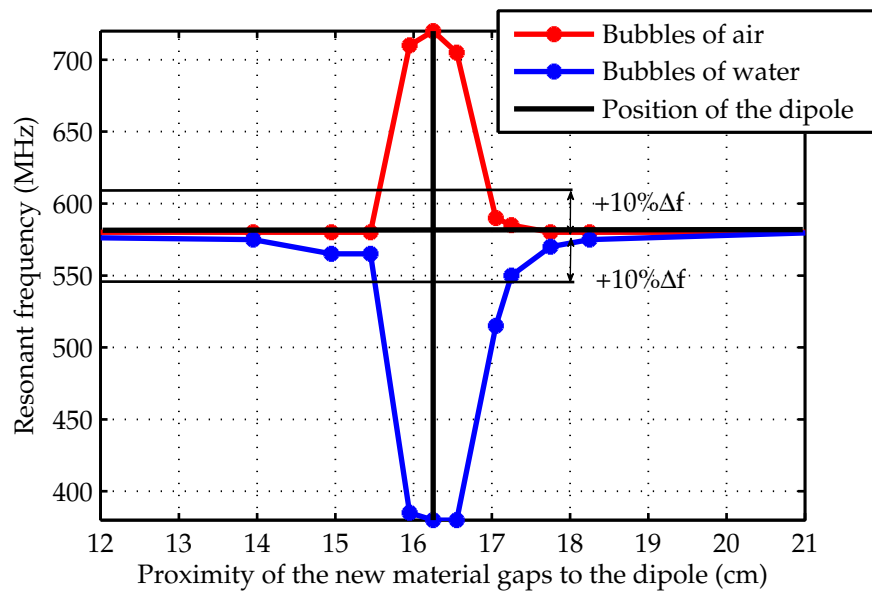


Figure 4.27: Evolution of the resonant frequency of the antenna in presence of a heterogeneous material.

#### 4.2.6 Laboratory-scale system

It has been shown that immersed measurements with a half-wave dipole antenna seem promising. When a half-wave antenna is put inside a pile of wood chips, the measurement of the resonance frequency seems directly related to the moisture content of the surrounding material.

In this section the system is tested in a small container with well-controlled MC wood chips of two kinds of wood. This allows to study if the specie of the wood has an influence on the results.

#### 4.2.6.1 Equipment

The antennas used to performed the measurements are 45-cm and 54-cm long half-wave dipoles fed at their center. They are made with double sided PCB Epoxy Fiber FR4 of 1.6-mm thickness,  $\epsilon' = 4.3$ . Two samples of  $0.5 \text{ m}^3$  of P45 chips of soft wood (pine) and hard wood (oak) are available to perform the measurements.

When placed into some media the antenna is sensitive to a given surrounding volume that depends on the length of the antenna. The longer the antenna, the larger the probed volume of wood chips. In order to take into account the effect of the container boundaries, a sample of chips humidified homogeneously up to 20% MC is used. 20% MC represents the minimal MC value in the industry and therefore the larger boundary influence. The internal dimension of the container is  $110 \times 71 \times 61 \text{ cm}^3$ , see Figure 4.28. The longest dipole (54 cm) is placed in different parts of the plastic container full of chips. As the longest axis is from 0 cm to 110 cm, the reflection coefficient  $\Gamma$  of the dipole is measured when this is located at different positions along this axis. The reflection coefficient is measured several times at each position changing the arrangement of wood chips. This way the variation of  $\Gamma$  can be observed when closer to the walls of the container. Figure 4.29 shows the average of the reflection coefficient  $\Gamma$  at different locations within the container. It is clear that the antenna probes more wood when it is in the middle position since its resonant frequency is slightly smaller. Also, other resonances or interferences are observed, this can be attributed to the presence of different objects in the room. Results show that  $\Gamma$  is very changeable depending on the location but when the antenna is covered by 40 cm up and down. This means that the antenna is sensitive to boundaries approximately 40 cm on each direction, which means that the minimal volume of wood chips to work with is approximately  $1 \text{ m}^3$ . Unfortunately, nor enough wood neither large enough devices are available in the laboratory. Considering the laboratory facility limitations an anechoic container has been designed. The internal surface of the plastic container is covered by ferrite, an electromagnetic absorbent material at the operating frequencies, in the range of 50 MHz to 1.3 GHz. A lid covered by ferrite has also been designed, this way the container simulates a complete anechoic chamber. This anechoic container presented in Figures 4.30 allows the study of the sensor preventing interferences caused by apparatus or material around the container. The reflection coefficient  $\Gamma$  at the antenna input when placed inside both samples is measured repeatedly using a 8722ES Vector Network Analyzer from Agilent Technologies.

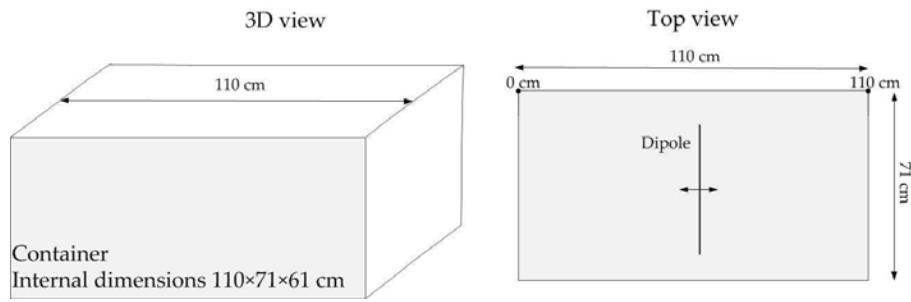
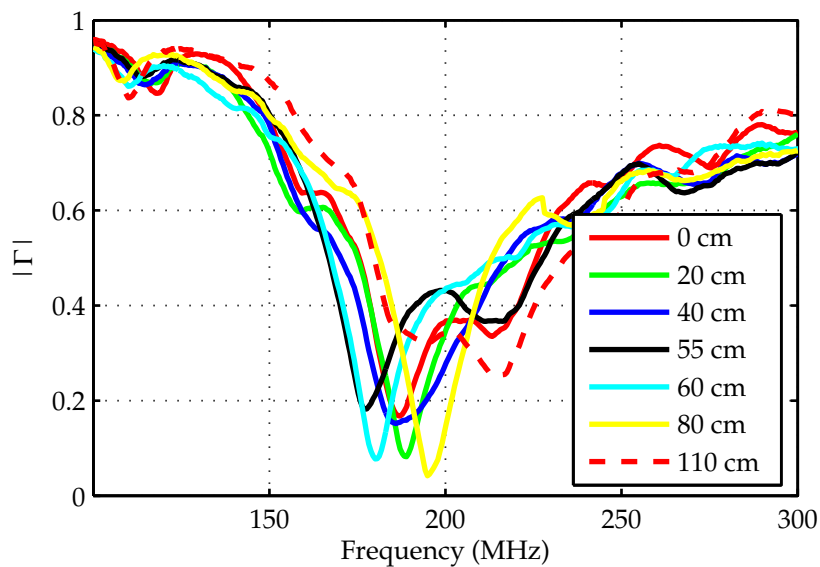


Figure 4.28: Plastic container.

Figure 4.29: Reflection coefficient  $\Gamma$  of the 54-cm dipole when placed at different positions within the plastic container.

#### 4.2.6.2 Methodology

The volume available of soft and hardwood is  $0.5 \text{ m}^3$ . The size of the chips is P45 for both species of wood. Samples of 36 kg of dry pine and 41 kg of dry oak are firstly humidified by adding water and then stirred regularly to get an homogeneous material. The reflection coefficient of the 45-cm and 54-cm long dipoles inside both samples have been measured during 32 days to follow the variation of the MC. The MC values are obtained by measuring concurrently each sample weight with a weighbridge following

$$\text{MC}(\%) = \frac{m_{wet} - m_{dry}}{m_{wet}} \times 100.$$

This monitoring process is presented in Figure 4.31. Sixteen different values of moisture have been tested in each sample. To reduce the dispersion caused by the heterogeneity of the material four measurements are performed at every moisture content changing the arrangement of chips



Figure 4.30: Photography of the anechoic container.

every time. Fans are used to speed up the drying process. Under these conditions, the MC range studied is comparable to the industrial wood chip MC range, from 17% to 50%.

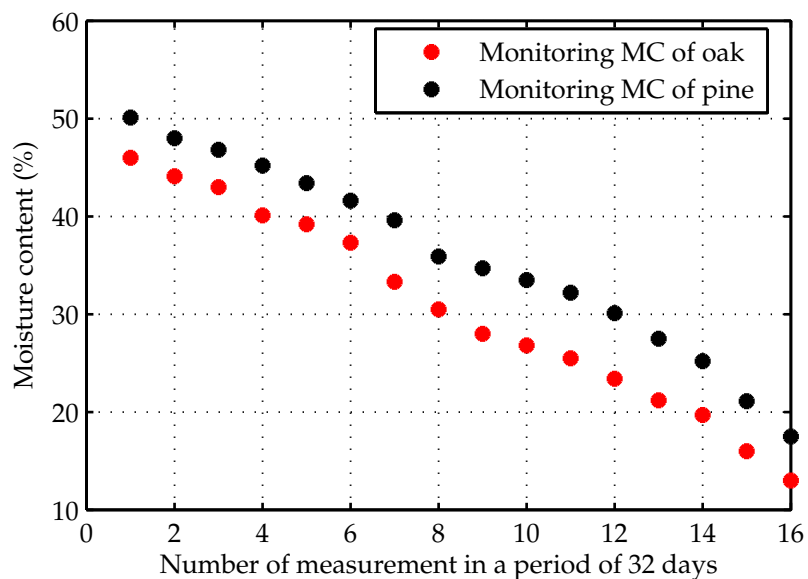


Figure 4.31: Monitoring of the MC of soft and hardwood.

#### 4.2.6.3 Sensor characterization

The 54-cm long dipole presents slightly better reproducibility than the 45-cm long one. Figure 4.32 shows the variation of the first resonance versus the MC for the 54-cm long dipole. Red (hard wood) and black (soft wood) curves represent the average resonance frequency at each MC. Their variation as a function of the MC are noticeable, with a constant sensitivity over the entire range of MC tested. The frequencies of every MC are clearly differentiated from each other, meaning that the arrangements of chips do not affect the final result. It is interesting to

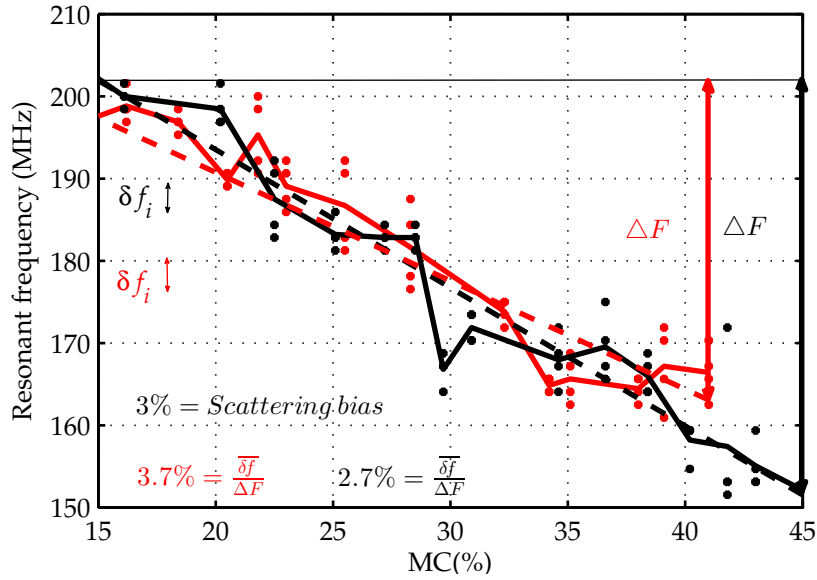


Figure 4.32: Firs resonance versus MC.

compare the frequency shift obtained for both species of wood. It shows that despite their different origins, the curves are very similar. This suggests that the measurements are relatively independent of the species of wood. A 3% relative scattering bias (Error rate in reproducibility) is estimated using

$$\text{Scattering bias} = \frac{1}{N} \sum_i^N \frac{f_{i,max} - f_{i,min}}{\bar{f}_i}, \quad (4.9)$$

where  $N = 16$  is the total number of measurement of MC,  $f_{i,max}$  and  $f_{i,min}$  are the maximum and minimum value of the resonance frequency for a given MC, and  $\bar{f}_i$  corresponds to the average resonance frequency for a given MC. It is estimated by

$$\bar{f}_i = \frac{1}{M} \sum_j^M f_j, \quad (4.10)$$

where  $M = 4$  is the number of measurements for each MC. The resolution of the method is estimated as  $\bar{\delta f} / \Delta F$ , where  $\bar{\delta f} = \sum (f_{i,max} - f_{i,min}) / N$  represents the average dispersion for measurements, and  $\Delta F = F_{max} - F_{min}$  is the general frequency range of a linear regression approximation of the first harmonic (dotted curves),  $F_{max}$  and  $F_{min}$  are the resonance frequencies for the maximum and minimum value of MC under test. This quantity approximately corresponds to the slope of the measurement versus the MC as presented in Figure 4.32. The behavior of the curve of the resonant frequency according to the MC is linear, this means that an average value of several samples of MC would agree with the average value of the respective resonant frequencies. A  $\pm 3.7\%$  resolution is obtained for hard wood and  $\pm 2.7\%$  for soft wood. When combining both kinds of wood  $\pm 3.4\%$  resolution is found [117][118]. Taking into



account the measurements dispersion, as the dispersion can be attributed to the arrangement of wood chips around the antenna but also to the slight variation of MC between the chips, 1% resolution requires an average over 20 measurements, thus 20 sensors would be required in the truck.

#### 4.2.6.4 Multivariate analysis

The calculation of the resonance frequency is not the only information given by the antenna inside the surrounding material. All the measured spectrum provides information but this requires more sophisticated methods as the implementation of non linear black box models applied to MC prediction. As mentioned above, for a given MC value several measurements of the reflection coefficient  $\Gamma$  have been performed. The reflection coefficient  $\Gamma$  has been measured at 801 frequencies between 50 MHz and 1.3 GHz. These measurements differ by the arrangement of the wood chips.

A non linear model based on Least Squares Support Vector Machine LS-SVM built by a machine learning specialist<sup>4</sup> is applied [119]. The LS-SVM modeling technique for non linear regression maps the input variable space to a high dimensional feature space where linear regression is possible. To rank and select the frequencies of the spectrum that are relevant for the model, the Gram-Schmidt orthogonalization procedure is applied. The validation error is calculated using the Virtual-Leave-One-Out (VLOO) method. This method reduces the computational burden and provides the validation error after performing a single training that involves all the available data. This method is exact when dealing with linear-in-their-parameters models such as the LS-SVM technique [120].

The description is summarized in the following diagram, see Figure 4.33 :

The first part of this analysis consists in the estimation of the reflection coefficients models  $[\hat{\Gamma}_1, \hat{\Gamma}_2, \dots, \hat{\Gamma}_N]$  at each MC. The number  $N$  is the quantity of MC under test. For this aim, the four measurements of  $\Gamma_j$  ( $j = 1, \dots, N$ ) corresponding to different arrangements of chips are taken into account. The values of reflection coefficient in all the spectrum  $f_i^M$ , where  $i$  represents one of the four wood-chip arrangements and  $M$  represents the 801 frequencies measured in each  $\Gamma$ . The reflection models are based on the LS-SVM with Gaussian kernel. This part leads to a set of  $N$  reflection models  $[\hat{\Gamma}_1, \hat{\Gamma}_2, \dots, \hat{\Gamma}_N]$ . In the second part, these models provide the inputs of the MC model. The model is optimized using the Gram Schmidt orthogonalization procedure that is dedicated to the frequency ranking and selection. The MC model is built using the LS-SVM technique with linear kernel. The 54-cm long dipole allows more efficient models than

---

<sup>4</sup>Hela Daassi-Gnaba.

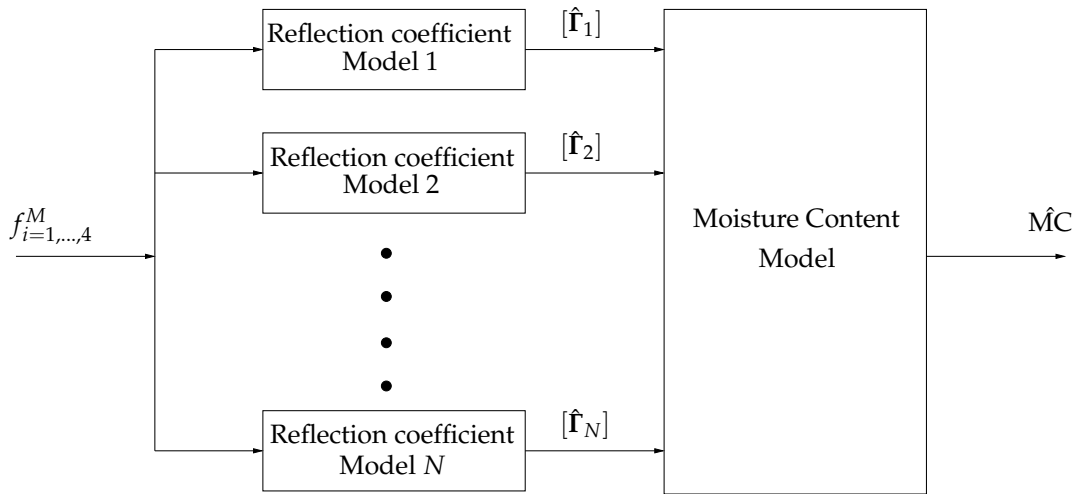


Figure 4.33: Model structure.

the 45-cm long one, for both types of wood. The bias for the oak is  $\pm 1.83\%$  and for the pine is  $\pm 1.42\%$ .

Since the goal is to provide a virtual sensor to determine the MC, a model that predicts MC regardless the type of wood is required. Thus, data from both wood types are combined to develop a global model. Eleven  $[\hat{\Gamma}]$  of softwood and eleven of hardwood have been used to build a new MC model. The remaining 10 reflection coefficient models  $[\hat{\Gamma}]$  are used to test the model.

#### 4.2.6.5 Summary

A small-scale prototype of a system to determine the MC of wood chips in bulk has been presented. Plastic containers with samples of  $0.5 \text{ m}^3$  simulate an industrial container full of chips. Pine and oak have been tested, they are respectively softwood and hardwood, the two kind of wood used in the french forest industry. One 54-cm long dipole fed perpendicularly is plunged inside the sample to test its reflection coefficient while the MC is decreasing from 50% to 20%. Results have shown that the final result is relatively independent of the kind of wood under test. A rough precision of  $\pm 3.4\%$  has been obtained. However, a method of implementation of non liner black box models based on the Least Squares Support Vector Machine LS-SVM provided a resolution of  $\pm 1.83\%$  for the oak and  $\pm 1.42\%$  for the pine. In a real application where the kind of wood is unknown or is just a mixed of several essences, the resolution given is  $\pm 2.15\%$ . This system presents promising results, it is non destructive, rapid, economical and can be very easily extended to a larger prototype and installed in a industrial container for real application.

### 4.3 Full-scale implementation

In view of the promising results offered by the small-scale system tested in the laboratory, an experimental larger prototype has been developed to perform measurements in the container of a real delivery truck, in a french forestry platform. The platform *Coopérative Forestière Bourgogne Limousin* (CFBL) allowed to use their installations and industrial equipment for this research. A long-term measurement campaign began in May 2015 for 7 months. The objective is to validate the performance of the sensor tested in the laboratory for real cases. Large piles of chips of different densities and sizes are available to test the system proposed. Nine piles of 45 m<sup>3</sup> of chips recently chipped (normally 50% MC) by an industrial woodchipper in the warehouse are available. Sensors are installed in 6 static piles to follow the behavior of the MC during months. The other 3 piles are used to load and unload a 35 m<sup>3</sup> container and perform measurements in it. The objective is to measure the moisture content of wood chips in bulk, so the installation of several sensors in the container of a delivery truck is here proposed. This allows to have several values of the reflection coefficient which provides several resonant frequencies that are respectively related to several values of MC. This system offers an average value of the MC of the total fuel up to purchase. Sensors can be positioned in a kind of portable grid or rope that can be easily attached or immersed in an industrial container. A measure in the container of a delivery truck could provide a first value of MC while chipping in the forest and a second value at the moment of the delivery to the client to determine the price of the fuel. The same system can then fulfill the requirements of the wood chip industry [121].

#### 4.3.1 Bulk measurements in static piles

Size P63	Birch	Pine	Oak
Measuring pile	45 m <sup>3</sup>	45 m <sup>3</sup>	45 m <sup>3</sup>
Sampling pile	45 m <sup>3</sup>	45 m <sup>3</sup>	45 m <sup>3</sup>

Table 4.3: Static available piles.

Three species of wood are available for the research. Two piles of every specie are located one beside the other on the platform of the warehouse. Each pile occupies a surface of around  $5 \times 5$  m<sup>2</sup> and 4 m high. The description of all six piles is presented in Table 4.3. Measuring piles are equipped with 14 antennas each at 3 different levels: 9 on a low level, 4 in the middle and 1 on the upper part of the pile. The antennas used are 56-cm long half-wave dipoles fed at their center, using single sided PCB Epoxy Fiber FR4 ( $\epsilon' = 4.3$ ) with 0.8-mm thickness for pine and oak and 1.6-mm thickness for birch. The dipoles are attached together by their centers all along the length of a rope, the separation between them is about 1 m. They have been installed in the

measuring piles while their formation as shown in Figure 4.34 All coaxial cables are respectively labeled indicating the position of every antenna and have been grouped in a box beside the pile. Figures 4.35 and 4.36 show this experiment when piles have been formed. Sampling piles are similar to the measuring piles but they are not equipped with antennas. They contain 12 small samples of chips in grid bags all spread within the pile. The bags are placed inside the piles while their formation, the bags are made of a grid in order for the sample to breath and to behave as a natural part of the whole pile. All samples are located about 1 m above the ground and 1 m inside the pile. They are accessible via a long rope that is attached to the bag, so the bags can be thrown out when required to check the MC of that specific in the sample. This is shown in Figure 4.37. A Keysight N9923A FieldFox Vector Network Analyzer is used to measure the reflection coefficient  $\Gamma$  of every antenna between 50 MHz and 1.3 GHz.



Figure 4.34: Installation of ropes of sensors while formation of the piles.



Figure 4.35: Piles of wood chips in the platform of the warehouse.



Figure 4.36: Security box for coaxial cables.



Figure 4.37: Samples of wood chips within the sampling piles.

The objective is to show how MC of a pile can differ a lot according to the position of the sensor, that is why an average value is needed. Inside a static pile of chips, the heat increases so the MC can increase or decrease irregularly depending on different locations within the pile. Every measurement day the corresponding samples have been taken out from the sampling piles to be dried in an oven at the laboratory in Paris, following the specifications of the official method. It is obvious that these samples do not represent a reliable value of MC of the whole pile but it gives the general tendency of MC for us to follow during the whole experiment. Table 4.4 shows the evolution of the MC of the samples in bags thrown out from the sampling piles of oak, pine and birch. Every measurement day the sample to dry is located in different parts of the same pile, that is why the evolution of the MC is irregular however it is clear how the general

tendency is towards drying out. This experiment allows to follow the behavior of the MC in

Day	0	6	12	22	29	36	54	65	96	112
Birch	36%	36.8%	35.1%	32.5%	30.1%	29.8%	28%	28%	25.8%	22.4%
Pine	45%	44.7%	46.3%	36%	38.7%	34.2%	38%	33%	31.2%	22.1%
Oak	34%	33.1%	30.7%	29.7%	27.6%	24.5%	26%	28%	26.7%	27.7%

Table 4.4: General tendency of sample MC in the sampling pile since the first measurement day.

different locations within a whole pile of chips during its natural drying process. As mentioned above, different parts of the pile hold different MC values. Measurements of the  $\Gamma$  at the entry of each antenna have been performed weekly for the three species. The comparison of the antenna labeled 5 located in the middle of the pile and the antenna labeled 14 located on the upper part of each pile is presented in Figure 4.38. One can see that the resonant frequency measured by the antenna on the top of the pile is always higher than the one from the middle of the pile. This is due to the different position of the sensor within the pile. Both curves of every specie follow a similar behavior, the three pairs of curves decrease equally respectively. The sensor that is closer to the air presents a resonant frequency higher than that of the sensor in the middle for the three species under test. The fact that the sensor is closer to the air means that obviously chips are drier in that part of the pile as it has been shown. Figure 4.39 shows the average value

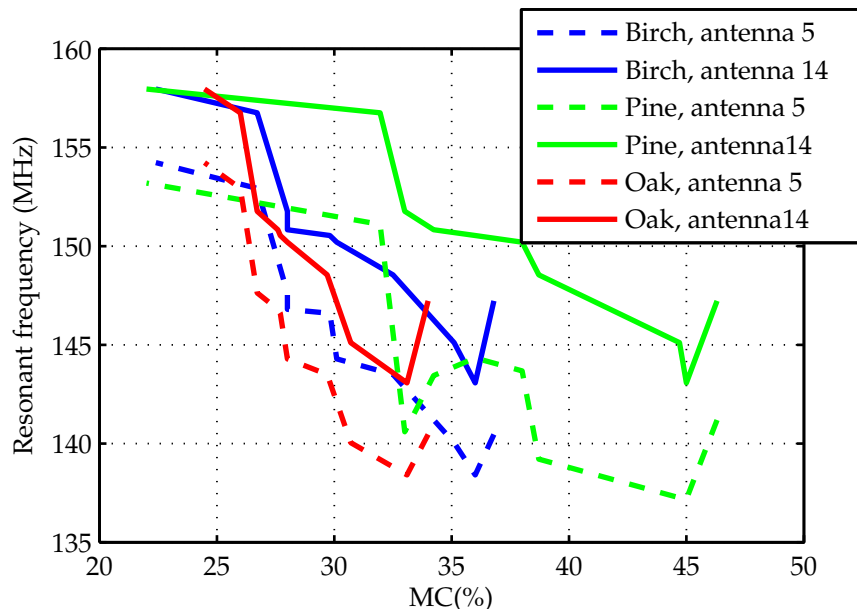


Figure 4.38: Comparison of sensors within the piles.

of the resonant frequency of all sensors during the experiment. It is well seen how the general MC value decreases. Results show that all piles have reached the same MC value after 16 weeks exposed in the warehouse. Measurements of all sensors present different values, the dispersion

is very high for the three species, the average frequency variation  $\Delta f = f_{max} - f_{min}$  is 17 MHz, where  $f_{max}$  and  $f_{min}$  are the maximum and minimum values of resonant frequency measured among the 14 sensors for every specie. This frequency variation is very important if comparing with the resonant frequency corresponding to the maximum and minimum MC measured of the whole experiment. Different species do dry also at different speeds. The speed drying value for birch and pine is similar. Oak seems to have a slower variation of MC in the same amount of time. This is because the oak was drier than birch and pine when first chipped in May. By the way, oak is a hardwood, therefore denser than the other species, which implies a slower speed of drying.

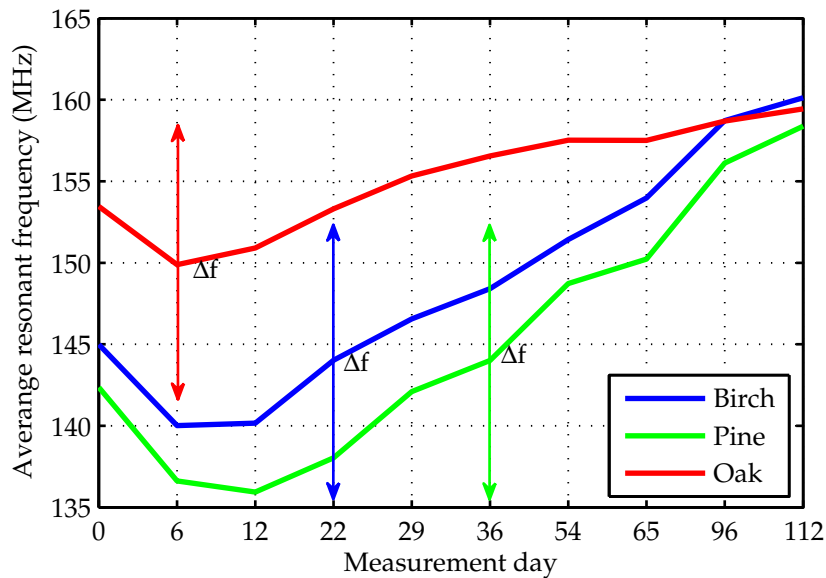


Figure 4.39: Evolution of the MC for three different species of wood.

### 4.3.2 Bulk measurements in a container

	Pine P63	Oak P63	Oak P45
Measuring pile	45 m <sup>3</sup>	45 m <sup>3</sup>	45 m <sup>3</sup>

Table 4.5: Piles available for measurements in a container.

Three piles of chips of different species and sizes are used to load and unload a 35 m<sup>3</sup> container of a delivery truck. Each pile occupies a surface of around 5 × 5 m<sup>2</sup> and 4 m high. Figure 4.40 shows the industrial truck used in this experiment. The piles available are described in Table 4.5. Contrarily to static measurement, here the antennas are subjected to a harsh environment, since tonnes of wood chips will flow on them. Therefore robust antennas have to be

used. Moreover, the container is available only days of measurements. Therefore the measurement system designed to install in the industrial container must be removable hanging chains equipped with antennas. Six ropes holding two antennas each have been built. They hang from three transverse bigger ropes located on the upper part of the truck. A photograph of the system installed in the container is presented in Figure 4.41. The ropes are hanged, this way they do not offer resistance at the moment of unloading the container since they move with the flow of chips. Each rope has been weighted at the bottom to limit their displacement toward the walls of the container while the process of loading. Antennas are fed at the center via a coaxial cable, the connection is protected with a plastic box filled with silicone to avoid water leaks. As every rope holds two antennas, a pair of coaxial cables is attached to the rope and left out of the truck. This way they do not resist stretching of any kind during loading and unloading.



Figure 4.40: Photography of the delivery truck and its specifications.

Since antennas are perpendicular to their power supply for sake of simplicity, the antennas are built with metal springs, which means that both arms are bendable so they are not an obstacle to the flow of chips while unloading, see Figure 4.42. This is key to minimize the damage of the system. Springs are 1-cm diameter and 56-cm long. In order to limit oxidation between the springs and thus to provide a good conduction a shielding braid is welded to the springs to improve their performance.

The target is to follow the MC of the piles since chipped (50% MC supposedly) until 20% MC and to study how different densities of wood and different sizes of chips affect the performance of the system. Measurements have been performed during 5 months since June 2015 to November 2015. Every measurement day the portable system of antennas is installed in the container and measured when empty. Then, a backhoe loader fills the truck with the pile of chips under test and the reflection coefficient  $\Gamma$  of every sensor is measured. Finally the unloading of the truck occurs. This is the most dangerous manouvre for the antennas because it represents a





Figure 4.41: Delivery truck equipped with the measuring system.

dramatic weight over the measuring system. The antennas must be checked after every unloading process, and re-welded if required. In a real system an in-line antenna, that is to say a parallel power supply would be required to offer more resistance and thus more robustness. In that case optic fiber should be used to power the system in order to keep the efficiency of the sensor (see subsection 4.2.4). Photographs 4.43, 4.44, 4.45 and 4.46 illustrate different stages of the procedure from loading and unloading the container, taking the samples, to drying them in the laboratory in Paris.

	MC(%)								
Pine P63	32	32.9	33	35.5	43.7	44.6	46.9	78.3	50.1
Dispersion	±5	±2.2	±0.5	±1	±1.5	±2.8	±6	±6.5	±0.7
Oak P63	21.3	23.8	24.5	24.7	42	42.7	43.7	44.2	
Dispersion	±4	±8.5	±2.3	±0.5	±2.5	±1.2	±1.6	±2	
Oak P45	23.8	25.5	27.6	31	41.2	41.8	43	43.1	
Dispersion	±0.5	±2	±1.5	±3.8	+2.4	±1.9	±2.5	±1.4	

Table 4.6: MC values tested in the platform.



Figure 4.42: Antennas built with metal springs.

In the experiments, chips are mixed during the loading and unloading process of the container, so the dispersion of MC between different locations of the pile is lower than in a static pile. However the arrangement of the wood chips is variable. Six samples of about 400 grammes are taken from every pile at the moment of unloading and dried in the laboratory to estimate the average MC value following the official method.

A total of 8 values of MC have been measured for the piles of oak and 9 for the pine. Table 4.6 shows the average value of the taken samples and their corresponding dispersion. It has been observed that the average dispersion in MC is  $\pm 2.6\%MC$ .



Figure 4.43: Loading the container of a delivery truck.



Figure 4.44: Unloading process.



Figure 4.45: Taking the samples.



Figure 4.46: Drying process in the oven at the laboratory in Paris.

The resonant frequency of every sensor at every MC is obtained from the reflection coefficient  $\Gamma$ . An algorithm based on a simple weighted sum applied to 80 MHz bandwidth centered at

the minimum value of  $\Gamma$  is applied in order to compensate possible external resonances due to the metallic container. It has been observed that the dispersion between the 12 sensors is similar to the measurements in static piles, about  $\Delta f=17$  MHz. This is due to the heterogeneity of the moisture content within a big amount of chips. This is the reason why an estimation based on the average must be calculated when buying large samples of this biofuel. Figure 4.47 shows the relationship between the average resonant frequency of the measuring system and the corresponding MC values obtained from drying the samples in the oven. It is well seen that the resonant frequency decreases with the MC and that there is no much difference between chipped oak and chipped pine, either between different size of chips used. These results are very positive because this can mean that the strong dependence on water dismissed other parameters to a given extent such as the density of the material and the size of chips used. The resolution of the method is estimated as  $\overline{\Delta f} / \Delta F$ , where  $\overline{\Delta f} = \sum (f_{i,max} - f_{i,min}) / N$  represents the average dispersion for measurements, and  $\Delta F = F_{max} - F_{min}$  is the general frequency range of a linear regression approximation for these curves (dotted curves),  $F_{max}$  and  $F_{min}$  are the resonance frequencies for the maximum and minimum value of MC under test. The rough resolution obtained for the pine is  $\pm 3.6\%$ , for the P63 oak is  $\pm 3.7\%$  and  $\pm 3.9\%$  for the P45 oak. For a common regression a global rough resolution of  $\pm 4.4\%$  is obtained, see Figure 4.48. However a  $\pm 2.6\%$  MC dispersion must be taken into account. This dispersion means that the  $\pm 4.4\%$  precision is not just related to the efficiency of the system but to the MC dispersion observed between the samples. Therefore the global rough precision is actually lower around  $\pm 1.8\%$ .

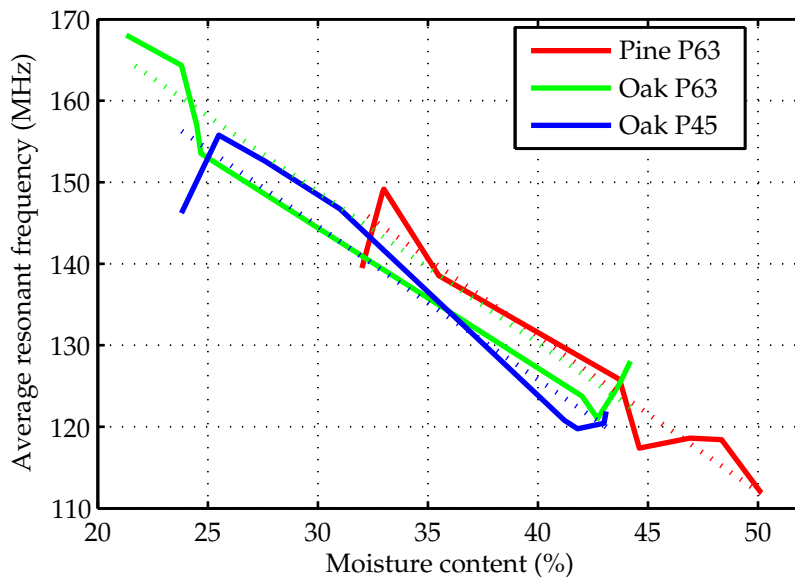


Figure 4.47: Performance of the system.

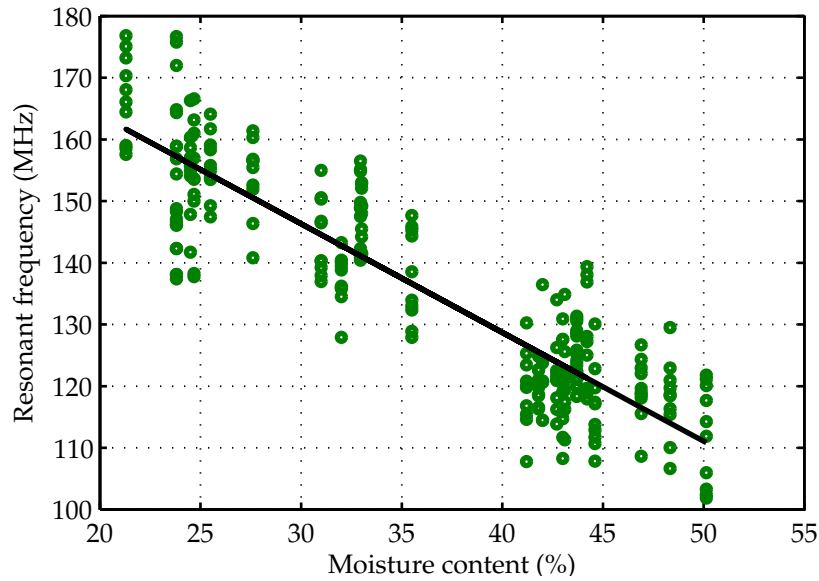


Figure 4.48: Global linear regression approximation.

### 4.3.3 Summary

The presented system is based on a resonator technology. Several resonator antennas have been firstly considered for this application, the half-wave dipole antenna responds better to the variation of the permittivity and also probes a larger volume than the others. Several species of wood at different chip size have been tested in a real experiment condition. In view of the results in the laboratory and on site it is clear that this technology is independent of external parameters such as the meteorology or the environment around, also of the density of the material and the size of chip used. A  $\pm 3.4\%$  rough precision is obtained at the laboratory for a system independent of the kind of wood under test using the same size of chips. Learning machine methods improve the precision to  $\pm 2.15\%$ . The rough precision obtained by the measurements on site is approximately  $\pm 1.8\%$ , notice that the samples measured on site present  $\pm 2.6\%$  MC dispersion. No learning machine methods are applied yet to these results on site so this precision can be easily improved. Different sizes of chips as well as different species have been tested. Bearing in mind the large quantity of material that must be probed and the difficult conditions that this application implies, it has been clearly demonstrated on site that an economical and robust system can be very easily implemented. It also offers versatility in terms of design, the system can be removable or fixed, used in a container or in a pile, and implemented in hanging chains or in a kind of grid.

## 4.4 Conclusion

This chapter is focused on in-contact technologies to determine the MC of wood chips in bulk. These technologies avoid the measurement of the surface of the material under test which is really changeable due to external parameters. In order to have a reliable prediction of MC the surface of the material must be avoided. Therefore the main idea presented here is a measurement of MC inside the container of a delivery truck, because this could provide a value of MC while chipping in the forest or in the warehouse, and also a value at the moment of the delivery to some client to set the price of the fuel.

The first proposal is based on a giant capacitor installed in the container of a delivery truck. The capacity of the chips between two or more electrodes installed in an industrial container can give a prediction of the MC. A laboratory-scale prototype has been designed and tested. This system would be very advantageous in terms of robustness for a real application. However results have shown that it is very sensitive to changes in the environment surrounding the container. If there is some water in the low part of the container or if it rains over the electrodes, the predictions become completely unreliable. This system also implies a fixed equipment precisely tuned in the container, this means that this one would be used specifically for transporting and testing wood chips.

The second system proposed is based on an internal technology. A resonant open antenna in contact with the material under test changes its impedance according to the permittivity of the medium around it. This implies a change of its resonant frequency. The resonant antenna is a half-wave dipole antenna. Measuring the reflection coefficient  $\Gamma$  of this antenna when it is placed inside wood chips allows to have a prediction of the MC of the material. This technology has provided very promising results so a real size prototype to test on site has been designed. The platform *Coopérative forestière Bourgogne Limousin CFBL* in Autun, provided the industrial machines and wood required for an experiment in real operating conditions. The real prototype designed in the laboratory in Paris has been used to test the MC of several tonnes of chips in a truck. The proposed implementation has turned out robust enough and the performance of the measuring system has provided promising results. These results are positive and inspiring for further investment into a real industrial prototype.



# Conclusion

Increasing the consumption of renewable energies is the best way to fight against climate change, which is one of the biggest issues of the twenty first century. That is why European policies as well as French National policies support the development of renewable sources in order to reach the target set by the European Union by 2020. Biomass is in the majority within the renewable sources and wood is the biggest source of biomass. The combustion of wood is a wide extended form of renewable energy and thus the increase of it is key to get the the expected objective.

Wood for combustion can be presented in logs, pellets or chips. Logs are the least efficient and more suitable for small boilers. Pellets and chips are more efficient and can be used in automatic systems, however pellets are a manufactured product, this means there is energy involved in their production. Wood chips are shredded wood that have many advantages for the production of thermal energy. They come from wood left over from the industry that otherwise would not be used and just 2% of all the energy recovered is invested in their production. Moreover, they come from an abundant source available in most countries.

This form of biofuel gets burned in specific boilers to create energy. During combustion, the water content is the most important and inconvenient parameter because heat is lost in the process of the evaporation of the water and more water results in less wood for a given mass of biofuel. Moreover, extra energy is wasted in the transportation of water. The calorific power is directly dependent on the moisture content. For example; the energy provided by 5 tonnes of chips at 50% moisture content (MC) is equivalent to 1 Toe, however at 20% MC, just 3 tonnes of chips would be required to produce the energy provided by 1 Toe. Boilers are designed for specific type of fuels and MC, therefore this parameter must be known in order to ensure the best efficiency.

Wood chips are an heterogeneous material. Measuring its MC presents many complexities because of the random nature, size and humidity of the chips. Nowadays the current applied method to determine the MC in large volumes of chips is called Oven Dry Method (EN 14774-1:2009). It is a sampling method, it takes small samples of a big pile of chips that are weighed



before and after drying to determine the humidity. It is a reliable method independent of parameters such as density or temperature of the fuel, but unfortunately it is too slow, it takes about 24 hours, and gives only an approximate measure of moisture because just small samples are tested. In view of these limitations, a new technique is required. Basically this technique should be rapid and most of all able to measure large samples.

This thesis is focused on the study of the permittivity of wood chips to predict the MC. Wood chips is a material formed by wood, water and air, water has a high dielectric constant when compared to other materials such as of the air and the wood. Therefore MC influences tremendously the dielectric constant of the material under test.

Radiofrequency (RF) is the most suited technology for bulk measurements due to its larger penetration depth. We can think of either external humidity sensors based on the study of the reflected energy by the material or the transmitted energy passing through it. Or internal devices based on resonator technologies. The MC measurement is required all along the production chain to monitor the quality of the fuel, but most of all at the final delivery to the client to determine the price of the fuel. According to the wood energy sector and to the way of handling wood chips, the container of a truck and the warehouse are the only possible scenes where the MC bulk measurements can be performed.

Progress on research and development of techniques for wood chips MC determination has been achieved. Specifically for bulk measurements. Several techniques has been developed, designed and tested. A technology that measures the reflected energy by wood chips is presented. It does not require a fixed equipment. For example a crossbar over the weighbridge in the sawmill is an alternative. When the truck brings chipped wood from the forests to the warehouse the fuel must be weighted, so then the MC measurement can be performed at the same time. The cross bar probes all along the surface of the fuel within the truck. Also, the crossbar could be portable and able to measure some different piles of chips in random places in the warehouse. This technology is dependent on the state of the surface of the fuel which can be very changeable according to climate conditions, thus this measurement of MC is then not trustworthy.

A small-scale technology that implies the equipment of a truck is also presented. This system is based on a huge capacitor installed in the container of a truck. This requires a specific equipment, that is to say that the equipped container would be useless for applications different than delivery of wood chips. MC determination is based on the capacitance measured in between both capacitors. Tests have shown that the results are very dependent on the environment around the container due to boundary conditions.

A removable technology based on open resonator antennas has been developed. The MC measurement is based on the resonant frequency at the entry of the antenna within the sample. A system of hanging chains equipped with twelve half-wave dipole antennas have been realized and tested. This way a full truck of chips can be probed. This method has provided a rough accuracy of 3.4% in the laboratory. Statistical analysis has been applied to optimize the precision to 2.15%. On site the rough accuracy has been found to be 4.4% but a ( $\pm 2.6\%$  MC) bias is caused by the MC dispersion observed in the measured samples. This means that the rough accuracy may be around 1.8%. Aside from the accuracy, this system provides an economical and simple measurement of MC. This technology is very convenient for the wood energy sector due to the flexibility of implementation. This removable system is installed in the container when a measurement is required, no modification in the truck, container or platform is needed. This technology implemented in a truck provides measurements in several stages all along the production chain: during chipping in the forest, in the meantime if deliveries are required and at the final delivery to the client. The implementation of this technology in the warehouse, to be applied on piles on site is also very conceivable.

In view of the initial issue, this technology seems to cover the requirements of the wood energy sector. A rapid and non destructive MC measurement able to probe large quantity of biofuel can be obtained. This work pertaining to MOQAPRO project, was supported by a grant overseen by the French National Research Agency (ANR) as part of the “*Bio-Matières et Energies (Bio-ME) 2012*” Programme (ANR-12-BIME-0007).



# Perspectives

The optimization of the wood energy sector is a priority in France. MOQAPRO is a scientific project whose main target is a large scale approach of quantity and quality monitoring of wood chips all along their production chain, from forest until final delivery to the client. This implies periodic measurements of mass and moisture content (MC) to check the quality of the fuel. The idea is to better control the wood production and to be able to give a Fuel Quality Certification. The goal of this thesis is to study possible technologies that can be applied on site to measure the moisture content of bulk chips to check the quality of the product and determine its price. This fuel is delivered in large samples, this and the rough site conditions represent complexities to the implementation of electronic devices on site. A non destructive, rapid and robust enough technology must be considered under these circumstances.

Conclusions and results achieved from the research carried out during this thesis allow to think ahead some perspectives that can contribute to the final objective. Regarding the capacitor technology, boundary conditions have presented some issues because the capacitance is sensitive to the environment. However, other geometry device that better confines the lines of electric field may be more convenient for this application. A pseudo-cylindrical-geometry capacitor can be considered. One or more electrodes disposed in the container can play the role of internal electrodes and the external electrode is the container itself, see Figure 4.49. Another way could be a smaller planar geometry inside the truck, which electrodes are immersed in wood, as illustrated in Figure 4.50. This both geometries could also be portable.

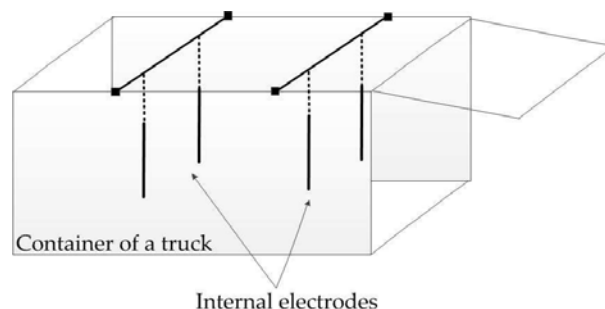


Figure 4.49: Pseudo-cylindrical capacitor.

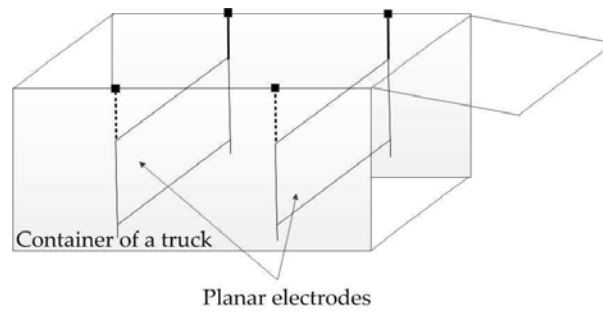


Figure 4.50: Capacitor technology.

Concerning the resonator technology using half-wave dipole antennas, tests performed in the laboratory and on site have provided promising results even though the implemented device is a prototype created in the laboratory. As an expectancy, learning machine methods can be applied to the real measurements performed in the *coopérative forestière CFBL* to try to improve the precision. Research in the laboratory has been carried out under some limitations because of storage restrictions. The performance of longer dipoles could be tested in the near future by the industry. More species of wood chips of all different sizes P16, P45, P63 and P100 may be also tested to compare reproducibility. Also, in view of the success obtained by the experiment on site, further effort should be directed towards the mechanics of the device. The most obvious weakness is its robustness overall because the dipole is fed perpendicularly. A parallel power supply opens up many possibilities of implementation. The dipoles could be installed along the length of a rope of rubber, for instance. The power supply can be wireless with inboard sensor supply or powered by non metallic means, using an optical fiber for instance. In this latter case, the signal as well as the energy supplied transits via the fiber. Thus, the performance of the antenna is not influenced by the presence of wires. This way a more robust and simple device is easily conceivable, see Figure 4.51. The sensors can be either inside the truck attached to the walls, or put into within the pile of chips by a drilling machine or by the staff while the pile is being built. This proposal is robust enough to be applied in the forest industry, and also can be installed and used by technicians who are not necessarily related to electrical engineering.

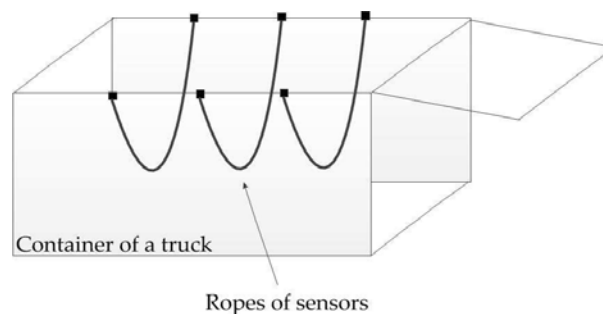


Figure 4.51: Rope of half-wave antennas.

# Bibliography

- [1] AEBIOM, "Final report 2013 european biomass association." <http://www.aebiom.org/blog/aebiom-annual-report-2013/>, 2013. Accessed 2015-08-17.
- [2] M. Wihersaari, "Greenhouse gas emissions from final harvest fuel chip production in finland," *Biomass and Bioenergy*, vol. 28, no. 5, pp. 435–443, 2005.
- [3] B. Wahlund, J. Yan, and M. Westermarck, "Increasing biomass utilisation in energy systems: A comparative study of co2 reduction and cost for different bioenergy processing options," *Biomass and Bioenergy*, vol. 26, no. 6, pp. 531–544, 2004.
- [4] S. Mahapatra and S. Dasappa, "Influence of surface area to volume ratio of fuel particles on gasification process in a fixed bed," *Energy for Sustainable Development*, vol. 19, pp. 122–129, 2014.
- [5] Biomass Energy Centre, "Chip fired boilers." [http://www.biomassenergycentre.org.uk/portal/page?\\_pageid=75,363210&\\_dad=portal&\\_schema=PORTAL](http://www.biomassenergycentre.org.uk/portal/page?_pageid=75,363210&_dad=portal&_schema=PORTAL). Accessed 2015-08-17.
- [6] Biomass Energy Centre, "Typical calorific values of fuels." [http://www.biomassenergycentre.org.uk/portal/page?\\_pageid=75,20041&\\_dad=portal&\\_schema=PORTAL](http://www.biomassenergycentre.org.uk/portal/page?_pageid=75,20041&_dad=portal&_schema=PORTAL). Accessed 2015-08-17.
- [7] Biomass trade centre, "Wood fuels hand book, production, quality requirements and trading." <http://www.biomasstradecentre2.eu/available-literature/>. Accessed 2015-08-17.
- [8] Forestry Commission United Kingdom, "Wood as fuel." <http://www.forestry.gov.uk/website/searchall.nsf/GoogleResults?open=&cx=001774383426470524382%3Aa5mnshoy9zo&cof=FORID%3A9&ie=UTF-8&q=FC-BEC>. Accessed 2015-08-17.
- [9] Biomass Energy Centre, "Calorific value as a function of moisture content." [http://www.biomassenergycentre.org.uk/portal/page?\\_pageid=75,177178&\\_dad=portal&\\_schema=PORTAL](http://www.biomassenergycentre.org.uk/portal/page?_pageid=75,177178&_dad=portal&_schema=PORTAL). Accessed 2015-08-17.

- [10] United Nations Economic Commission for Europe/Food and agriculture Organization of the United Nations. UNECE/FAO 2011, "Wood biomass." <http://www.unece.org/forests/areas-of-work/markets/forestsfpoutputs/wood-energy.html>. Accessed 2015-08-17.
- [11] European Commission, "2020 climate and energy package." [http://ec.europa.eu/clima/policies/strategies/2020/index\\_en.htm](http://ec.europa.eu/clima/policies/strategies/2020/index_en.htm). Accessed 2015-08-17.
- [12] The French National Research Agency, "Omicage project, developpement des technologies de mesures, des systemes dinformation et des outils de production pour une approche holistique des chaines dapprovisionnement de grande echelle en biomasse ligneuse." <http://www.agence-nationale-recherche.fr/?Projet=ANR-06-BIOE-0008>, 2006. Accessed 2015-08-03.
- [13] The French National Research Agency, "Moqapro project, methods and tools for quantitative and qualitative woodchips production monitoring in a large scale supply chain." <http://www.agence-nationale-recherche.fr/?Project=ANR-12-BIME-0007>, 2012. Accessed 2015-08-03.
- [14] European Committee for Standardization, CENT/TC 335 EN 14774-1, "Determination of moisture content." <http://standards.cen.eu/dyn/www/f?p=204:105:0>. Accessed 2015-07-03.
- [15] G. I. Torgovnikov, *Dielectric Properties of Wood and Wood-Based Materials*. Springer Series in Wood Science, Berlin, Heidelberg: Springer Berlin Heidelberg, 1993.
- [16] J. Nyström and E. Dahlquist, "Methods for determination of moisture content in woodchips for power plants—a review," *Fuel*, vol. 83, pp. 773–779, 2004.
- [17] P. Jensen, H. Hartmann, T. Böhm, M. Temmerman, F. Rabier, and M. Morsing, "Moisture content determination in solid biofuels by dielectric and nir reflection methods," *Biomass and Bioenergy*, vol. 30, pp. 935–943, 2006.
- [18] N. Panwar, S. Kaushik, and S. Kothari, "Role of renewable energy sources in environmental protection: A review," *Renewable and Sustainable Energy Reviews*, vol. 15, no. 3, pp. 1513–1524, 2011.
- [19] G. Toth and C. Szigeti, "The historical ecological footprint: From over-population to over-consumption," *Ecological Indicators*, vol. 60, pp. 283–291, 2016.
- [20] S. Mohr, J. Wang, G. Ellem, J. Ward, and D. Giurco, "Projection of world fossil fuels by country," *Fuel*, vol. 141, pp. 120–135, 2015.

- [21] "M. king hubbert, peak of oil production." <http://www.hubbertpeak.com/hubbert/>. Accessed 2015-09-26.
- [22] S. Shafiee and E. Topal, "An econometrics view of worldwide fossil fuel consumption and the role of US," *Energy Policy*, vol. 36, no. 2, pp. 775–786, 2008.
- [23] L. E. Ekpeni, K. Y. Benyounis, F. Nkem-Ekpeni, J. Stokes, and A. Olabi, "Energy diversity through renewable energy source *res* - a case study of biomass," *Energy Procedia*, vol. 61, pp. 1740–1747, 2014.
- [24] A. González, J.-R. Riba, R. Puig, and P. Navarro, "Review of micro- and small-scale technologies to produce electricity and heat from mediterranean forests' wood chips," *Renewable and Sustainable Energy Reviews*, vol. 43, pp. 143–155, 2015.
- [25] F. Manzano-Agugliaro, A. Alcayde, F. Montoya, A. Zapata-Sierra, and C. Gil, "Scientific production of renewable energies worldwide: An overview," *Renewable and Sustainable Energy Reviews*, vol. 18, pp. 134–143, 2013.
- [26] S. Gerssen-Gondelach, D. Saygin, B. Wicke, M. Patel, and A. Faaij, "Competing uses of biomass: Assessment and comparison of the performance of bio-based heat, power, fuels and materials," *Renewable and Sustainable Energy Reviews*, vol. 40, pp. 964–998, 2014.
- [27] E. Agbor, X. Zhang, and A. Kumar, "A review of biomass co-firing in north america," *Renewable and Sustainable Energy Reviews*, vol. 40, pp. 930–943, 2014.
- [28] 4planet Energy Group, "Biomass power." <http://www.4planetenergy.com/index.php/products/biogas-biomass-generation>. Accessed 2015-11-27.
- [29] Biomass Energy Centre, "Carbon emissions of different fuels." [http://www.biomassenergycentre.org.uk/portal/page?\\_pageid=75,163182&\\_dad=portal&\\_schema=PORTAL](http://www.biomassenergycentre.org.uk/portal/page?_pageid=75,163182&_dad=portal&_schema=PORTAL). Accessed 2015-09-26.
- [30] European biomass industry association EUBIA, "Eubia project publications - a valuable model for local biomass supply chain development in european regions." <http://www.eubia.org/index.php/publications/eubia-project-publications/viewdownload/1-eubia-project-publications/51-bioenergy-nw-a-valuable-model-for-local-biomass-supply-chain-development-in-european-regions>. Accessed 2015-08-03.
- [31] T. M. Maker, "Wood-chip heating systems," *A guide for institutional and commercial biomass installations*, 2004.
- [32] D. Timmons and C. V. Mejía, "Biomass energy from wood chips: Diesel fuel dependence?," *Biomass and Bioenergy*, vol. 34, no. 9, pp. 1419–1425, 2010.



- [33] Spanish Confederation of Consumers and Users -CECU- Environment, "Biomass boilers for domestic householding-res and rue dissemination project." <http://www.ceu.es/campanas/medio%20ambiente/res&rue/htm/dossier/5%20biomasa.htm#1.%20La%20biomasa%20como%20combustible%20renovable%20para%20la%20calefacci%C3%B3n>. Accessed 2015-08-03.
- [34] Spanish Confederation of Consumers and Users -CECU- Environment, "Energy from biomass and thermal chimneys-res and rue dissemination project." <http://ceu.es/campanas/medio%20ambiente/res&rue/htm/guia/biomasa.htm>. Accessed 2015-08-03.
- [35] Eurostat News Release, 11 March 2015, "Share of renewable energy up to 15% of energy consumption in the eu28 in 2013." [https://en.wikipedia.org/wiki/Renewable\\_energy\\_in\\_the\\_European\\_Union#cite\\_note-eurostat-PDF-2013-2](https://en.wikipedia.org/wiki/Renewable_energy_in_the_European_Union#cite_note-eurostat-PDF-2013-2). Accessed 2015-08-17.
- [36] T. A. Smit, J. Hu, and R. Harmsen, "Unravelling projected energy savings in 2020 of EU Member States using decomposition analyses," *Energy Policy*, vol. 74, pp. 271–285, 2014.
- [37] European Commission, "Energy strategy." <http://ec.europa.eu/energy/en/topics/energy-strategy>. Accessed 2015-08-17.
- [38] European Commission, "The new eu forest strategy - agriculture and rural development." [http://ec.europa.eu/agriculture/forest/strategy/index\\_en.htm](http://ec.europa.eu/agriculture/forest/strategy/index_en.htm). Accessed 2015-03-03.
- [39] A. Sergent, "Sector-based political analysis of energy transition: Green shift in the forest policy regime in france," *Energy Policy*, vol. 73, pp. 491–500, 2014.
- [40] Forest Energy Portal, "Small scale harvesting of whole trees with chipping at roadside." [http://forestenergy.org/pages/images/?get\\_page=gallery&contentareaid=314&PHPSESSID=08f494025b32326f048658ad295b0a93](http://forestenergy.org/pages/images/?get_page=gallery&contentareaid=314&PHPSESSID=08f494025b32326f048658ad295b0a93). Accessed 2015-11-27.
- [41] Biomass Energy Centre, "The biomass storage facility." [http://www.biomassenergycentre.org.uk/portal/page?\\_pageid=75,17730&\\_dad=portal&\\_schema=PORTAL](http://www.biomassenergycentre.org.uk/portal/page?_pageid=75,17730&_dad=portal&_schema=PORTAL). Accessed 2015-09-26.
- [42] S. Rinne, H. Holmberg, T. Myllymaa, K. Kontu, and S. Syri, "Wood chip drying in connection with combined heat and power or solar energy in Finland," vol. 79, p. 3008, 2014.
- [43] J. K. Gigler, W. K. P. Van Loon, M. M. Vissers, and G. P. A. Bot, "Forced convective drying of willow chips," *Biomass and bioenergy*, vol. 19, no. 4, pp. 259–270, 2000.
- [44] Forestry Commission Scotland, "Biomass wood chip-usewoodfuel scotland." <http://www.usewoodfuel.co.uk/supplying-woodfuel/standards-and-accreditation/wood-fuel-standards,-properties-and-specifications/wood-chip-specifications.aspx>. Accessed 2015-08-03.

- [45] Wikipedia, "Woodchipper." <https://en.wikipedia.org/wiki/Woodchipper>. Accessed 2015-11-27.
- [46] "Trucks for wood chips transportation." <http://brenner.eu/buy-wood-biomass-timber/?lang=en>. Accessed 2015-12-08.
- [47] "Handling wood chips in a warehouse." [http://www.chaudieres-morvan.com/fr/le-chauffage-au-bois-dechiquete\\_16.html](http://www.chaudieres-morvan.com/fr/le-chauffage-au-bois-dechiquete_16.html). Accessed 2015-12-08.
- [48] "Excavator for wood chips transportation." <http://live.pege.org/2005-wood/transport.htm>. Accessed 2015-12-08.
- [49] Intelligent Energy Europe, "Forest guides and documents—fostering efficient long term supply partnerships." <http://www.forestprogramme.com/tools-resources/guides/>. Accessed 2015-03-03.
- [50] "Fuelchip - local renewable wood supply." <http://www.fuelchip.co.uk/about-us/our-approach/quality-specification>. Accessed 2015-08-03.
- [51] "Quality and sustainability standards for biofuels." <http://www.solidstandards.eu/standardisation/result-document.html>. Accessed 2015-08-03.
- [52] "Cen european committee for standardization." <https://www.cen.eu/Pages/default.aspx>. Accessed 2015-08-03.
- [53] European Committee for standardization CEN, "Cen/tc 335 solid biofuels." [http://standards.cen.eu/dyn/www/f?p=204:7:0::::FSP\\_ORG\\_ID:19930&cs=17158638AB0C35D5E52A369017E54A1D6](http://standards.cen.eu/dyn/www/f?p=204:7:0::::FSP_ORG_ID:19930&cs=17158638AB0C35D5E52A369017E54A1D6). Accessed 2015-08-03.
- [54] European Committee for standardization CEN, "Cen/tc 335 technical bodies." [http://standards.cen.eu/dyn/www/f?p=204:32:0::::FSP\\_ORG\\_ID,FSP\\_LANG\\_ID:19930,25&cs=19F087DBDE0BACDFD4078ABA84D4941DC](http://standards.cen.eu/dyn/www/f?p=204:32:0::::FSP_ORG_ID,FSP_LANG_ID:19930,25&cs=19F087DBDE0BACDFD4078ABA84D4941DC). Accessed 2015-08-03.
- [55] British Standards Institution and European Committee for Standardization, *Solid biofuels: determination of moisture content, oven dry method. Simplified method EN 14774-1:2009*. London: British Standards Institution, 2010.
- [56] H. Hartmann and T. Böhm, "Rapid moisture content determination of wood chips—results from comparative trials," in *Proceedings of the first World conference on biomass for energy and industry*, pp. 5–9, 2000.
- [57] J. Nyström and E. Dahlquist, "Methods for determination of moisture content in wood-chips for power plants—a review," *Fuel*, vol. 83, no. 7-8, pp. 773–779, 2004.

- [58] R. Samuelsson, J. Burvall, and R. Jirjis, "Comparison of different methods for the determination of moisture content in biomass," *Biomass and Bioenergy*, vol. 30, no. 11, pp. 929–934, 2006.
- [59] P. Jensen, H. Hartmann, T. Bohm, M. Temmerman, F. Rabier, and M. Morsing, "Moisture content determination in solid biofuels by dielectric and NIR reflection methods," *Biomass and Bioenergy*, vol. 30, no. 11, pp. 935–943, 2006.
- [60] C. Ratti, "Hot air and freeze-drying of high-value foods: a review," *Journal of food engineering*, vol. 49, no. 4, pp. 311–319, 2001.
- [61] "Christ alpha 1-2 ld freeze dryer. freeze dryers." <http://www.freeze-dryers.co.uk/store/products/christ-alpha-1-2-ld-freeze-dryer/>. Accessed 2015-09-27.
- [62] "Heating /drying ovens." <http://www.memmert.com/products/heating-drying-ovens/universal-oven/UN55plus/>, 2015. Accessed 2015-09-27.
- [63] "Infrared moisture analyzer ma35m-000115v1 - sartorius ag." <https://www.sartorius.us/us/product/product-detail/ma35m-000115v1/>. Accessed 2015-09-27.
- [64] "Moisture analyser pce-mwm 300 pce instruments." [https://www.pce-instruments.com/english/weighing-equipment/scales-and-balances/moisture-analyser-moisture-analyzer-pce-instruments-moisture-analyser-pce-mwm-300-det\\_2208249.htm?\\_list=qr.art&\\_listpos=2](https://www.pce-instruments.com/english/weighing-equipment/scales-and-balances/moisture-analyser-moisture-analyzer-pce-instruments-moisture-analyser-pce-mwm-300-det_2208249.htm?_list=qr.art&_listpos=2). Accessed 2015-09-27.
- [65] C. Wyman, *Handbook on bioethanol: Production and Utilization*. Washington: Taylor and Francis, 1996.
- [66] "Kf titrando: water determination with high-end karlfischer titrators metrohm." <http://www.metrohm.com/en/products/karl-fischer-titration/kf-titrando/>. Accessed 2015-09-27.
- [67] International Conference on Electromagnetic Wave Interaction with Water and Moist Substances, *Electromagnetic aquametry: electromagnetic wave interaction with water and moist substances*. Berlin ; New York: Springer, 2005.
- [68] J. Nystrom and B. Franzon, "Radio frequency system for measuring characteristics of biofuels," *Instrumentation and Measurement Technology Conference, 2005. IMTC 2005. Proceedings of the IEEE*, vol. 2, pp. 978–983, 2005.
- [69] "Detection of decay in wood using microwave characterization," in *Microwave Conference Proceedings (APMC), 2011 Asia-Pacific, IEEE*.

- [70] C. Vallejos and W. Grote, "Wood moisture content measurement at 2.45 GHz," in *Microwave and Optoelectronics Conference (IMOC), 2009 SBMO/IEEE MTT-S International*, pp. 221–225, IEEE, 2009.
- [71] Y. Zhang and S. Okamura, "New density-independent moisture measurement using microwave phase shifts at two frequencies," *Instrumentation and Measurement, IEEE Transactions on*, vol. 48, no. 6, pp. 1208–1211, 1999.
- [72] H. S. Chua, G. Parkinson, A. D. Haigh, and A. A. Gibson, "A method of determining the moisture content of bulk wheat grain," *Journal of Food Engineering*, vol. 78, no. 4, pp. 1155–1158, 2007.
- [73] S. Trabelsi, A. W. Kraszewski, and S. O. Nelson, "A microwave method for on-line determination of bulk density and moisture content of particulate materials," *Instrumentation and Measurement, IEEE Transactions on*, vol. 47, no. 1, pp. 127–132, 1998.
- [74] R. Cerny, "Time-domain reflectometry method and its application for measuring moisture content in porous materials: A review," *Measurement*, vol. 42, no. 3, pp. 329–336, 2009.
- [75] K. Sarabandi and E. S. Li, "Microstrip ring resonator for soil moisture measurements," *Geoscience and Remote Sensing, IEEE Transactions on*, vol. 35, no. 5, pp. 1223–1231, 1997.
- [76] J. Skulski and B. A. Galwas, "Planar resonator sensor for moisture measurements," in *Microwaves and Radar, 1998. MIKON'98., 12th International Conference on*, vol. 3, pp. 692–695, IEEE, 1998.
- [77] "Resonator sensor for moisture content measurement," in *Intelligent Control and Automation, 2006. WCICA 2006. The Sixth World Congress on*, vol. 1, IEEE.
- [78] A. Fuchs, M. J. Moser, H. Zangl, and T. Bretterklieber, "Using capacitive sensing to determine the moisture content of wood pellets-investigations and Application," *International journal on smart sensing and intelligent systems*, vol. 2, no. 4, pp. 293–308, 2009.
- [79] "Moisture Meter for woodchips and biofuels." <http://www.exotek-instruments.com/Moisture-meters/Wood-Chips/FMG3000e.htm>. Accessed 2015-09-27.
- [80] "Wood moisturemeter pce instruments." [https://www.pce-instruments.com/english/measuring-instruments/test-meters/wood-moisture-meter-kat\\_151728\\_1.htm](https://www.pce-instruments.com/english/measuring-instruments/test-meters/wood-moisture-meter-kat_151728_1.htm). Accessed 2015-09-27.
- [81] "Nir spectrometer uv-vi/optical /for process applications - kjt70 - ket." <http://www.directindustry.com/prod/kett/product-71402-1101007.html>. Accessed 2015-09-27.

- [82] "Infrared moisture meter analyzer -ir 5000 quality measurement greco." <http://www.grecon.us/measurement/infrared-moisture-meter/>. Accessed 2015-09-27.
- [83] P. Tangirala, J. R. Heath, A. Radun, and T. Conners, "Development and validation of a programmable logic device (pld) based sensor and processor microarchitecture system for equilibrium moisture content calculation in wood industries," in *Sensors Applications Symposium, 2006. Proceedings of the 2006 IEEE*, pp. 135–140, IEEE, 2006.
- [84] S. Hermansson, F. Lind, and H. Thunman, "On-line monitoring of fuel moisture-content in biomass-fired furnaces by measuring relative humidity of the flue gases," *Chemical Engineering Research and Design*, vol. 89, no. 11, pp. 2470–2476, 2011.
- [85] "Humimeter bma professional wood chip moisture meter." <http://www.humimeter.com/fr/bioenergy/humimeter-bma-woodchip-moisture-meter/>. Accessed 2015-09-27.
- [86] M. Hultnas and V. Fernandez-Cano, "Determination of the moisture content in wood chips of Scots pine and Norway spruce using Mantex Desktop Scanner based on dual energy X-ray absorptiometry," *Journal of Wood Science*, vol. 58, no. 4, pp. 309–314, 2012.
- [87] P. J. Barale, C. G. Fong, M. A. Green, P. A. Luft, A. D. McInturff, J. A. Reimer, and M. Yahnke, "The use of a permanent magnet for water content measurements of wood chips," *Lawrence Berkeley National Laboratory*, 2001.
- [88] A. Z. Nagy and P. Vertes, "Correction for dry bulk density in measurements with neutron moisture gauges," *Journal of Physics E: Scientific Instruments*, vol. 1, no. 11, p. 1097, 1968.
- [89] J. Lewiner, S. Hole, E. Geron, N. Cuvigny, and T. Ditchi, *Method and device for measuring humidity on a stream of wood chippings*. Google Patents, 2013. WO Patent App. PCT/FR2012/052,922.
- [90] F. Ding, *Method and apparatus for estimating surface moisture content of wood chips*. Google Patents, 2007. US Patent 7,292,949.
- [91] S. Osaki, K. Sakai, and S. Nagata, *Apparatus for determining water content of powder/granule*. Google Patents, Sept. 1991. US Patent 5,046,356.
- [92] P. Jakkula, *Method and apparatus for measuring the moisture content or dry-matter content of materials using a microwave dielectric waveguide*. Google Patents, 1988. US Patent 4,755,743.
- [93] P. Jakkula and E. Tahkola, *Method and apparatus for determining the moisture content of a material*. Google Patents, 1994. US Patent 5,315,258.

- [94] A. Ullberg, R. Kullenberg, E. Odén, and F. Danielsson, "Method and apparatus for measuring moisture content in a biological material," 2013. US Patent 8,467,496.
- [95] T. Lappalainen, V.-J. Aho, and M. Tiitta, *Method and arrangement for determining the moisture content of wood chips*. Google Patents, 2003. US Patent 6,526,119.
- [96] A. M. Krause, *Method of wood chip moisture analysis*. Google Patents, 2000. US Patent 6,131,442.
- [97] S. Ramo, J. R. Whinnery, and T. Van Duzer, *Fields and waves in communication electronics*. John Wiley & sons, 1984.
- [98] G. I. Torgovnikov, *Dielectric Properties of Wood and Wood-Based Materials*. Springer Series in Wood Science, Berlin, Heidelberg: Springer Berlin Heidelberg, 1993.
- [99] S. Drabowitch, A. Papiernik, H. Griffiths, J. Encinas, and B. L. Smith, *Modern antennas*. Springer Science & Business Media, 2010.
- [100] J. C. Slater and N. H. Frank, *Electromagnetism*. Courier Corporation, 2012.
- [101] "Electromagnetic spectrum." [https://en.wikipedia.org/wiki/Electromagnetic\\_spectrum](https://en.wikipedia.org/wiki/Electromagnetic_spectrum). Accessed 2015-11-30.
- [102] X. Su and Q. Zhang, "Dynamic 3-d shape measurement method: A review," *Optics and Lasers in Engineering*, vol. 48, no. 2, pp. 191 – 204, 2010.
- [103] H. Schwenke, U. Neuschaefer-Rube, T. Pfeifer, and H. Kunzmann, "Optical methods for dimensional metrology in production engineering," *{CIRP} Annals - Manufacturing Technology*, vol. 51, no. 2, pp. 685 – 699, 2002.
- [104] R. Correal, G. Pajares, and J. Ruz, "Automatic expert system for 3d terrain reconstruction based on stereo vision and histogram matching," *Expert Systems with Applications*, vol. 41, no. 4, Part 2, pp. 2043 – 2051, 2014.
- [105] G. Li, X. Zhang, C. Li, H. Jin, and J. Zhao, "Design and application of parallel stereo matching algorithm based on cuda," *Microprocessors and Microsystems*, 2015.
- [106] "Stereo vision camera. heden webcam 3d." <http://www.ldlc.com/fiche/PB00097117.html>. Accessed 2015-11-30.
- [107] H. Daassi-Gnaba and Y. Oussar, "External vs. internal svm-rfe: The svm-rfe method revisited and applied to emotion recognition," *Neural Network World*, vol. 25, no. 1, pp. 75–91, 2015.

- [108] H. Daassi-Gnaba, Y. Oussar, M. Merlan, T. Ditchi, E. Géron, and S. Holé, "Woodpile moisture content recognition by using svm-rfe method," *Neurocomputing*, In submission 2015.
- [109] I. Guyon and A. Elisseeff, "An introduction to variable and feature selection," *The Journal of Machine Learning Research*, vol. 3, pp. 1157–1182, 2003.
- [110] T. Hastie, R. Tibshirani, and J. Friedman, *Unsupervised learning*. Springer, 2009.
- [111] A. J. Stamm, "The fiber-saturation point of wood as obtained from electrical conductivity measurements," *Industrial & Engineering Chemistry Analytical Edition*, vol. 1, no. 2, pp. 94–97, 1929.
- [112] J. S. Seybold, *Introduction to RF propagation*. Hoboken, N.J: Wiley, 2005.
- [113] C. A. Balanis, *Antenna theory: analysis and design*. Hoboken, NJ: John Wiley, 3rd ed ed., 2005.
- [114] R. E. Collin, *Antennas and radiowave propagation*, vol. 6. McGraw-Hill New York, 1985.
- [115] P. Mabire, A. Mayer, S. Holé, T. Ditchi, E. Géron, and Z. Mokthari, "Mesure non-destructive du taux d'humidité d'un materiau," 2015-03-11. Patent FR1552032.
- [116] A. Cataldo, E. PiuZZi, G. Cannazza, E. De Benedetto, and L. Tarricone, "Quality and anti-adulteration control of vegetable oils through microwave dielectric spectroscopy," *Measurement*, vol. 43, pp. 1031–1039, 2010.
- [117] M. Merlan, T. Ditchi, S. Holé, Y. Oussar, J. Lucas, and E. Géron, "Application of resonant half-wave antenna for determination of moisture content in wood chips," *Biomass and bioenergy*, in submission Jan 2016.
- [118] M. Merlan, T. Ditchi, S. Holé, Y. Oussar, J. Lucas, and E. Géron, "Systeme électromagnétique de mesure de l'humidité de plaquettes forestieres," in *Journées Scientifiques de l'Union Radio-scientifique Internationale, Probing matter with electromagnetic waves*, Paris (France), 2015.
- [119] H. Daassi-Gnaba, Y. Oussar, M. Merlan, T. Ditchi, E. Géron, and S. Holé, "Wood moisture content prediction using feature selection techniques and a kernel method," *Neurocomputing*, Submitted in 2015.
- [120] G. C. Cawley and N. L. Talbot, "Preventing over-fitting during model selection via bayesian regularisation of the hyper-parameters," *The Journal of Machine Learning Research*, vol. 8, pp. 841–861, 2007.

- [121] M. Merlan, T. Ditchi, S. Holé, Y. Oussar, J. Lucas, and E. Géron, "Electromagnetic systeme to determine the moisture content of wood chips," in *Third International Congress on Energy Efficiency and Energy Related Materials (ENEFM)*, Oludeniz, Fethiye/Mugla (Turkey), 2015.







## Abstract

Global warming is one of the major problems of this century. Thus, European policies support the development of renewable energies in order to reach the target set by the European Union by 2020: 20% of the energy consumption must come from renewable resources. The combustion of wood biomass is the larger of the renewable energies and thus the increase of it is a key factor to get the expected target. Wood chips are shredded wood that present many advantages for the production of thermal energy. In particular, they are considered a carbon neutral fuel.

During combustion, the water content does not produce energy but causes a heat loss in the process of the evaporation of the water. Moreover, for a given mass of biofuel, the larger water content, the smaller the wood available. Therefore knowing the moisture content (MC) allows to determine the calorific value of the biofuel and then its price.

In this thesis several techniques based upon the study of the permittivity of large samples of wood chips have been proposed to predict the MC. External systems based on measurements of the reflected energy by the material are not reliable because of their dependence on the surface of the fuel, which can be very changeable under rough industrial and weather conditions. Internal devices are more efficient. They are based on either a capacitive technology or on open resonator technology. Due to promising results, a prototype of a resonator device was implemented and tested in real operating conditions.

## Résumé

Le réchauffement climatique est l'un des principaux problèmes de ce siècle. Les politiques européennes soutiennent le développement des énergies renouvelables afin d'atteindre, d'ici 2020, l'objectif fixé par l'Union Européenne (UE). Ce dernier stipule que 20% de l'énergie produite devra provenir d'une source renouvelable. La combustion de la biomasse sous forme de bois est la plus importante des ressources renouvelables. Par conséquent, le développement de celle-ci est fondamental pour atteindre l'objectif de l'UE. Les plaquettes forestières sont des morceaux de bois déchiquetés. Elles présentent de nombreux avantages pour la production d'énergie thermique, en particulier, elles possèdent un bilan carbone neutre.

Lors de la combustion, la présence d'eau dans le bois ne produit pas d'énergie mais provoque une perte de chaleur dans le processus de l'évaporation de l'eau. Par ailleurs, plus il y a d'eau moins il y a de bois pour une masse donnée de combustible. De ce fait, la connaissance de la teneur en eau dans le bois permet de déterminer son pouvoir calorifique et donc son prix.

Dans cette thèse, plusieurs techniques fondées sur l'étude de la permittivité ont été proposées afin de prédire la teneur en eau des plaquettes forestières à grande échelle. Les systèmes externes fondés sur la réflectivité électromagnétique du matériau sont peu fiables en raison de leur dépendance à l'état de surface du combustible. Celui-ci est très variable en fonction des conditions d'utilisation et climatiques. Les dispositifs internes sont plus performants. Des systèmes internes capacitifs et à base de résonateurs ouverts ont été étudiés. Un prototype de dispositif à résonateur a été réalisé et testé en conditions réelles de production.